FINAL REPORT

U.F. Project No. 4910-4504-797-12
Contract No: BC-354
RPWO# 26

EVALUATION OF SHRINKAGE CRACKING POTENTIAL OF CONCRETE USED IN BRIDGE DECKS IN FLORIDA

Mang Tia
Rajarajan Subramanian
Danny Brown
Chuck Broward

September 2005

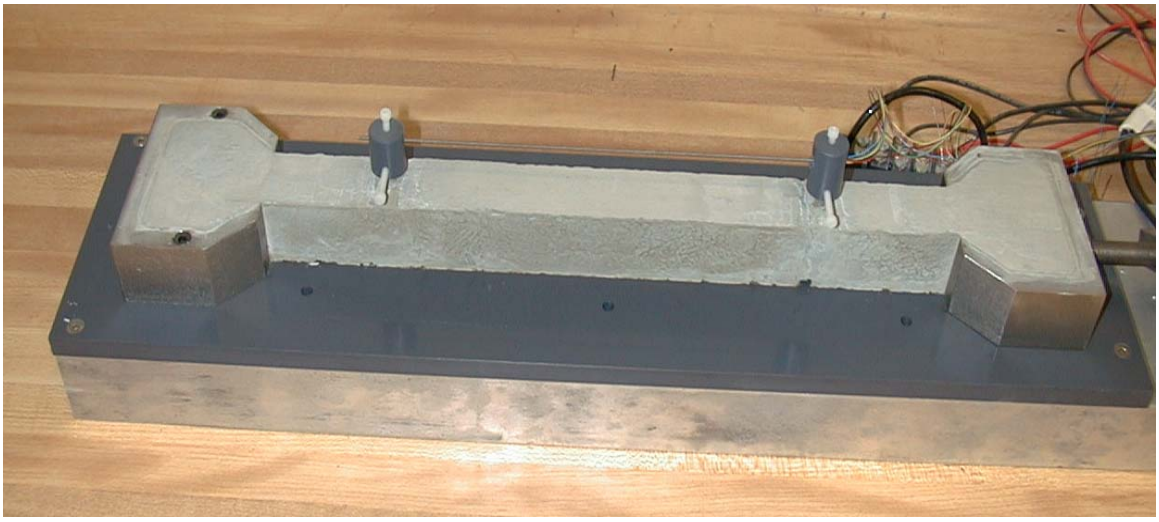

Department of Civil & Coastal Engineering
College of Engineering
University of Florida
Gainesville, Florida

Technical Report Documentation Page

1. Report No.	2. Government Accession No.	3. Recipient's Catalog No.
Final Report		

4. Title and Subtitle

EVALUATION OF SHRINKAGE CRACKING POTENTIAL OF CONCRETE USED IN BRIDGE DECKS IN FLORIDA

5. Report Date: September 2005

6. Performing Organization Code:

8. Performing Organization Report No.: 4910-4504-797-12

7. Author(s): Mang Tia, Raja Subramanian, Danny Brown, and Chuck Broward

9. Performing Organization Name and Address:
University of Florida
Department of Civil and Coastal Engineering
365 Weil Hall / P.O. Box 116580
Gainesville, FL 32611-6580

10. Work Unit No. (TRAIS):

11. Contract or Grant No.: BC 354 – RPWO #26

13. Type of Report and Period Covered: Final Report
November, 2000 – June, 2005

12. Sponsoring Agency Name and Address:
Florida Department of Transportation
Research Management Center
605 Suwannee Street, MS 30
Tallahassee, FL 32399 Phone: (804) 414-4615

14. Sponsoring Agency Code:

15. Supplementary Notes

Prepared in cooperation with the U.S. Department of Transportation and the Federal Highway Administration

16. Abstract

The main objectives of this research are (1) to develop an effective and convenient laboratory set-up and procedure for evaluating concrete mixtures for their resistance to shrinkage cracking in service, (2) to evaluate the different concrete mixtures that have various different admixtures added for reducing the shrinkage in the concrete, and (3) to make recommendations for concrete mix designs for improved resistance to shrinkage cracking in service.

The constrained long specimen apparatus, which was previously developed for the FDOT by the University of Florida for evaluation of resistance to shrinkage cracking of concrete, was further refined and evaluated. The major refinements included (1) using a load cell to measure the induced force in the constrained long specimen, (2) using an embedment strain gage to measure the strain of the long specimen, (3) using an automatic data acquisition system to collect the load and strain data continuously, (4) using a water-resistant and low-friction Teflon sheet as a base plate to minimize the friction between the concrete specimen and its supporting base, and (5) a modification to the test procedure to correct for the specimen contraction.

The results of the testing program indicated that the use of a shrinkage-reducing admixture was effective in reducing the free shrinkage strains and shrinkage-induced stresses of all the concrete mixtures tested, while the compressive strength, splitting tensile strength and elastic modulus of the concrete were not significantly affected. The addition of fly ash as a mineral admixture was found to be effective in reducing the free shrinkage strain and shrinkage-induced stresses of all the concrete.

17. Key Words: Concrete Shrinkage, Constrained Long Specimen Apparatus, Shrinkage-Induced Stress, Indirect Tensile Strength, Compressive Strength, Modulus of Elasticity, Fly Ash, Ground Blast Furnace Slag, Shrinkage-Reducing Admixture

19. Security Classif. (of this report)	20. Security Classif. (of this page)	21. No. of Pages	22. Price
Unclassified	Unclassified	141	

DISCLAIMER

"The opinions, findings and conclusions expressed in this publication are those of the authors and not necessarily those of the Florida Department of Transportation or the U.S. Department of Transportation.

Prepared in cooperation with the State of Florida Department of Transportation and the U.S. Department of Transportation."

SI* (MODERN METRIC) CONVERSION FACTORS

APPROXIMATE CONVERSIONS TO SI UNITS

Symbol	When You Know	Multiply By	To Find	Symbol
	LENGTH			
in	inches	25.4	millimeters	mm
ft	feet	0.305	meters	m
yd	yards	0.914	meters	m
mi	miles	1.61	kilometers	km
	AREA			
in^2	square inches	645.2	square millimeters	mm^2
ft^2	square feet	0.093	square meters	m^2
yd^2	square yards	0.836	square meters	m^2
ac	acres	0.405	hectares	ha
mi^2	square miles	2.59	square kilometers	km^2
	VOLUME			
fl oz	fluid ounces	29.57	milliliters	ml
gal	gallons	3.785	liters	l
ft^3	cubic feet	0.028	cubic meters	m^3
yd^3	cubic yards	0.765	cubic meters	m^3
NOTE: Volumes greater than 1000 l shall be shown in m^3.				
	MASS			
oz	ounces	28.35	grams	g
lb	pounds	0.454	kilograms	kg
T	short tons (2000 lb)	0.907	megagrams	Mg
	TEMPERATURE (exact)			
°F	Fahrenheit temperature	5(F-32)/9 or (F-32)/1.8	Celcius temperature	°C
	ILLUMINATION			
fc	foot-candles	10.76	lux	l
fl	foot-Lamberts	3.426	candela/m^2	cd/m^2
	FORCE and PRESSURE or STRESS			
lbf	poundforce	4.45	newtons	N
psi	poundforce per square inch	6.89	kilopascals	kPa

APPROXIMATE CONVERSIONS FROM SI UNITS

Symbol	When You Know	Multiply By	To Find	Symbol
	LENGTH			
mm	millimeters	0.039	inches	in
m	meters	3.28	feet	ft
m	meters	1.09	yards	yd
km	kilometers	0.621	miles	mi
	AREA			
mm^2	square millimeters	0.0016	square inches	in^2
m^2	square meters	10.764	square feet	ft^2
m^2	square meters	1.195	square yards	yd^2
ha	hectares	2.47	acres	ac
km^2	square kilometers	0.386	square miles	mi^2
	VOLUME			
ml	milliliters	0.034	fluid ounces	fl oz
l	liters	0.264	gallons	gal
m^3	cubic meters	35.71	cubic feet	ft^3
m^3	cubic meters	1.307	cubic yards	yd^3
	MASS			
g	grams	0.035	ounces	oz
kg	kilograms	2.202	pounds	lb
Mg	megagrams	1.103	short tons (2000 lb)	T
	TEMPERATURE (exact)			
°C	Celcius temperature	1.8C + 32	Fahrenheit temperature	°F
	ILLUMINATION			
lx	lux	0.0929	foot-candles	fc
cd/m^2	candela/m^2	0.2919	foot-Lamberts	fl
	FORCE and PRESSURE or STRESS			
N	newtons	0.225	poundforce	lbf
kPa	kilopascals	0.145	poundforce per square inch	psi

* SI is the symbol for the International System of Units. Appropriate rounding should be made to comply with Section 4 of ASTM E380.

(Revised August 1992)

TABLE OF CONTENTS

LIST OF TABLES

LIST OF FIGURES

ACKNOWLEDGMENTS

The Florida Department of Transportation (FDOT) is gratefully acknowledged for providing the financial support, testing equipment, materials and personnel that made this investigation possible. The project manager of this study is Mr. Michael Bergin, whose valuable technical guidance, coordination and cooperation throughout the entire study is greatly appreciated. Sincere gratitude is due to Mr. Charles Ishee for his valuable contribution towards this study. Mr. Mario Paredes is acknowledged for his expert help with the instrumentation for this study. The investigators would like to thank Mr. Richard Delorenzo for his patience and hard work in completing the necessary physical tests for this study. The research team would like to thank Messrs. Toby Dillow, Joseph Fitzgerald, and Craig Roberts for their help in conducting the physical tests on concrete. W. R. Grace & Co. is acknowledged for providing the shrinkage reducing admixture, water reducing admixture and air entraining admixture used in this study. Ms. Candace Leggett and Ms. Irene Scarso are duly acknowledged for their cheerful support in editing and printing this report.

CHAPTER 1
INTRODUCTION

1.1 Background

Shrinkage cracking of concrete bridge decks is a critical problem in the State of Florida. Many concrete bridge decks have been observed to develop plastic shrinkage cracks soon after construction. These cracks shorten the service lives of the decks and increase the cost for maintenance and repairs. In recent years, the increasing use of high performance concretes might have made this problem worse. High-performance concretes, which are usually produced by using a high cement content, are known to have higher free shrinkage and are thus more likely to develop shrinkage cracking.

One of the possible solutions to this problem is to modify the concrete mix designs such that the concretes could be less susceptible to shrinkage cracking while maintaining their other high-performance properties. However, the tendency of a concrete to shrinkage cracking is not a simple function of its free shrinkage. It is also affected by factors such as the constraint on the concrete, rate of strength gain, temperature and the elastic modulus of the concrete. The creep of the concrete during its plastic stage can also relieve some of the induced stress due to shrinkage. All these factors need to be fully considered in evaluating a concrete mix for its resistance to shrinkage cracking.

In a prior research project entitled, "Development of a Laboratory Procedure for Evaluating Concrete Mixes for Resistance to Shrinkage Cracking in Service," sponsored by the FDOT, a testing and analysis method was developed for evaluation of concrete mixes for resistance to shrinkage cracking. The developed testing procedures included

characterizing the tensile strength and elastic modulus of the concrete at early ages by means of the conventional strength tests, and to characterize the creep, free shrinkage and elastic properties of the concrete by means of a constrained long specimen apparatus, which was developed as part of this project. Results from this study show that the developed test method is very effective in measuring the pertinent properties of concrete that are related to shrinkage cracking, and is a very promising tool for evaluating the resistance to shrinkage cracking of concrete in service. This testing and analysis method should be further evaluated, refined and implemented as a standard procedure for evaluating shrinkage cracking resistance of concrete used by FDOT.

1.2 Study Objectives

The main objectives of this research are as follows:

1. To develop an effective and convenient laboratory set-up and procedure for evaluating concrete mixtures for their resistance to shrinkage cracking in service of bridge decks in Florida.
2. To implement the developed testing and analysis method using the developed constrained long specimen apparatuses as a standardized tool for evaluation of shrinkage cracking resistance of concrete in Florida.
3. To evaluate the different concrete mixtures that have various different admixtures added for reducing the shrinkage in the concrete.
4. To make recommendations for modification of concrete mix designs based on the evaluation of the different concrete mixtures that were used in bridge decks of Florida for improved resistance to shrinkage cracking in service.

CHAPTER 2
LITERATURE REVIEW

2.1 Introduction

This chapter presents a literature review on the basics of concrete shrinkage and the results of some studies on admixtures for reducing shrinkage in concrete.

2.2 Mechanism of Concrete Shrinkage

Concrete shrinks as it dries under normal atmospheric conditions. Tensile stresses develop when the concrete is prevented from shrinking freely. The combination of high tensile stresses with the low fracture resistance of concrete often results in cracking. Cracks reduce load carrying capacity and accelerate deterioration, resulting in increased maintenance costs and reduced service life. Although free shrinkage measurements are useful in comparing different mixture compositions, they do not provide sufficient information to determine if the concrete will crack in service. Cracking is a complex phenomenon, which is dependent on several factors including free shrinkage, age-dependent material property development, creep relaxation, shrinkage rate, and degree of restraint. The types of shrinkages can be listed as plastic shrinkage, drying shrinkage, carbonation shrinkage and autogenous shrinkage.

Water-related shrinkage is a volumetric change caused by the movement and the loss of water (i.e., change in the internal pore pressure caused by drying or self-desiccation). Drying is driven by the environmental conditions in which the relative humidity of the concrete structure strives to bring into balance with the humidity of the surrounding environment. Water is squeezed out from the capillary pores resulting in the development of tensile stresses since the internal humidity attempts to make uniform with

a lower environmental humidity. The cause of compressing the concrete matrix is the tensile stress that explains partially the phenomenon of drying shrinkage. Water-related shrinkage is the most significant in thinner structures (with large surface area to volume ratio) due to the more rapid loss of water. Pavements, bridge decks, and slabs are examples of thin structures that may be susceptible to drying shrinkage cracking [Bazant 1986; Bazant and Carol 1993; and Tazawa 1998].

This report will focus on water-related shrinkage and as a result the following sections will be used to provide a brief summary of the terms that are used to describe shrinkage of concrete. Also, the effects of ingredients and their physical characteristics on the shrinkage of concrete are discussed in this chapter. While plastic and carbonation shrinkage can occur in structures, this research report will focus primarily on drying shrinkage.

2.2.1 Plastic Shrinkage

Plastic shrinkage is a term reserved for freshly poured concrete. Plastic shrinkage occurs when water is allowed to evaporate from the fresh concrete surface. Environmental considerations including solar effects, wind speed, high temperature and low relative humidity drastically influence the potential of plastic shrinkage cracking [Schaels and Hoover 1988]. Generally, plastic shrinkage cracking can be prevented by limiting early-age evaporation through the use of plastic sheeting, mono-molecular films, water fogging, or wind breaks in conjunction with properly designed concrete mixtures. Results of several studies suggest the benefits of using short fibers as a possible alternative solution to this problem [Swamy and Stavarides 1979; Kraai 1985; Berke and Dallaire 1993].

2.2.2 Carbonation Shrinkage

Carbonation occurs as a result of a reaction that occurs between hydrated cement and carbon dioxide in the atmosphere which causes the concrete to shrink. Carbonation shrinkage occurs along the surface of concrete and as such it is usually not a main cause for concern in structural concrete. Carbonation shrinkage will not be considered in this study.

2.2.3 Drying Shrinkage

Drying shrinkage is by far the most common cause of shrinkage. Drying shrinkage occurs in hardened concrete as a result of water movement. The reaction of cement and water results in the formation of a calcium silicate hydrate gel (CS-H) with water-filled space. The size of the pores in the water-filled space varies from large capillary pores (> 5 nm) to smaller voids in the C-S-H gel that are filled with adsorbed water (0.5~2.5 nm). As drying occurs, disjoining pressure removes adsorbed water from these pores and hydrostatic forces (capillary stresses) form a meniscus that exerts stresses on the C-S-H skeleton causing the cement paste to shrink.

One of the most substantial factors influencing free shrinkage is the water-to cement ratio (w/c). The w/c required for complete hydration is typically assumed to be approximately 0.42 depending on the amount of gel porosity that is assumed. The amount of water has a direct influence on the size and magnitude of the porosity (i.e., higher w/c pastes have higher porosity). Therefore, specimens with a lower w/c have a lower amount of pore water and consequently exhibit lower drying shrinkage. It should be noted that recently the use of high-range water-reducing admixtures (HRWRA) has led to increased workability for lower w/c mixtures.

Another factor that influences shrinkage is the degree of hydration. At later ages, more water has chemically combined; consequently less water is available to move and lower shrinkage is frequently observed. It can be argued however in some cases that the shrinkage may not decrease as the hydration of the specimen is increased since hydration also results in a reduction in pore size. Other factors that influence shrinkage include chemical admixtures, mineral admixtures, and cement composition, since they typically alter the reaction products, porosity, and mechanical stiffness [Powers and Brownyard 1948].

2.2.4 Autogenous Shrinkage

Autogenous shrinkage occurs under sealed concrete (i.e., no moisture loss) without temperature change. Autogenous shrinkage occurs primarily as a result of chemical shrinkage (i.e., volume reduction due to the hydration reaction) and self-desiccation (i.e., the internal consumption of water by the hydration reaction). Consequently, concrete can be made with significantly lower water demands ($0.2 < w/c < 0.42$) resulting in concrete which may be susceptible to self-desiccation shrinkage. Self-desiccation describes a process where the internal water is consumed by hydration and the internal surfaces can no longer be saturated. Self-desiccation occurs even in specimens that are sealed during curing and can lead to incomplete hydration. Although autogenous shrinkage was described as early as the 1930's [Lyman 1934], it did not pose significant problems in construction until recently since a high w/c was typically required to maintain sufficient workability. This changed however with the development of water-reducing and high-range water-reducing agents that have permitted common use of low w/c mixtures (i.e., less than ~0.42) and as a result autogenous shrinkage has become

a cause of concern. Currently, many investigations are currently being conducted on chemical and autogenous shrinkage [Persson 1998; Tazawa 1998].

2.3 Influence of Aggregates on Concrete Shrinkage

Aggregates affect concrete deformation through water demand, aggregate stiffness and volumetric concentration, and paste/aggregate interaction [Han 1994]. The primary source of shrinkage is the cement paste. Aggregates that require a lower water demand for workability will therefore produce concretes with a lower cement content, which will result in lower shrinkage. Shape and texture of coarse aggregate play a role on the behavior of fresh and hardened concrete. Shape and texture affect the demand for sand. Flaky, elongated, angular, and rough particles have high voids and require more sand to fill the voids and to provide a workable concrete, thus increasing the demand for water and thereby increasing shrinkage [Legg 1998]. Spherical or cubical aggregates have less specific surface area than flat and elongated particles. Consequently, spherical or cubical aggregates require less paste and less water for workability [Shilstone 1999; Dewar 1992]. For a given workability, flaky and elongated aggregates increase the demand for water thus affecting strength of hardened concrete as well as increase the shrinkage in concrete. Spherical or cubical particles lead also to better pumpability and finishability as well as produce higher strengths and lower shrinkage than flaky and elongated aggregates [Shilstone 1990].

Aggregates with higher stiffness will give greater restraining effects to shrinkage stresses and result in lower shrinkage in concrete [Neville 1996]. Aggregates that shrink considerably upon drying usually have a low stiffness. This type of aggregate may also have a large water absorption value, which will result in a concrete with higher shrinkage

[Troxell 1996]. Aggregates with low absorption tend to reduce shrinkage and creep [Washa 1998].

A concrete using a well-graded aggregate and with large maximum aggregate size requires less cement paste, thus decreasing bleeding, creep, and shrinkage [Washa 1998; Shilstone 1999]. However, it is to be noted that although an excess of coarse aggregate could decrease drying shrinkage, it will increase the amount of micro-cracks within the paste [Aitcin 1998].

In some parts of the world, high absorption aggregates exist and use of these aggregates will increase the water content and may increase shrinkage. However, it should be noted that recently the use of high porosity lightweight aggregate (LWA) has been proposed as one method to minimize autogenous shrinkage. In these works, the LWA is saturated to various degrees before casting and the aggregate acts as a water reservoir to supply water that counteracts the self-desiccation of the paste [van Breugel and deVries 1998; Bentur et al. 1999].

2.4 Influence of Cement on Concrete Shrinkage

Tazawa and Miyazawa [1997a] found that cement composition has a greater influence on autogenous shrinkage than drying shrinkage. As compared with normal Portland cement, larger autogenous shrinkage was observed for high early strength cement at an early age, and blast furnace slag cement at later ages. Less autogenous shrinkage was observed for moderate heat cement paste, and low heat Portland cement with a high C_2S content. Autogenous shrinkage depends on the hydration of C_3A and C_4AF and it increases with an increase in these compounds.

The use of an expansive cement was found to produce a large shrinkage reduction in the cement mortar, but negligible effect in the concrete in a study by Saito [et al. 1991]. The aggregate was found to play an important role in the shrinkage of the concrete. It was found that at the beginning of shrinkage, some cracks had already existed around the coarse aggregate particles used in the expansive cement concretes. The formation of cracks was found to lead to a partial loss of restraint of coarse aggregate particles against drying shrinkage.

2.5 Influence of Water Content on Concrete Shrinkage

The water content has a large influence on the drying shrinkage of cement paste and concrete. For a given w/c ratio, concretes of a wet consistency have a higher paste content and have a greater amount of shrinkage than a stiffer mixture [Troxell 1996]. For a given proportion of cement and aggregate, concretes of a wet consistency have a higher water content and thus have a greater amount of shrinkage than a stiffer mixture.

2.6 Influence of Concrete Specimen Size and Shape on Shrinkage

The size and shape of a concrete specimen definitely influence the rate of loss or gain of moisture under a given storage condition, and this can affect the rate of volume change as well as total expansion or contraction.

Almudaiheem and Hansen [1987] observed the shrinkage of concrete specimens of various sizes over a one-year period. The shrinkage decreased with increasing specimen size. The ultimate shrinkage of paste, mortar, and concrete was found to be independent of specimen size and shape according to the dynamic shrinkage/weight loss curves. They concluded that the ultimate drying shrinkage may be estimated from the

shrinkage versus drying time curves for small laboratory specimens of $1 \times 1 \times 11$ in. ($25 \times 25 \times 279$ mm) with the same mixture proportions as the larger structural members.

2.7 Shrinkage-Reducing Admixtures

Shrinkage-reducing admixtures (SRA) can be divided into two types namely, mineral and chemical admixtures. They typically reduce the shrinkage strain in concrete specimens.

2.7.1 Mineral Admixtures

Fly Ash

Fly ash used in mortar samples reduces the drying shrinkages by about 30 to 40% when compared with pure Portland cement mortar. The mortar samples containing 40% fly ash expanded instead of shrinking. Based on the strength and shrinkage measurement results, it was concluded that the nonstandard Afsin-Elbistan fly ash (from Afsin-Elbistan Power plant, Turkey) could be utilized in cement-based materials as a mineral additive, particularly in concrete pavement, large industrial concrete floors, parking lot applications or rock bolt applications of rock engineering where shrinkage should be avoided. Based on the expansive property of this fly ash, it may also be concluded that this fly ash may be utilized as cement reducing agent or in production of a shrinkage compensating cement. However, further studies are needed to investigate long-term properties of the concrete made with this fly ash before it can be used as a mineral additive or in production of a shrinkage compensating cement [Duran et al. 2004].

Tangtermsirikul [et al. 1995] tested $0.56 \times 1.56 \times 6.24$ in. ($15 \times 40 \times 160$ mm) prism specimens to measure length change due to drying shrinkage. The drying shrinkage tests were conducted in a controlled environment of 77° F (25° C) and 60%

relative humidity. Three types of Class C fly ash and one type of Class F fly ash were used in the experiment. The class C fly ash had a smaller drying shrinkage than the ordinary cement paste mixtures. The addition of the fly ash reduced the water requirement of the mixtures, thus reducing the shrinkage. The Class C fly ash also reduced the autogenous shrinkage due to chemical expansion of the concrete mixture.

The morphology, particle size distribution and surface characteristics of fly ash used as a mineral admixture has a considerable influence on the water requirement, workability, and rate of strength development of concrete [Mehta 1986]. Particle sizes range from less than 1 micron to 100 microns in diameter, with more than 50% under 20 microns. The Class C high calcium fly ash is more chemically active than the low calcium Class F fly ash.

Silica Fume

Silica fume is an industrial by-product with a particle size about 100 times finer than Portland cement [Mehta 1986]. Tazawa and Yonekura [1991] examined shrinkage and creep of mortar and concrete. Drying shrinkage of concrete was tested using 3.9 × 3.9 × 15.6-in. (100 × 100 × 400-mm) prism specimens. The specimens were in a controlled environment of 68° F (20° C), 50% relative humidity. The drying shrinkage of the concrete mixtures with the silica fume was lower than that of the same type mixtures without the silica fume.

Haque [1996] measured the drying shrinkage on 3.35 × 3.35 × 11.22-in. (85 × 85 × 285-mm) prism specimens. The addition of both 5 and 10% silica fume (by weight) in concrete mixtures resulted in a substantial reduction of drying shrinkage.

A dozen high strength concrete prisms of size $3 \times 3 \times 11.25$ in. ($76 \times 76 \times 286$ mm) were examined for assessing the drying shrinkage strain that the silica fume concrete experienced [Alsayed 1998]. These prisms were monitored over a three-year time period. All of the mixtures were identical except for the admixture content. Three mixtures were compared; the first had a superplasticizer as the admixture, the second had a superplasticizer and 10% silica fume by weight, and the third mixture had a regular plasticizer and 10% silica fume by weight. The specimens were submerged in water for seven days. Six specimens were then put in a laboratory-controlled environment, while the other six specimens were exposed to field conditions. By adding 10% silica fume, the shrinkage was reduced over time. The mixture with the superplasticizer and silica fume showed a reduction in shrinkage. Specimens with the normal plasticizer showed a larger drying shrinkage than those with the superplasticizer. The combined superplasticizer and silica fume mixtures showed a reduced drying shrinkage rate in the first month. The addition of the silica fume helped to reduce the sensitivity of the concrete to curing conditions. After the first 90 days of exposure, 75% to 80% of the drying shrinkage occurred depending on the curing conditions

Silane

Silane is an aqueous admixture, called aqueous amino vinyl silane. Silane treatment of silica fume and/or carbon fiber is highly effective for decreasing the drying shrinkage of cement paste. The increase of the hydrophilic character of fibers and particles after the treatment and the formation of chemical bonds between fibers/particles and cement are believed to be the main reasons for the observed decrease of the drying shrinkage. By adding silane-treated carbon fibers and replacing as-received silica fume

by silane-treated silica fume, the shrinkage at 28 days is decreased by 32% [Yunsheng Xu 2001].

Onada Expan

ONADA EXPAN™ is an expansive additive currently used in Japan for concrete. This admixture expands when it is hydrated, without strength loss. It uses calcium silicate and glass interstitial substitute rather than CaO. This material is stable but it must be moist cured and requires longer mixing [Tazawa and Miyazawa 1995].

2.7.2 Chemical Admixtures

The use of chemical shrinkage-reducing admixture (SRA) in high-performance concrete was found to significantly reduce drying shrinkage and restrained shrinkage cracking in laboratory ring specimens.

The following effects were observed when an organic SRA (shrinkage-reducing admixture) was added [Bentz et al. 2001]:

1. Comparing to distilled water, there is a significant reduction in the surface tension of a solution containing the SRA.
2. The drying rate of the cement pastes is reduced.
3. A significant decrease in autogenous shrinkage in low w/c ratio mortars cured under sealed conditions.

There was no significant change in 28-day compressive strength of mortar specimens with the addition of an SRA, for w/c = 0.35 (8% silica fume) and cured under sealed conditions at 86° F (30° C).

A shrinkage reducing admixture (SRA) has been suggested for use in reducing the rate of shrinkage in concrete at early-ages when concrete is most vulnerable, even though reductions in overall shrinkage have also been observed [Weiss 1999].

Tests were conducted on concrete with SRA added according to ASTM C 157-93 [Balogh 1996]. A larger percentage of decrease in shrinkage was noted in concretes with a lower w/c ratio. For concretes with a w/c ratio of less than 0.60, the SRA reduced the 28-day shrinkage by 80% or more, and the 56-day shrinkage was reduced by about 70%. The applied admixture dosage rate was 1.5% by weight of cement. For concretes with a w/c ratio of 0.68, the SRA reduced the 28- and 56-day shrinkage by 37% and 36%, respectively. The SRA was tested with different cements, one with fly ash, one with fly ash and slag cement. The long-term shrinkage reductions without moist-curing the concretes ranged from 25% to 38%, depending on the composition of the concrete mixtures.

Concrete specimens were cured for 1 to 14 days and tests were conducted to evaluate the drying shrinkage of concrete [Berke et al. 1997]. The specimens were stored at 37.4° F (3° C) and 50% relative humidity. The concrete specimens having 2% SRA by weight of cement showed less shrinkage at early ages after controlled drying. For the same cement content, the drying shrinkage of the concrete increased as the w/c ratio increased for all the mixtures tested. The drying shrinkage was greatly reduced with the addition of the SRA. Drying shrinkage was significantly reduced with increased curing time. Longer curing periods reduced the sensitivity to changes in the w/c ratio with respect to shrinkage reduction.

The shrinkage strain of concretes using a silica fume slurry, a superplasticizer and an SRA was studied [Folliard 1997]. The fresh concrete had a slump of 6 to 8 in. (150 to 200 mm). Concrete prisms of $3 \times 3 \times 11.25$ in. ($75 \times 75 \times 285$ mm) were cast to measure free drying shrinkage. The use of a SRA reduced the drying shrinkage of the high strength concretes both with and without silica fume. The ring test was used to determine the restrained shrinkage. The restrained shrinkage was significantly reduced when the SRA was used. The shrinkage reduction was more significant with the silica fume mixtures.

The ring test was used to determine the restrained shrinkage of concretes containing different SRAs by Shah, Karaguler, and Sarigaphuti [1992]. The specimens were placed in a controlled environment of 68° F (20° C) and 40% relative humidity. Three different SRAs were used. Tests were also conducted on $4 \times 4 \times 11.25$-in. ($100 \times 100 \times 285$-mm) prism specimens. The SRAs were found to possibly decrease the compressive strength of the concrete. The addition of the SRA did reduce the amount of shrinkage. As the amount of SRA added increases, the shrinkage further decreases. The addition of SRA reduced the restrained shrinkage crack width. Free shrinkage was also measured on $3.9 \times 3.9 \times 15.6$-in. ($100 \times 100 \times 400$-mm) prism specimens. The addition of SRA greatly improved the reduction of free shrinkage. An equal amount of water was removed when the SRA was added. The addition of the SRA caused a delay in the restrained shrinkage cracking.

CHAPTER 3
MATERIALS

3.1 Introduction

This chapter describes the mix proportions and the mix ingredients of the concrete mixtures evaluated in this study. The method of preparation of the concrete mixtures, fabrication of the test specimens and testing procedures used in this study are also presented.

3.2 Concrete Mixtures Evaluated

Concrete mixtures were prepared in the laboratory and tested for their resistance to shrinkage cracking to evaluate (1) the effectiveness of the shrinkage test apparatuses used, (2) the shrinkage characteristics of typical concretes used in bridge deck applications in Florida, and (3) the effects of adding a shrinkage-reducing admixture. A typical mix design for a Florida Class IV concrete with a total cementitious materials content of 700 lb per cubic yard (lb/yd^3), or 415.7 kg per cubic meter (kg/m^3), of concrete was selected for use. Various percentages of fly ash and ground blast-furnace slag were incorporated into this basic mix design to form six different mix designs to be evaluated in the laboratory testing program. For each of the concrete mixtures evaluated, a pair of concrete mixes was prepared at the same time – one with the addition of a shrinkage-reducing admixture (SRA) and one without. Since various different test apparatuses were used during different stages of this study, several replicate batches of the same mixes were used, resulting in a total of 15 pairs of concrete mixes tested in this study.

Tables 3-1 through 3-15 show the mix proportions for the 15 pairs of concrete mixtures evaluated in this study. The concrete mixes were numbered according to the order by which they were prepared and tested in this study. Mixes 1 and 13 had a cement content of 350 lb/ yd^3 (207.8 kg/m^3) and a slag content of 350 lb/yd^3 (207.8 kg/m^3) of concrete. Mixes 2 and 3 had a cement content of 210 lb/ yd^3 (124.7 kg/m^3) and a slag content of 490 lb/yd^3 (291 kg/m^3). Mixes 4, 7, 8 and 11 had a cement content of 560 lb/yd^3 (332.5 kg/m^3) and a fly ash content of 140 lb/yd^3 (83.1 kg/m^3). Mixes 5, 9, 10 and 14 had a cement content of 455 lb/yd^3 (270.2 kg/m^3) and a fly ash content of 245 lb/yd^3 (145.5 kg/m^3). Mixes 6 and 12 had a cement content of 210 lb/yd^3 (124.7 kg/ m^3), a fly ash content of 140 lb/yd^3 (83.1 kg/m^3) and a slag content of 350 lb/yd^3 (207.8 kg/ m^3). Mix 15 had a cement content of 700 lb/yd^3 (415.7 kg/ m^3), and no mineral admixture. The slump of the fresh concrete was targeted to be 8 ± 1.5 inches (203 ± 38 mm).

Table 3-1. Mix Proportions for Mix 1

Mix – 1				
Ingredients	**Weight (pounds per cubic yard, lb/yd^3)**			
	Standard		**SRA**	
	Design Batch	**Actual Batch**	**Design Batch**	**Actual Batch**
Cement	350	350	350	350
Fly ash	-	-	-	-
Slag	350	350	350	350
Water	287	234	274	219
F.A.	1257	1252	1257	1252
C.A.	1513	1572	1513	1572
Air Entrainer	0.0625	0.0625	0.0625	0.0625
Admixture (WRDA 64)	0.875	0.875	0.875	0.875
Admixture (Adva 120)	1.313	1.313	1.313	1.313
Admixture (SRA)	-	-	12	12
Slump (in inches)	6.25	6.25	7.25	7.25
Air (%)	3.75	3.75	3	3
Workability	Good	Good	Good	Good
W/C Ratio	0.41	0.33	0.41	0.33
Unit Weight (pcf)	139.1	139.2	139.1	139.1

Table 3-2. Mix Proportions for Mix 2

Mix – 2				
Ingredients	**Weight (lb/yd^3)**			
	Standard		**SRA**	
	Design Batch	**Actual Batch**	**Design Batch**	**Actual Batch**
Cement	210	210	210	210
Fly ash	-	-	-	-
Slag	490	490	490	490
Water	224	176	211	165
F.A.	1336	1331	1336	1331
C.A.	1583	1633	1583	1633
Air Entrainer	0.0625	0.0625	0.0625	0.0625
Admixture (WRDA 64)	0.875	0.875	0.875	0.875
Admixture (Adva 120)	2.063	2.063	2.063	2.063
Admixture (SRA)			12	12
Slump (in inches)	8	8	9.25	9.25
Air (%)	2.75	2.75	1.75	1.75
Workability	Sticky	Sticky	Sticky	Sticky
W/C Ratio	0.32	0.25	0.32	0.25
Unit Weight (pcf)	142.3	142.2	142.3	142.3

Table 3-3. Mix Proportions for Mix 3

Mix – 3				
Ingredients	**Weight (lb/yd^3)**			
	Standard		**SRA**	
	Design Batch	**Actual Batch**	**Design Batch**	**Actual Batch**
Cement	210	210	210	210
Fly ash	-	-	-	-
Slag	490	490	490	490
Water	287	213	274	200
F.A.	1253	1248	1253	1253
C.A.	1507	1586	1507	1507
Air Entrainer	0.0625	0.0625	0.0625	0.0625
Admixture (WRDA 64)	0.875	0.875	0.875	0.875
Admixture (Adva 120)	1.313	1.313	1.313	1.313
Admixture (SRA)			12	12
Slump (in inches)	9	9	8.5	8.5
Air (%)	3.5	3.5	2.5	2.5
Workability	Good	Good	Good	Good
W/C Ratio	0.41	0.30	0.39	0.29
Unit Weight (pcf)	138.8	138.8	138.3	135.5

Table 3-4. Mix Proportions for Mix 4

Mix – 4				
Ingredients	**Weight (lb/yd^3)**			
	Standard		**SRA**	
	Design Batch	**Actual Batch**	**Design Batch**	**Actual Batch**
Cement	560	560	560	560
Fly ash	140	140	140	140
Slag	-	-	-	-
Water	287	244	275	232
F.A.	1250	1246	1250	1246
C.A.	1486	1533	1486	1533
Air Entrainer	0.0625	0.0625	0.0625	0.0625
Admixture (WRDA 64)	1.75	1.75	1.75	1.75
Admixture (Adva 120)	2.188	2.188	2.188	2.188
Admixture (SRA)			12	12
Slump (in inches)	7.5	7.5	9	9
Air (%)	3.25	3.25	2.5	2.5
Workability	Good	Good	Good	Good
W/C Ratio	0.41	0.35	0.39	0.33
Unit Weight (pcf)	137.9	137.9	137.4	137.4

Table 3-5. Mix Proportions for Mix 5

Mix – 5				
Ingredients	**Weight (lb/yd^3)**			
	Standard		**SRA**	
	Design Batch	**Actual Batch**	**Design Batch**	**Actual Batch**
Cement	455	455	455	455
Fly ash	245	245	245	245
Slag	-	-	-	-
Water	287	228	275	216
F.A.	1217	1213	1217	1213
C.A.	1469	1533	1469	1533
Air Entrainer	0.0625	0.0625	0.0625	0.0625
Admixture (WRDA 64)	1.75	1.75	1.75	1.75
Admixture (Adva 120)	2.188	2.188	2.188	2.188
Admixture (SRA)			12	12
Slump (in inches)	9.25	9.25	8.75	8.75
Air (%)	3.25	3.25	3.25	3.25
Workability	Good	Good	Good	Good
W/C Ratio	0.41	0.33	0.41	0.33
Unit Weight (pcf)	136.0	136.1	136.0	136.1

Table 3-6. Mix Proportions for Mix 6

Mix – 6				
Ingredients	**Weight (lb/yd^3)**			
	Standard		**SRA**	
	Design Batch	**Actual Batch**	**Design Batch**	**Actual Batch**
Cement	210	210	210	210
Fly ash	140	140	140	140
Slag	350	350	350	350
Water	289	246	275	232
F.A.	1240	1236	1240	1236
C.A.	1475	1522	1475	1522
Air Entrainer	0.0625	0.0625	0.0625	0.0625
Admixture (WRDA 64)	1.75	1.75	1.75	1.75
Admixture (Adva 120)	2.188	2.188	2.188	2.188
Admixture (SRA)			12	12
Slump (in inches)	9.25	9.25	9	9
Air (%)	1.75	1.75	2.75	2.75
Workability	Good	Good	Good	Good
W/C Ratio	0.41	0.35	0.41	0.35
Unit Weight (pcf)	137.2	137.2	137.1	137.1

Table 3-7. Mix Proportions for Mix 7

Mix – 7				
Ingredients	**Weight (lb/yd^3)**			
	Standard		**SRA**	
	Design Batch	**Actual Batch**	**Design Batch**	**Actual Batch**
Cement	560	560	560	560
Fly ash	140	140	140	140
Slag	-	-	-	-
Water	254	235	242	223
F.A	1334	1330	1257	1330
C.A	1561	1554	1513	1554
Air Entrainer	0.0625	0.0625	0.0625	0.0625
Admixture (WRDA 64)	1.31	1.31	0.88	0.88
Admixture (Adva 120)	1.31	1.31	1.31	1.31
Admixture (SRA)			12	12
Slump (in inches)	8	8	9	9
Air (%)	2.75	2.75	3.25	3.25
Workability	Good	Good	Good	Good
W/C Ratio	0.36	0.34	0.36	0.34
Unit Weight (pcf)	142.6	141.4	137.9	141.4

Table 3-8. Mix Proportions for Mix 8

Mix – 8				
Ingredients	**Weight (lb/yd^3)**			
	Standard		**SRA**	
	Design Batch	**Actual Batch**	**Design Batch**	**Actual Batch**
Cement	560	560	560	560
Fly ash	140	140	140	140
Slag	-	-	-	-
Water	224	264	212	252
F.A	1453	1449	1455	1451
C.A	1453	1417	1455	1419
Air Entrainer	0.0625	0.0625	0.0625	0.0625
Admixture (WRDA 64)	0.88	0.88	0.88	0.88
Admixture (Adva 120)	2.06	2.06	2.06	2.06
Admixture (SRA)			12	12
Slump (in inches)	2.5	2.5	2.25	2.25
Air (%)	4.5	4.5	3.75	3.75
Workability	Stiff	Stiff	Stiff	Stiff
W/C Ratio	0.32	0.38	0.32	0.38
Unit Weight (pcf)	141.9	141.9	142.0	142.0

Table 3-9. Mix Proportions for Mix 9

Mix – 9				
Ingredients	**Weight (lb/yd^3)**			
	Standard		**SRA**	
	Design Batch	**Actual Batch**	**Design Batch**	**Actual Batch**
Cement	455	455	455	455
Fly ash	245	245	245	245
Slag	-	-	-	-
Water	287	324	275	312
F.A.	1351	1347	1351	1347
C.A.	1351	1318	1351	1318
Air Entrainer	0.0625	0.0625	0.0625	0.0625
Admixture (WRDA 64)	0.88	0.88	0.88	0.88
Admixture (Adva 120)	1.31	1.31	1.31	1.31
Admixture (SRA)			12	12
Slump (in inches)	3.25	3.25	4.5	4.5
Air (%)	2.75	2.75	2.5	2.5
Workability	O.K	O.K	O.K	O.K
W/C Ratio	0.41	0.46	0.41	0.46
Unit Weight (pcf)	136.6	136.6	136.6	136.6

Table 3-10. Mix Proportions for Mix 10

Mix – 10				
Ingredients	**Weight (lb/yd^3)**			
	Standard		**SRA**	
	Design Batch	**Actual Batch**	**Design Batch**	**Actual Batch**
Cement	455	455	455	455
Fly ash	245	245	245	245
Slag	-	-	-	-
Water	252	289	240	278
F.A	1265	1261	1265	1261
C.A	1513	1480	1513	1480
Air Entrainer	0.0625	0.0625	0.0625	0.0625
Admixture (WRDA 64)	0.88	0.88	0.88	0.88
Admixture (Adva 120)	1.31	1.31	1.31	1.31
Admixture (SRA)			12	12
Slump (in inches)	3.25	3.25	4.5	4.5
Air (%)	2.75	2.75	2.5	2.5
Workability	O.K	O.K	O.K	O.K
W/C Ratio	0.36	0.41	0.36	0.41
Unit Weight (pcf)	138.2	138.2	138.1	138.2

Table 3-11. Mix Proportions for Mix 11

Mix – 11				
Ingredients	**Weight (lb/yd^3)**			
	Standard		**SRA**	
	Design Batch	**Actual Batch**	**Design Batch**	**Actual Batch**
Cement	560	560	560	560
Fly ash	140	140	140	140
Slag				
Water	287	321	275	308
F.A.	1250	1246	1250	1246
C.A.	1486	1456	1486	1456
Air Entrainer	0.0625	0.0625	0.0625	0.0625
Admixture (WRDA 64)	1.75	1.75	1.75	1.75
Admixture (Adva 120)	2.188	2.188	2.188	2.188
Admixture (SRA)			12	12
Slump (in inches)	8.5	8.5	9	9
Air (%)	3	3	2.75	2.75
Workability	Good	Good	Good	Good
W/C Ratio	0.41	0.46	0.41	0.46
Unit Weight (pcf)	137.9	137.9	137.9	137.9

Table 3-12. Mix Proportions for Mix 12

Mix – 12				
Ingredients	**Weight (lb/yd^3))**			
	Standard		**SRA**	
	Design Batch	**Actual Batch**	**Design Batch**	**Actual Batch**
Cement	210	210	210	210
Fly ash	140	140	140	140
Slag	350	350	350	350
Water	224	194	212	183
F.A.	1516	1511	1516	1511
C.A.	1376	1410	1376	1410
Air Entrainer	0.0625	0.0625	0.0625	0.0625
Admixture (WRDA 64)	1.75	1.75	1.75	1.75
Admixture (Adva 120)	2.188	2.188	2.188	2.188
Admixture (SRA)			12	12
Slump (in inches)	3	3	6.5	6.5
Air (%)	3.25	3.25	3	3
Workability	Stiff	Stiff	Sticky	Sticky
W/C Ratio	0.32	0.28	0.32	0.28
Unit Weight (pcf)	141.3	141.3	141.3	141.3

Table 3-13. Mix Proportions for Mix 13

Mix – 13				
Ingredients	**Weight (lb/yd^3)**			
	Standard		**SRA**	
	Design Batch	**Actual Batch**	**Design Batch**	**Actual Batch**
Cement	350	350	350	350
Fly ash				
Slag	350	350	350	350
Water	224	285	212	273
F.A.	1547	1543	1547	1543
C.A.	1405	1348	1405	1348
Air Entrainer	0.0625	0.0625	0.0625	0.0625
Admixture (WRDA 64)	1.75	1.75	1.75	1.75
Admixture (Adva 120)	2.188	2.188	2.188	2.188
Admixture (SRA)			12	12
Slump (in inches)	1.75	1.75	7 (Sheared off)	7 (Sheared off)
Air (%)	3.75	3.75	3.25	3.25
Workability	Stiff	Stiff	Stiff	Stiff
W/C Ratio	0.32	0.41	0.32	0.41
Unit Weight (pcf)	143.6	143.5	143.6	143.6

Table 3-14. Mix Proportions for Mix 14

Mix – 14				
Ingredients	**Weight (lb/yd^3)**			
	Standard		**SRA**	
	Design Batch	**Actual Batch**	**Design Batch**	**Actual Batch**
Cement	455	455	455	455
Fly ash	245	245	245	245
Slag				
Water	224	209	212	197
F.A.	1502	1499	1502	1499
C.A.	1364	1383	1364	1383
Air Entrainer	0.0625	0.0625	0.0625	0.0625
Admixture (WRDA 64)	1.75	1.75	1.75	1.75
Admixture (Adva 120)	2.188	2.188	2.188	2.188
Admixture (SRA)			12	12
Slump (in inches)	Sheared off	Sheared off	Sheared off	Sheared off
Air (%)	3.5	3.5	4.5	4.5
Workability	Stiff	Stiff	Stiff	Stiff
W/C Ratio	0.32	0.30	0.32	0.30
Unit Weight (pcf)	140.4	140.4	140.4	140.4

Table 3-15. Mix Proportions for Mix 15

Mix – 15				
Ingredients	**Weight (lb/yd^3)**			
	Standard		**SRA**	
	Design Batch	**Actual Batch**	**Design Batch**	**Actual Batch**
Cement	700	700	700	700
Fly ash				
Slag				
Water	224	202	212	190
F.A.	1557	1553	1557	1553
C.A.	1415	1441	1415	1441
Air Entrainer	0.0625	0.0625	0.0625	0.0625
Admixture (WRDA 64)	0.875	0.875	0.875	0.875
Admixture (Adva 120)	1.313	1.313	1.313	1.313
Admixture (SRA)			12	12
Slump (in inches)	0.25	0.25	0.25	0.25
Air (%)	4.5	4.5	4	4
Workability	Stiff	Stiff	Stiff	Stiff
W/C Ratio	0.32	0.29	0.32	0.29
Unit Weight (pcf)	144.3	144.3	144.3	144.3

3.3 Mix Constituents

The mix constituents that are used in producing the concrete mixture are described in this section.

3.3.1 Water

Water used was obtained from the local city water supply system.

3.3.2 Fine Aggregate

The silica sand mined from Goldhead, Florida, was used as fine aggregate for the concrete mixtures. The oven-dried silica sand was used for producing the concrete for this study. The gradation plot of the Goldhead silica sand is displayed in the Figure 3-1. The physical properties of fine aggregate are given Table 3-16.

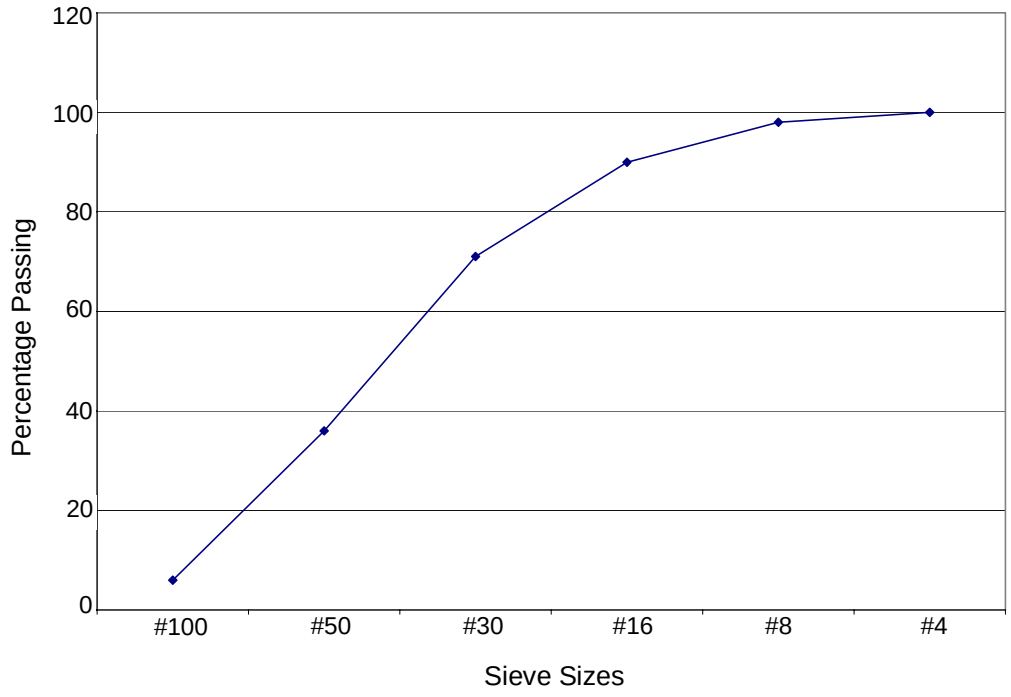

Figure 3-1. Gradation chart for the fine aggregate (Goldhead silica sand)

Table 3-16. Physical Properties of the Fine Aggregate

Physical Property	Value
Bulk specific gravity	2.63
Bulk specific gravity SSD	2.68
Apparent specific gravity	2.64
Absorption	0.73%

3.3.3 Coarse Aggregate

The coarse aggregate used was a #89 limestone obtained from Mine 08-0057. The coarse aggregate was used as-is at its natural moisture condition. The gradation of the coarse aggregates is shown in Figure 3-2. Its physical properties are given in Table 3-17.

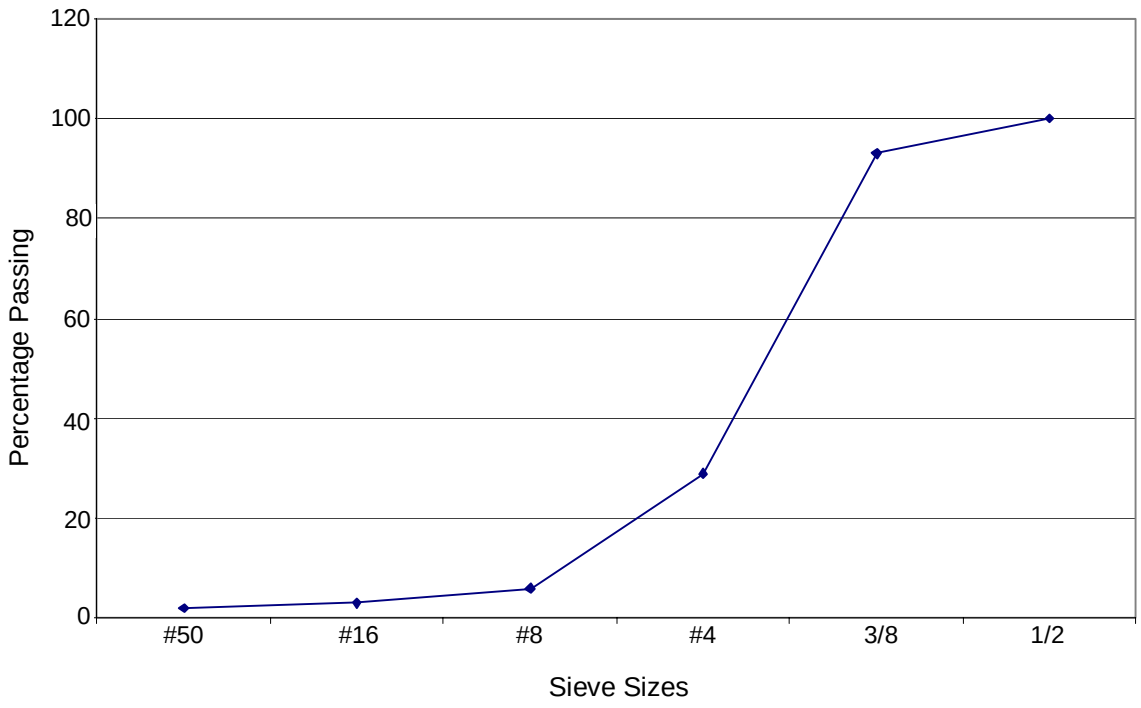

Figure 3-2. Gradation chart for the coarse aggregate (#89 limestone)

Table 3-17. Physical Properties of the Coarse Aggregate

Physical Property	Value
Bulk Specific Gravity	2.23
Bulk Specific Gravity SSD	2.40
Apparent Specific Gravity	2.56
Absorption	4.55%

3.3.4 Cement

Cemex Cement Company provided the Type I Portland cement for use in the concrete mixtures that were used for this study. The physical characteristics and the chemical composition of the cement are shown in Tables 3-18 and 3-19, respectively.

Table 3-18. Physical Properties of the Type I Cement Used

Tests	Specification	Cement	Spec. Limits
Autoclave Expansion	ASTM C151	0.01%	<= 0.80%
Fineness by Apparatus	ASTM C204	402 m^2 /kg	>= 260.0 & <= 420.0
Loss on Ignition	ASTM C114	1.50%	<= 3.0%
Time of setting (Initial)	ASTM C226	125 min.	>= 60
Time of setting (Final)	ASTM C226	205 min.	<= 600
3-day Compressive Strength Test	ASTM C109	2400 psi	>= 1740
7-day Compressive Strength Test	ASTM C109	2930 psi	>= 2760
Cement acid insoluble test	ASTM C114	0.48% Insoluble	<= 0.75

Table 3-19. Chemical Composition of the Type I Cement Used

Constituents (%)	%
SiO_2	20.3
Al_2O_3	4.8
CaO	63.9
SO_3	3.1
Na_2O-K_2O	0.51
MgO	2
Fe_2O_3	3.3
C_3A	7
C_3S	59
C_2S	13.8
C_4AF+C_2F	15.8

3.3.5 Fly Ash

Class F fly ash, which was derived from the combustion of ground or powdered coal and met the requirements of ASTM C 618, was used for this project. Boral Company provided the fly ash for this project. The chemical composition of the fly ash is shown in Table 3-20. Its physical properties are shown in Table 3-21.

Table 3-20. Chemical Composition of the Class F Fly Ash Used

Chemical	Value
Sulfur Trioxide	0.30%
Oxides of Si, Fe, Al	12.1094%

Table 3-21. Physical Properties of the Class F Fly Ash Used

Property	Fly ash	Limits
% Moisture	0.10%	<= 3.0
Loss on Ignition	4.30%	<= 6.0

3.3.6 Ground Blast-Furnace Slag

The ground blast-furnace slag used in this project met the requirements of ASTM C 989. The slag used in this project was provided by Boral Company. The chemical composition of the slag used is shown in Table 3-22.

Table 3-22. Chemical Composition of the Slag Used

Chemical	Value
Sulfur Trioxide	1.70%
Total Alkali as Na2O	0.7

3.3.7 Air-Entraining Admixture

The air-entraining admixture used in this study was Darex AEA, which was an aqueous solution of a complex mixture of organic acid salts. It is specially formulated for

use as an air-entraining admixture for concrete. It was supplied as ready-to-use admixture and did not require pre-mixing with water. The air-entraining admixture was used to improve the workability, and to reduce bleeding and segregation of the fresh concrete. It also imparts high durability to the concrete mixture in which it is used. In this project, 0.1 lb of Darex was used for one cubic yard (0.059 kg/m^3) of concrete.

3.3.8 Water-Reducing Admixtures

Water-reducing admixtures were used in the concrete to reduce the demand of water in the mix. Two types of water-reducing admixtures were used in the concrete mixtures for this project. They were WRDA 64 and Adva Flow, which are described in the following sections.

WRDA 64

WRDA 64 is a polymer-based aqueous solution of complex organic compounds. It is a ready-to-use low viscosity liquid which contains no calcium chloride. It can reduce the water demand of concrete by typically 8 to 10%. Setting times and water reduction are more consistent due to the presence of polymer components. It also performs especially well in concretes containing fly ash and other pozzolans. In this project, 1.75 lb of WRDA 64 was used per cubic yard (1.04 kg/m^3) of concrete.

Adva Flow (Super plasticizer)

Adva Flow Superplasticizer is a high range water-reducing admixture and does not have any chloride added. In this project, 2.2 lb of Adva Flow was used per cubic yard (1.31 kg/m^3) of concrete.

3.3.9 Shrinkage-Reducing Admixture

The shrinkage-reducing admixture (SRA) is a liquid admixture specially formulated for use in indoor slab-on-grade concrete construction. The SRA has no expansive agent, but acts chemically to dramatically reduce the primary internal forces that cause shrinkage and curling. The SRA at a dosage of 1.5 gal/yd^3 7.43 liter/m^3) has been shown to reduce drying shrinkage, as measured by ASTM C 157, by as much as 80% at 28 days, and up to 50% at one year or beyond. It is a clear liquid admixture. In this project, 12 lb of the SRA was used per cubic yard (7.13 kg/m^3) of the concrete mixtures that required the shrinkage-reducing admixture.

3.4 Preparation of Concrete Mixtures

3.4.1 Mixing of Concrete

Fifteen pairs of concrete mixtures were produced and tested in this project. The concrete batches were mixed in two rotary drum mixers of capacities of 3.5 cubic feet (ft^3), or 0.098 cubic meters (m^3), for small mix and 6 ft^3 (0.168 m^3) according to the requirement. The photo of the 6 ft^3 (0.168 m^3) mixer is shown in Figure 3-3. The surface of interior portion of the drum was rinsed with a butter mix (i.e., the original mix in small quantity) before mixing to avoid absorption and to ensure the same mixing conditions for all mixes.

The following procedures of mixing of concrete were followed in the preparation of each concrete mixture:

1. Place the coarse and fine aggregates in the mixer, and mix for about two minutes with one half of mixing water added to ensure uniform dispersion of the aggregates.

2. Add the cement, fly ash, slag, air entraining admixture, water-reducing admixtures and the remaining water into the mixer, and continue the mixing for an additional three minutes. Stop the mixer as needed to break loose the materials sticking to the mixer to facilitate thorough mixing. It is then followed by a 3-minute rest period.
3. Continue the mixing for an additional two minutes after the rest period.
4. After the mix appeared uniformly mixed, run the slump test on the fresh concrete. Add additional water-reducing admixtures if the slump is too low. While adding water-reducing admixtures, take care not to exceed the allowable dosages. Otherwise, the mixtures may become segregated and start bleeding.

Figure 3-3. Concrete mixer used

3.4.2 Preparation of Concrete Specimens for Mechanical Tests

The following steps were followed in making the concrete specimens for evaluation of mechanical properties:

1. After mixing is complete, fill each of the 4 × 8-in. (101.6 × 203.2-mm) cylindrical molds with the fresh concrete to one half of its height, and place the mold on a vibrating table for 30 seconds of vibration.
2. After that, fill the cylinder mold to overflowing and then place it on the vibrating table for an additional 30 seconds.
3. Finish the surface of the concrete specimen with a hand trowel, and cover the cylinder with a plastic sheet to prevent evaporation of water.
4. Demold the concrete specimens after 24 hours of curing, and put them in a standard moist room for proper curing until the specific tests (compressive strength, modulus of elasticity and splitting tensile strength tests) are to be performed at the specified curing times (such as 3, 7, 14 and 28 days).

3.4.3 Preparation of Concrete Specimens for ASTM C157 Shrinkage Test

A portion of the fresh concrete was used to produce the 3 × 3 × 11.25-in. (76 × 76 × 286-mm) square prism specimens for the ASTM C157 Shrinkage Test. The procedures for the making of these specimens are described in Section 4.3.4 of this report.

3.4.4 Preparation of Concrete Specimens for Long Specimen Tests

The rest of the fresh concrete from the mixer was used to make the long specimens for the constrained shrinkage test and the free shrinkage test. The procedures for making the long specimens for free shrinkage test are described in Section 4.3.5, while those for the constrained shrinkage test are described in Chapter 5 of this report.

CHAPTER 4
LABORATORY TESTING PROGRAM

4.1 Introduction

This chapter describes the laboratory testing program on the concretes to be evaluated for their resistance to shrinkage cracking in this study. It includes the description of the tests on fresh and hardened concretes and the associated instrumentation.

4.2 Tests on Fresh Concrete

The following tests were performed on the fresh concrete:

1. Slump test (ASTM C143);
2. Unit weight test (ASTM C138);
3. Air content by volumetric method (ASTM C173); and
4. Temperature measurement (ASTM C1064).

4.3 Tests on Hardened Concrete

The following tests were run on the hardened concrete:

1. Compressive strength (ASTM C39) tests using 4 × 8-in. (101.6 × 203.2-mm) specimens at 3, 7, 14 and 28 days (3 replicates per condition).
2. Elastic modulus (ASTM C469) tests using 4 × 8-in. (101.6 × 203.2-mm) specimens at 3, 7, 14 and 28 days (2 replicates per condition).
3. Splitting tensile strength test (ASTM C496) using 4 × 8-in. (101.6 × 203.2-mm) specimens at 3, 7 and 14 days (3 replicates).

4. Free shrinkage measurement (ASTM C157) using 3 × 3 × 11.25-in. (76 × 76 × 286-mm) specimens (3 replicates).
5. Free shrinkage measurement using the long specimen apparatus without the constraint, monitored continuously for a minimum of 14 days (2 replicates).
6. Constrained shrinkage test using the long specimen apparatus, monitored continuously for a minimum of 14 days (2 replicates).

The equipment, instrumentation and procedures for these tests on hardened concrete are described in the following section.

4.3.1 Compressive Strength Test

The compressive strength test was run in accordance with ASTM Test Method C39. Figure 4-1 shows the set-up for the compressive strength test. The testing machine used was a servo-controlled compression testing machine with a capacity of 500,000 lb (227,000 kg). All the tests were run with a rate of loading ranging from 400 to 500 lb (1,780 to 2,225 N) per second.

Figure 4-1. Set-up for compressive strength test

Three 4 × 8-in. (101.6 × 203.2-mm) cylindrical specimens per batch per curing condition were tested for the analysis. Before testing, the cylinders were ground by using a grinding stone so that two end surfaces are made even to support the applied load uniformly.

Compressive strengths were determined at moist-curing times of 3, 7, 14 and 28 days. The compressive strength of the specimen was calculated using the following equation (Eq.):

$$\text{Compressive Strength, } f_c = P/A \qquad \text{(Eq. 4.1)}$$

where

P = ultimate load attained during the test in pounds (lb); and

A = loading area in square inches (in^2).

Of the three replicate specimens per condition used, one specimen was first tested to determine its ultimate compressive strength, so that the modulus of elasticity test could be run at 40% of the ultimate strength of the concrete. The modulus of elasticity test was then run on the other two replicate specimens before they were tested for their compressive strength.

4.3.2 Modulus of Elasticity Test

The modulus of elasticity test was run in accordance with ASTM Test Method C469. Cylindrical specimens of size 4 × 8 in. (101.6 × 203.2-mm), which were also used in the compressive strength test, were used for this test. Similar to the compressive strength test, the modulus of elasticity test was performed at curing times of 3, 7, 14 and 28 days. The test set-up is shown in Figure 4-2. The test set-up consisted of a compression testing machine, a digital key panel (for controlling the testing machine) and a laptop computer (for downloading the data from the test.) The rate of loading adopted for this

Figure 4-2. Set-up for modulus of elasticity test

test was the same as that for the compressive strength test, and ranged from 400 to 500 lb (1,780 to 2,225 N) per second. The output from the load cell (in the testing machine) and the output from the LVDT (which was connected to the specimen to measure its vertical deformation) were connected to the laptop computer via a USB connection. The software "Virtual BenchLink Data Logger" was used to capture the output data from the LVDT and load cell and convert them into a readable CSV (Comma Separated Variable) Microsoft Excel format. A close-up view of the LVDT used is shown in Figure 4-3.

Figure 4-3. Close-up view of elastic modulus test wet-up with a LVDT for strain measurement

Before the test of Modulus of Elasticity is run, one of the three cylinders was tested for ultimate compressive strength until breaking. On the remaining two cylinders, the Modulus of Elasticity Test was run at a strength level of 40% of the ultimate compressive strength of the concrete. After that, those two specimens from the Modulus of Elasticity test are tested for ultimate compressive strengths. The data from the first load cycle were disregarded. The data values from the last two cycles of loading were recorded and converted into CSV (comma separated variable) format which is readable by the Excel spreadsheet, the modulus of elasticity was determined using regression analysis embedded in the Excel spreadsheet charts.

4.3.3 Splitting Tensile Strength Test

The splitting tensile strength test was run in accordance with the procedures laid out in ASTM C496 method. Three 4 × 8-in. (101.6 × 203.2-mm) cylindrical specimens per condition were used for this test. The test set-up is shown in Figure 4-4. The splitting tensile strength of the specimen was calculated using the expression below:

$$\text{Splitting tensile strength, } f_t = 2P/\pi ld \qquad \text{(Eq. 4.2)}$$

where

P = maximum applied load;

l = length of the cylindrical specimen; and

d = diameter of the cylindrical specimen.

Figure 4-4. Set-up for splitting tensile strength test

4.3.4 Free Shrinkage Measurement (ASTM C157) Using LVDTs Specimen Molds

Square prism specimens with dimensions of 3 × 3 × 11.25 in. (76 × 76 × 286 mm) were used in the free shrinkage test in accordance with ASTM C157 Method. Figure 4-5 shows a mold used to cast the shrinkage test specimens. Steel end plates with a hole at their centers were used to hold the contact points in place at each end of the specimen.

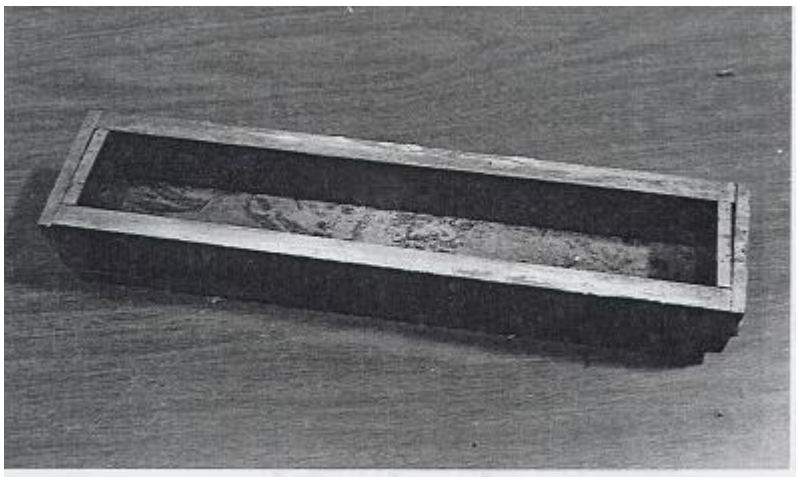

Figure 4-5. Mold for 3 × 3 × 11.25-in. (76 × 76 × 286-mm) shrinkage test specimen

Test Set-Up

The setup for the ASTM C157 free shrinkage test consisted of a DC-powered LVDT connected to a shrinkage test frame that held the specimen. The output from the LVDT was connected to a Data Acquisition System (DAS). A laptop computer was used to download the data from the DAS. The data downloaded from the Data Acquisition System was in readable form with Microsoft Excel CSV (Comma Separated Variable) format.

A Lucas Schaevitz spring loaded model GCD-121-050 LVDT was used to monitor the vertical movement of the specimen. The LVDT had a travel range of ± 0.050 in. (1.27 mm) with a sensitivity of 200 V/in. (7.874 /mm). Thus, over the travel range of 0.10 in. (2.54 mm), there would be a 20 V difference in output voltage readings, i.e., –10 V to +10 V. The linearity range cited by the manufacturer of 0.25% for the full range output produced readings with errors within ± 0.025 V, which translated into displacement measurement errors within ± .000125 in. (.031750 mm).

These LVDTs are made of AISI 400 series stainless steel. They are complete and ready-to-use displacement transducers with a sleeve bearing structure on one end that supports a spring-loaded shaft attached to the core. The bearing is threaded externally to facilitate mounting. By using a spring loaded LVDT, the need for core rods or core support structures is eliminated. All LVDTs are hermetically sealed to operate in harsh environments such as a moist room, and have an operating temperature range of 0° F to 160° F (–17.8° C to 71.1° C) to facilitate testing of temperature effects.

The data acquisition system used is an Agilent 34970A unit (by Agilent Technologies) with a HP 34901A (20-channel armature multiplexer) plug-in module. The data acquisition unit can be set up to take readings at specified time intervals and for a specified length of time. The HP 34901A multiplexer module can read up to 20 channels of AC or DC voltages with a maximum capacity of 300 V. It has a switching speed of up to 60 channels per second. It also has a built-in thermocouple reference junction for use in temperature measurement by means of thermocouples. Thus, the Agilent 34970A data acquisition unit with one HP 34901A multiplexer module will be adequate for the job of recording load and displacement readings from 10 testing

apparatuses. The Agilent 34970A unit can take up to three plug-in modules. Thus, if needed, it can be expanded to take up to 60 channels of output.

The test setup for measuring the free shrinkage using a LVDT is shown in Figure 4-6. Figure 4-7 shows a picture of several test set-ups that were used simultaneously. Figure 4-8 shows the schematics of these test set-ups.

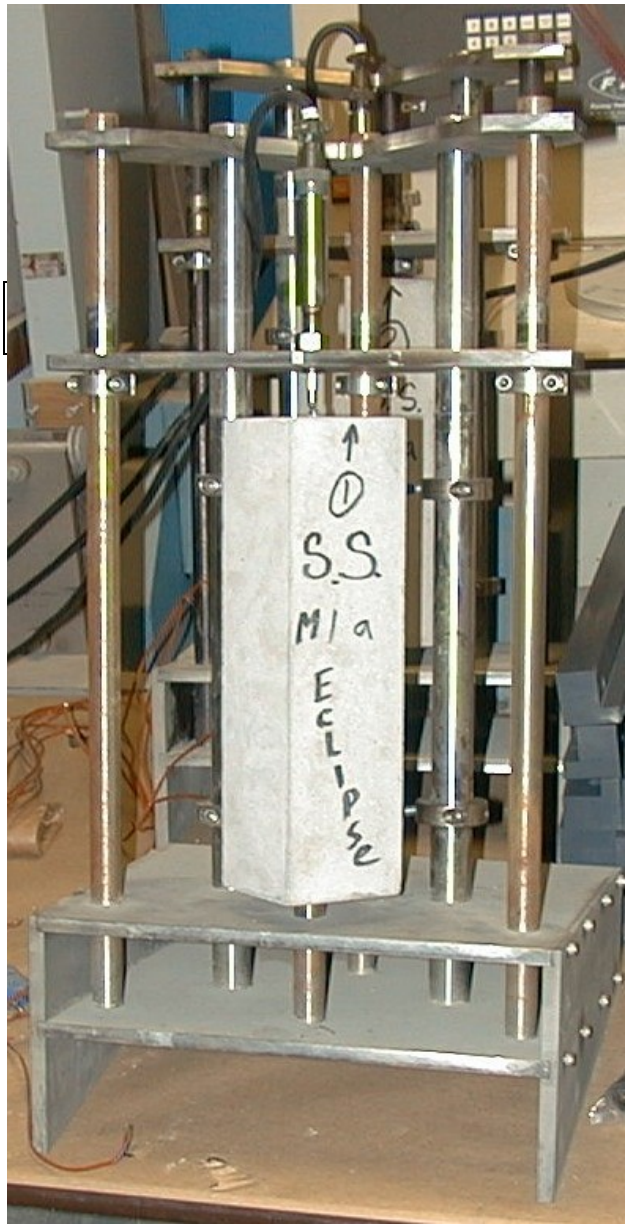

Figure 4-6. Set-up for ASTM C157 free shrinkage measurement using a LVDT

Figure 4-7. Picture of several test setups for free shrinkage measurement using LVDTs

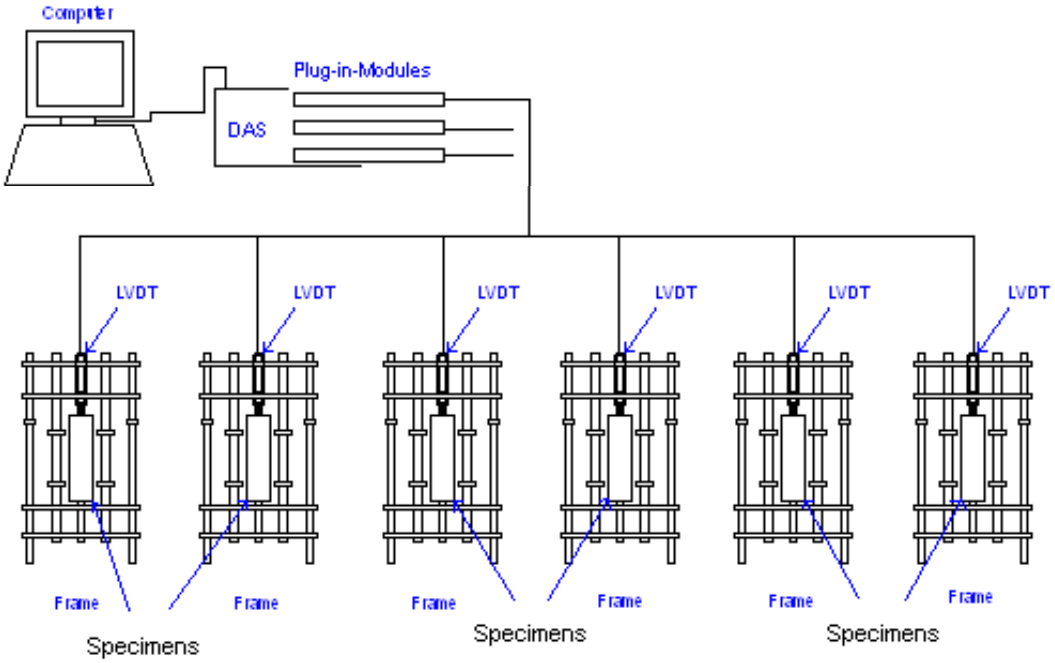

Figure 4-8. Schematics of test set-ups for measurement of free shrinkage using LVDTs

Test Procedure

The following steps were used in conducting ASTM C157 free shrinkage test:

1. Cover the interior surfaces of the specimen molds with transmission oil.
2. Set up the gage set points on the sides of the mold carefully, keeping them clean, and free of oil, grease and foreign matter.
3. After concrete mixing is done, place the fresh concrete into the molds in two equal layers with each layer vibrated for 30 seconds by placing the molds over a vibrating table.
4. Cover the concrete samples with plastic sheets for one day.
5. After one day, remove the concrete samples from the molds and place them into the shrinkage test frames as shown in Figures 4-6 and 4-7.
6. Adjust the LVDT readings to zero by observing output displays in the DAS. It is somewhat difficult to set the LVDT reading to zero, because of its high sensitivity. Thus, just adjust it to as close to zero as possible.
7. After the LVDT readings are set to zero (or close to zero), set the DAS to record readings every 15 minutes continuously.
8. Download the readings from the DAS to a computer after 7 to 14 days, using the software "Bench Link Data Logger."

4.3.5 Free Shrinkage Measurement Using Embedment Gage in the Long-Specimen Apparatus

Test Set-Up

The test setup for free shrinkage measurement using the long-specimen apparatus consisted of a long-specimen mold, an embedment strain gage, a Bridge-sensor (which

was a strain indicator), a laptop computer, a data acquisition system and a temperature gage. The schematics for the test setup are shown in Figure 4-9. Figure 4-10 shows a picture of two long-specimen molds before the placement of concrete in them.

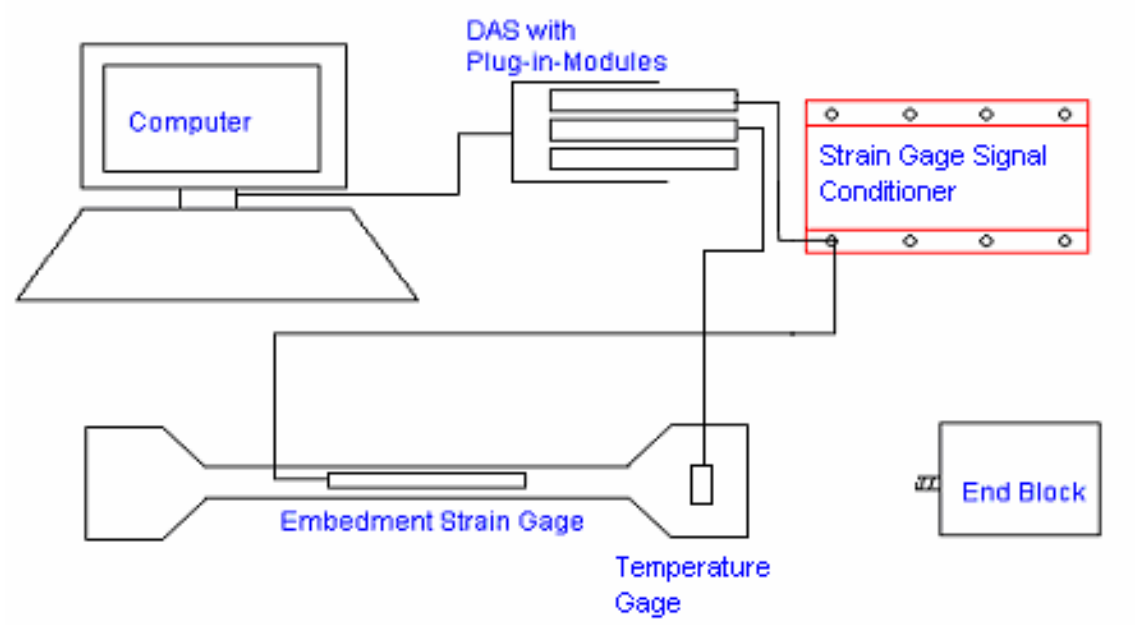

Figure 4-9. Schematics for test setup for free shrinkage measurement using the long-specimen apparatus

An OMEGA OM2-8608 Backplane 8-channel signal conditioner was used to connect the embedment strain gages in a quarter bridge circuit and to amplify the output signals from the bridge circuits. The embedment strain gages used have a length of 4.68 in. (120 mm), a resistance of 120 Ohms and a gage factor of 2.0. An excitation voltage of 4 V and a gain of 333.33 for the output signal were used. The outputs from the signal condition were connected to the data acquisition system. The following equation relates the un-amplified voltage output to the measured strain:

$$\begin{aligned} \text{Strain} &= 4\,(\text{voltage output}) / (\text{gage factor})(\text{excitation voltage}) \\ &= 4\,(\text{voltage output}) / 2.0\,(4\text{V}) \\ &= (\text{voltage output in V}) / 2 \end{aligned} \qquad \text{(Eq. 4.4)}$$

Figure 4-10. Picture of two long-specimen molds

With a gain of 333.33 was used, the measured strain is related to the amplified voltage output as follows:

$$\text{Strain} = (\text{Amplified voltage output in V}) / (2 \times 333.33)$$

$$= (\text{Amplified voltage output in V}) / (666.67) \qquad \text{(Eq. 4.5)}$$

Test Procedure

The following steps were used for running the free shrinkage test using the long-specimen apparatus:

1. Assemble the side blocks and the end blocks of the long-specimen molds together and fix them to the base plate firmly by using screws.

2. Coat the surfaces of the support base plate and the side blocks with a thin layer of transmission fluid to avoid friction between the concrete specimen and the bottom support plate and the side plates.
3. Configure the DAS to record the data for the test. The desired parameters such as the time interval for the DAS to scan the data, the unit for temperature, type of thermocouple, unit for voltages, etc., have to be set in the DAS by using the knobs and buttons in the front panel of the DAS.
4. Set the DAS unit to start scanning with a time interval of 15 minutes.
5. Place the fresh concrete into the mold in two equal layers, and tamp each layer with fingers for consolidation. After the first layer is done, place the embedment gage in the concrete at the center of the mold. Then, apply the second layer of concrete on top of the gage. The gage should be placed about half an inch from the top of the mold.
6. Finish the surface of the specimen with a hand trowel.
7. Turn on the DAS to start recording data.
8. After the concrete has set sufficiently, remove the side blocks so that the concrete specimen will not have restraint on all sides except the bottom portion, which has been coated with a thin layer of transmission oil to reduce friction. Usually the side blocks can be removed within several hours to a day's time.
9. Keep the specimen undisturbed for the entire duration of the test.
10. Download the data to a laptop computer at the desired times. Data from seven days may be downloaded at one time. The software "Bench Link Data Logger" can be used to download data from the DAS to the readable Excel CSV format files.

4.3.6 Free Shrinkage Measurement using Whittemore Gage in the Long-Specimen Apparatus

Test Set-up

In this test set-up, a pair of gage point studs was embedded in the long concrete specimen at a distance of 10 inches (254 mm) apart from one another, and a Whittemore gage was used to measure the change in distance between these two gage points due to shrinkage in the specimen. The Whittemore gage used is shown in Figure 4-11. The long concrete specimen with the two gage point studs installed is shown in Figure 4-12.

Figure 4-11. Whittemore gage for measuring the distance between two gage points

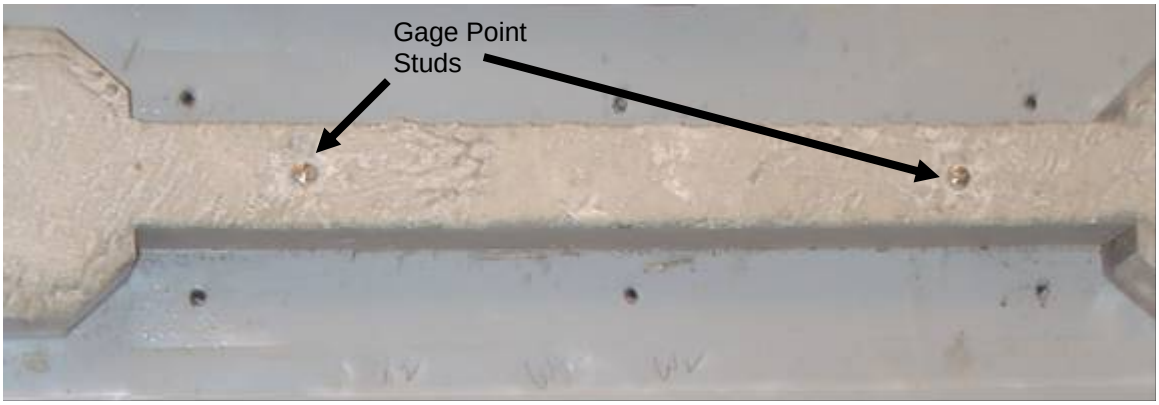

Figure 4-12. Long concrete specimen with gage point studs installed

Procedure

The following steps are followed in conducting the free shrinkage measurement using the Whittemore gage in the long specimen apparatus:

1. Assemble the side blocks and the end blocks of the long-specimen molds together and fix them to the base plate firmly by using screws.
2. Coat the surfaces of the support base plate and the side blocks with a thin layer of transmission fluid to avoid friction between the concrete specimen and the bottom support plate and the side plates.
3. Place the fresh concrete into the mold in two equal layers, and tamp each layer with fingers for consolidation. After both layers are done, press two gage studs into the surface of the long concrete specimen, at the middle of the specimen and at a distance of 10 in. (254 mm) from one another. Make sure that the gage point studs are well pressed into the concrete so that after hardening, the Whittemore gage can be placed on top of the studs securely and the readings can be taken.
4. Finish the surface of the specimen with a hand trowel
5. After the concrete has set sufficiently, remove the side blocks so that the concrete specimen will not have any restraint on all sides except the bottom portion, which has been coated with a thin layer of transmission oil to reduce friction. Usually the side blocks can be removed within several hours to a day's time.
6. After the concrete has hardened sufficiently (usually after 24 hours of curing), take the first reading of the distance between the two gage points using the Whittemore gage. Take additional readings at the specified times as needed.

4.3.7 Free Shrinkage Measurement Using Whittemore Gage on Cylindrical Specimens

In this method, 6 × 12-in. (152.4 × 304.8-mm) cylindrical concrete specimens are cast, and the free shrinkage of the concrete specimens are measured by means of a Whittemore gage. Three pairs of gage points with a gage distance of 10 in. (254 mm) are to be placed in each test concrete specimen. A Whittemore gage is to be used to measure the change in distance between the gage points due to drying shrinkage.

A gage-point positioning guide, as shown in Figure 4-13, was used in positioning the gauge-points on the plastic cylinder mold. The guide can be placed around a 6 × 12-in. (152.4 × 304.8-mm) cylinder mold. By tightening the six screws on the guide, the precise locations for the three pairs of gage points, with a gage distance of 10 in. (254 mm), can be marked conveniently on the mold. Figure 4-14 shows the picture of gauge-position guide. Figure 4-15 shows a picture with the plastic cylinder mold inside the gauge-position guide.

Test Procedure

Figure 4-16 shows a picture of the concrete cylinders with the gauge points attached on them after the molds have been removed. A Whittemore gauge was used to measure the change in the distance between the gage points as the concrete cylinder shrinks. The Whittemore gauge has a resolution of 0.0005 in. Three sets of measurements were taken from each specimen at each specified time. The original distances between the gauges are to be measured immediately after the plastic mold is removed. The shrinkage strain is taken as the average of the three readings from each specimen, and can be expressed as follows:

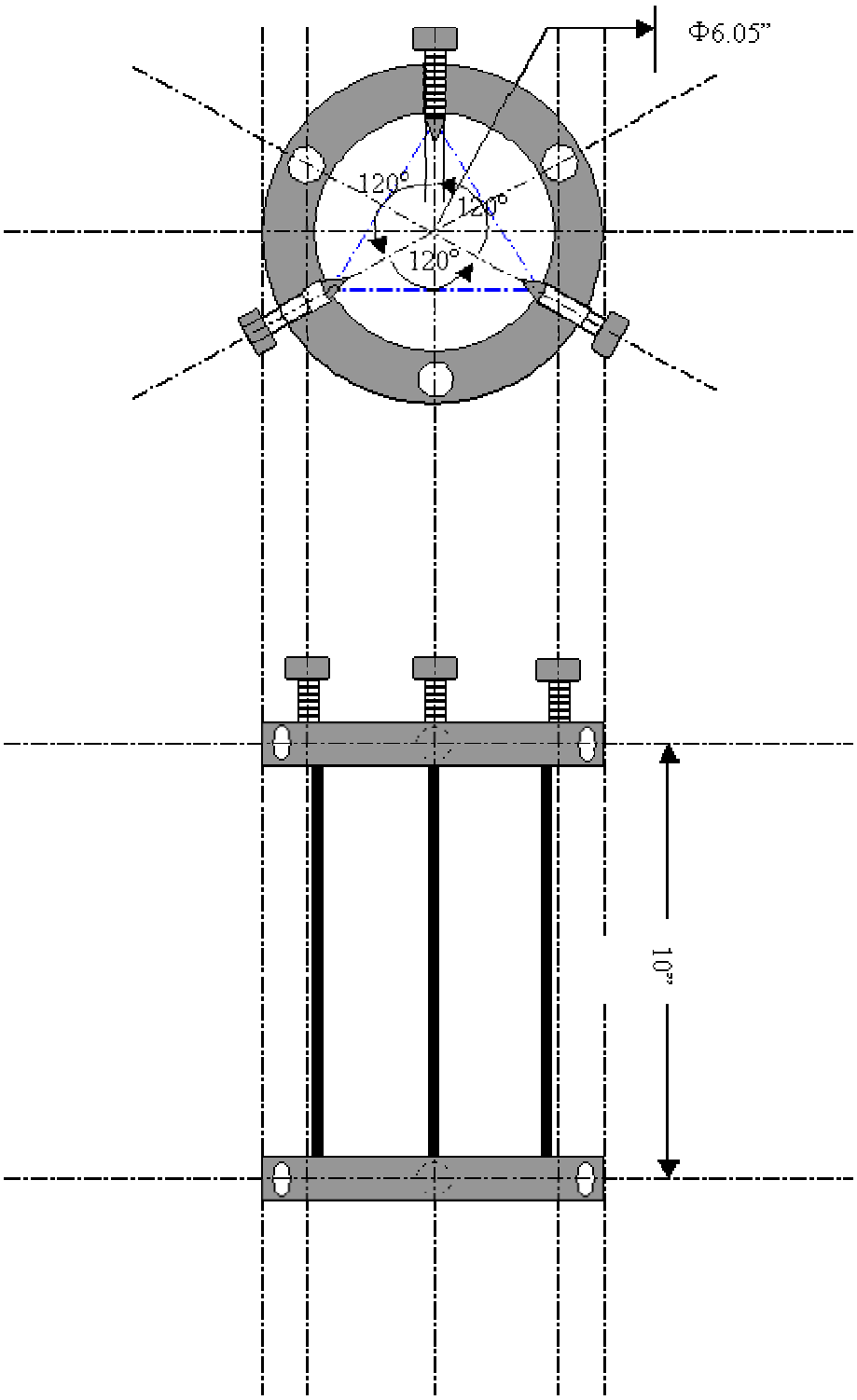

Figure 4-13. Gage-point positioning guide

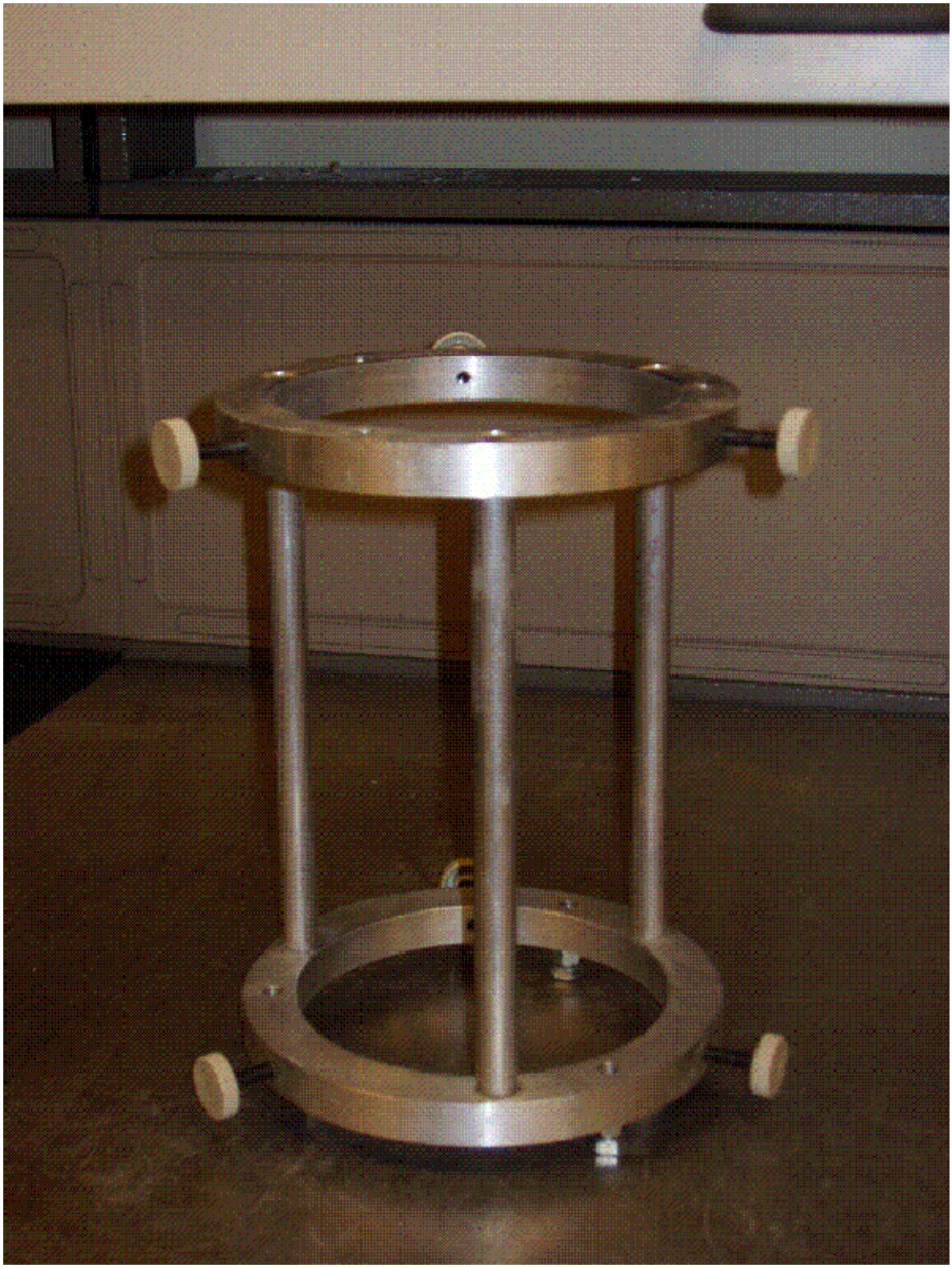

Figure 4-14. Gauge-position guide

Figure 4-15. Plastic cylinder mold inside gauge-position guide

Figure 4-16. Concrete cylinders with gauge point installed on them

$$\varepsilon_{sh} = \frac{1}{3}\sum_{i=1}^{3}\frac{(l_i - l_0)}{l_0} \qquad \text{(Eq. 4.6)}$$

where

l_i = measured distance between i^{th} pair of gage points

l_0 = original distance between i^{th} pair of gage points measured immediately after demolding.

4.3.8 Constrained Shrinkage Test Using the Long Specimen Apparatus

The test setup and procedure for the constrained shrinkage test went through numerous stages of development and refinement during the course of this study. The description of the test setups and procedures used in this study, and their evaluation are presented in Chapter 5 of this report.

CHAPTER 5
DEVELOPMENT AND EVALUATION OF THE MODIFIED CONSTRAINED LONG SPECIMEN APPARATUS

5.1 Introduction

This chapter presents the development and evaluation of the modified constrained long specimen apparatus for evaluation of resistance to shrinkage cracking of concrete. Based on the evaluation of the various designs that have been tried out, a final design was adopted for use in the laboratory testing program in this study.

5.2 Fundamentals of the Constrained Long Specimen Method

5.2.1 Original Design

The constrained long specimen set-up had a dog-bone shaped mold with an overall length of 27.30 in. (700 mm). The actual portion of the mold that holds the concrete is 17.55 in. (450 mm) long and 1.56 × 1.56 in. (40 × 40 mm) in cross section. It has two flared ends each of which has a width of 4.29 in. (110 mm). One end is fixed to the bottom plate, and the other end was free to move. Meanwhile, in order to give restraint to the free movement of concrete, it was clamped with an end aluminum block through a proving ring so that the induced tensile force can be measured. This aluminum block was fixed to the bottom plate. When there is any shrinkage movement in the concrete specimen, the proving ring will get stretched because of its fixity to the end block and it will read a value equal to the tensile force that is induced in the specimen. Figure 5-1 illustrates the design of the originally developed Constrained Long Specimen Apparatus.

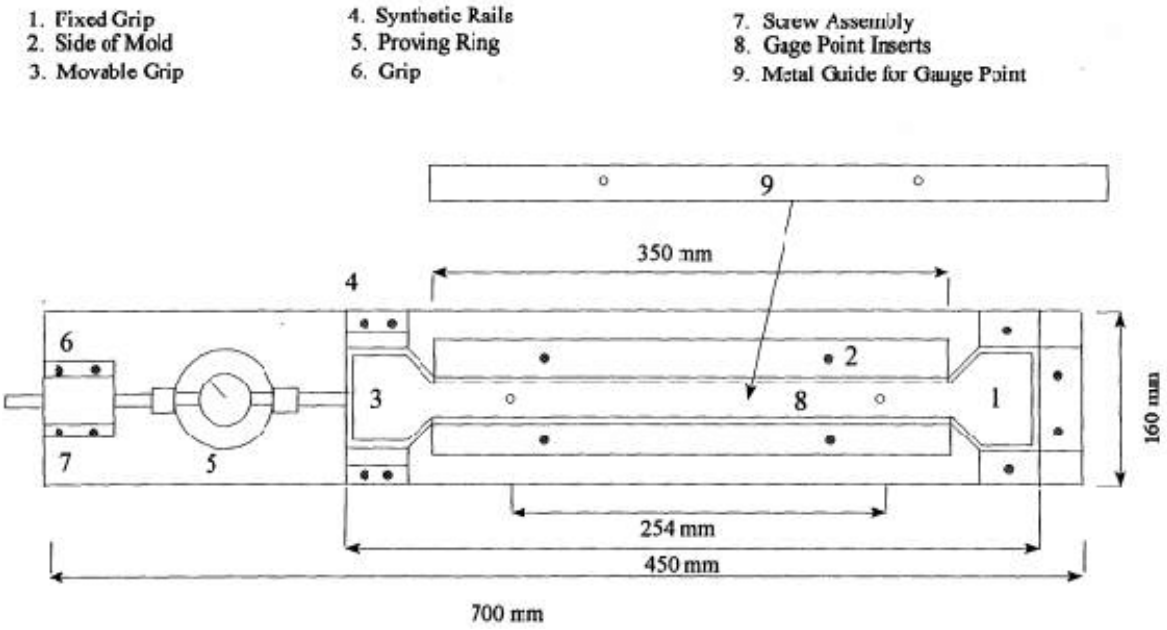

Figure 5-1. The original constrained long specimen apparatus [Tia et al., 1998]

5.2.2 Test Procedure

The test procedure for the original constrained long specimen apparatus test consisted of the following steps:

1. Spread a thin layer of motor oil on the surface of the metal guide that is in contact with the concrete specimen.
2. Place the fresh concrete into mold.
3. Place the whole apparatus on a vibrating table for one minute.
4. Place two gage-point inserts which are attached under the metal guide (#9 in Figure 5-1) into the concrete specimen.
5. Place the entire apparatus again on the vibrating table for an additional minute.
6. Press the two gage point inserts into the concrete firmly by fingers to make sure that they are completely inside the concrete mass. Two gage point inserts are used to hold the Whittemore gage to the concrete.

7. Finish the surface of the specimen with a hand trowel.
8. After 12 hours, remove the two side pieces of the mold, and remove the metal guide from the gage point inserts.
9. Attach the Whittemore gage to the two inserts with two screws.
10. Record the initial readings of both the proving ring and the Whittemore gage.
11. After the removal of the side pieces and the attachment of the Whittemore gage, monitor the induced load by means of the proving ring, and the movement of the concrete specimen by means of the Whittemore gage for a period of 14 days.

Though the concrete specimen was constrained from movement at the two ends, the Whittemore gage would usually measure a slight shortening of the concrete specimen. This could be explained by the movement of the proving ring as load was induced. Figure 5-2 shows how the movement of the proving ring (δ_{PR}) is equal to the movement of the constrained long specimen (δ_{CL}).

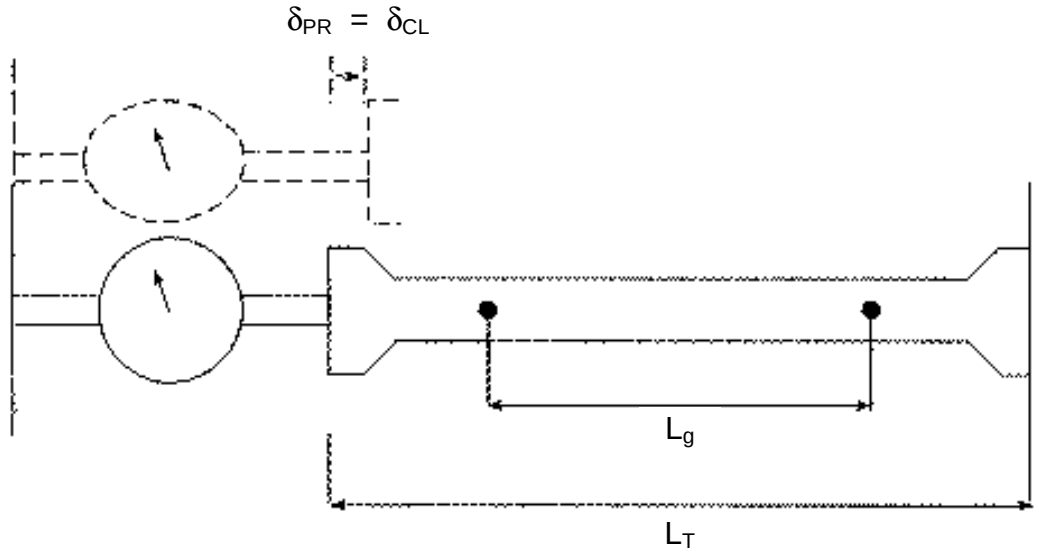

Figure 5-2. Schematics of the restrained long specimen under contraction

5.2.3 Method of Analysis

The analysis part consists of several equations involving three different deformation components in the concrete specimen. The first component is the shortening due to shrinkage (δ_{sh}). The second component is the elastic lengthening due to induced tensile stress (δ_E). The third one is the creep due to the induced stresses (δ_{CR}). These three components are related to the total movement of the specimen as follows:

$$\delta_{CL} = \delta_{sh} - \delta_E - \delta_{CR} \qquad \text{(Eq. 5.1)}$$

In terms of strains (ε's), the relationship can be written as:

$$\varepsilon_{CL} = \varepsilon_{sh} - \varepsilon_E - \varepsilon_{CR} \qquad \text{(Eq. 5.2)}$$

The total strain in the constrained long specimen (ε_{CL}) can be calculated from the deformation read by the Whittemore gage (δ_g) as follows:

$$\text{Total Strain, } \varepsilon_{CL} = \delta_g / L_g \qquad \text{(Eq. 5.3)}$$

where L_g = gage length = 10 in. (254 mm).

The elastic strain (ε_E) can be calculated from the induced stress (σ_E) and the elastic modulus of the concrete (E) as follows:

$$\varepsilon_E = \sigma_E / E = F_{PR} / AE \qquad \text{(Eq. 5.4)}$$

where F_{PR} = force measured by the proving ring; and

A = cross-sectional area of concrete specimen = 2.48 in^2 (16.0 cm^2).

The shrinkage strain (ε_{sh}) can be assumed to be equal to the free shrinkage strain measured by the length comparator. From Equation 5.2, the creep strain (ε_{CR}) can be calculated from the other strains as follows:

$$\varepsilon_{CR} = \varepsilon_{sh} - \varepsilon_E - \varepsilon_{CL}$$

$$= \varepsilon_{sh} - (F_{PR}/AE) - \delta_g/L_g \qquad \text{(Eq. 5.5)}$$

If a concrete member is fully constrained from movement, the induced stress due to drying shrinkage can be expressed as:

$$\Phi_{FC} = (\varepsilon_{sh} - \varepsilon_{CR}) E \qquad \text{(Eq. 5.6)}$$

where Φ_{FC} = induced stress in a fully constrained concrete.

The free shrinkage strains as obtained from the free shrinkage measurements by means of the length comparator are used as the shrinkage strain (ε_{sh}), while the creep strains from the long constrained specimen test (as computed from Equation 5.5) are used as the creep strains, ε_{CR}. The actual creep strain should be slightly more than the one experienced by the long constrained specimen, since the long constrained specimen is not fully constrained. Thus, using the creep strains from the long constrained specimen would result in a slightly higher (or more conservative) estimation of the induced stresses.

When the computed expected shrinkage stress (Φ_{FC}) as computed by Equation 5.6 exceeds the expected tensile strength of the concrete (Φ_t) at any particular time, the concrete will be likely to crack due to shrinkage stresses at that time.

5.3 First Refinement of Apparatus – Use of LVDT, Load Cell and Data Acquisition System

5.3.1 Changes Made to the Original Design

The constrained long specimen apparatus, which was previously developed for the FDOT by the University of Florida and described in Section 5.2, was further refined by automating the data acquisition system process. The apparatus was refined by (1) replacing the Whittemore gage, which was used to measure the deformation of the specimen by a high-sensitivity Linear Variable Differential Transformer (LVDT), and (2) replacing the proving ring, which was used to measure the induced force in the

constrained long specimen by a load cell. A convenient and effective method of attaching an LVDT to the constrained long concrete specimen, and using the LVDT to measure the deformation of the specimen was designed and tested. After some comparative evaluation, an AC LVDT, instead of a DC LVDT was selected for use. An AC LVDT has two major advantages over a DC LVDT in this application. First, an AC LVDT is much lighter in weight. Second, it has less noise and is more accurate.

The selected AC LVDT is a CD375-025 by Macro Sensors. It has a stroke of ±0.025 in. (0.635 mm), a weight of 0.1 oz (2.8 grams) and gives an output of 10 mV per 0.001 in. (0.0254 mm) of deformation under the normal operating condition. Gage studs, brackets for holding the gage studs, and lightweight holders for the LVDT body and LVDT core were designed, fabricated and tested. Figure 5-3 shows the setup used for measuring the deformation of the constrained long specimen using an LVDT. When there is any shrinkage movement in the concrete specimen, the load cell will get stretched because of its fixity to the end block and it will read a value equal to the tensile force that is induced in the specimen. The constrained long specimen mold used a concrete specimen of a length of 21.25 in. (539.75 mm) with 1.5 × 1.5 in. (38.1 × 38.1 mm) as cross-section. The end collar blocks have a width of 4.25 in. (111.95 mm) each.

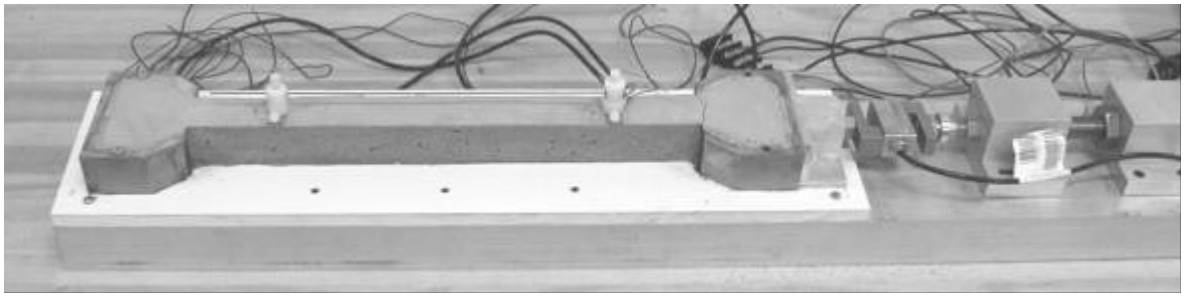

Figure 5-3. Constrained long specimen apparatus using a LVDT

A drawing of the top and the side views of the apparatus is shown in Figure 5-4. The long constrained concrete specimen with its dog bone shape has two ends of steel collars with a width of 4.25 in. each. The steel collar blocks are shown in Figure 5-5. Figure 5-6 displays the front and Side views of the PVC side pieces for the Long Constrained Specimen apparatus. Figure 5-7 shows the aluminum bracket support for the gage studs that hold the LVDT and the core rod holders to the concrete specimen.

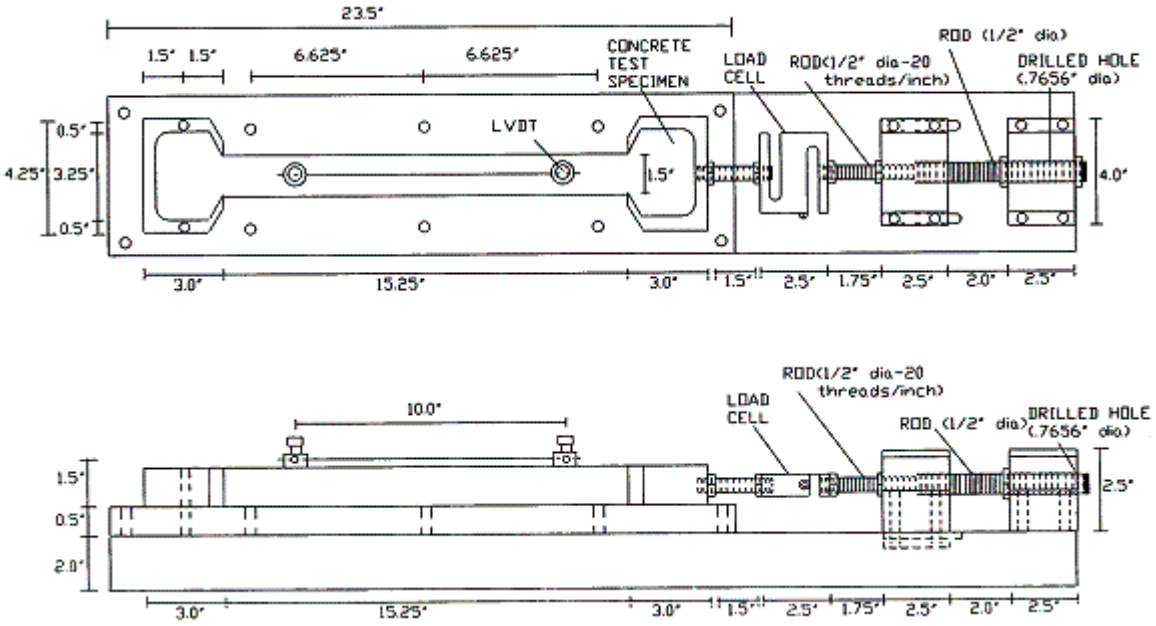

Figure 5-4. Top and side views of the constrained long specimen apparatus

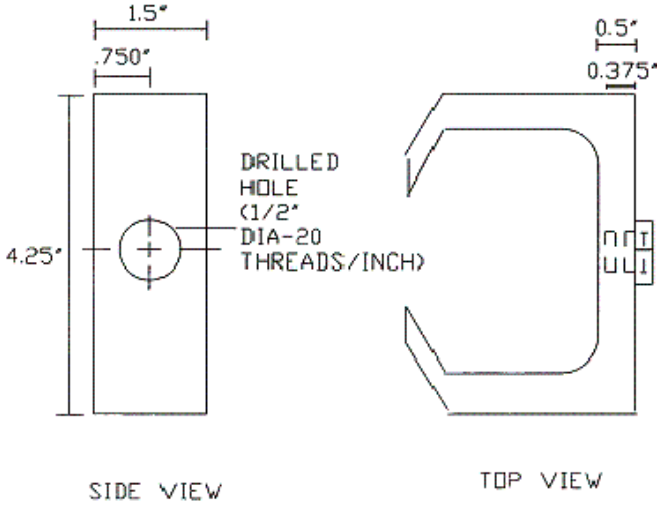

Figure 5-5. Side and top views of the end collar block of the mold

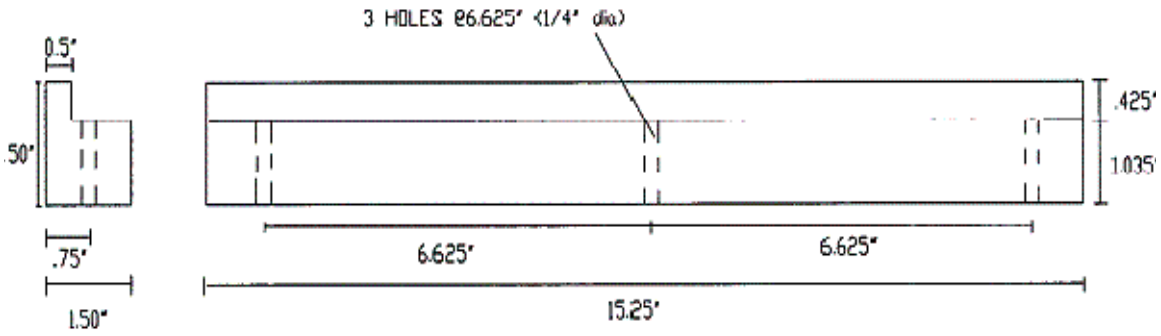

Figure 5-6. Front and side views of the PVC side pieces for the constrained long specimen apparatus

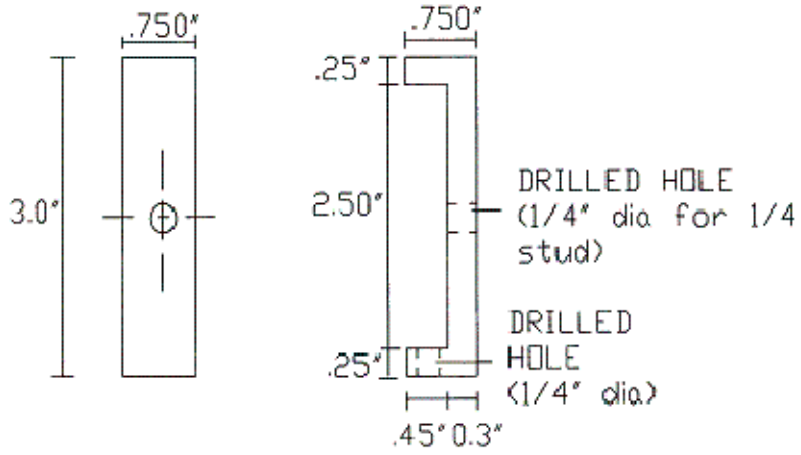

Figure 5-7. Aluminum bracket support for the gage studs that hold the LVDT and the core rod holders to the concrete specimen

5.3.2 LVDTs for Measurement of Strain

An AC LVDT (Linear Variable Differential Transformer) is used to measure the displacement between two gage studs, which are placed on the concrete specimen at a spacing of 10 inches (mm) apart. An LVDT is an electromechanical device that produces an electrical output proportional to the displacement of a separate movable core. It consists of a primary coil and two secondary coils symmetrically spaced on a cylindrical form. A free-moving, rod shaped magnetic core inside the coil assembly provides a path for the magnetic flux linking the coils. The cross-sectional view of a typical LVDT is shown in Figure 5-8.

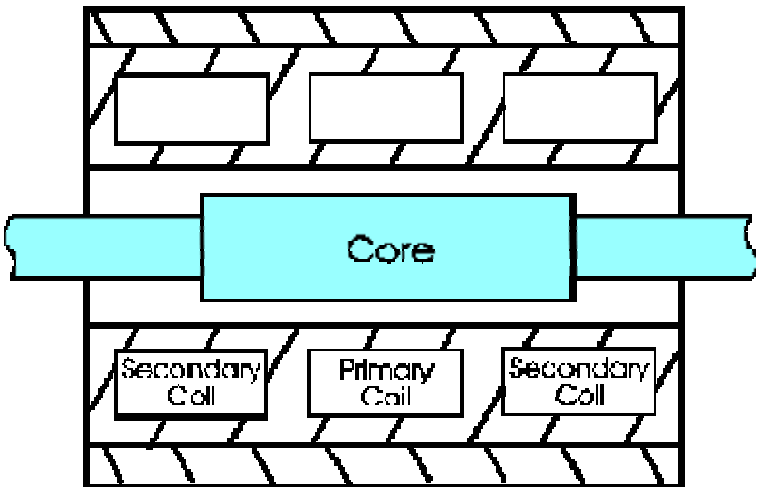

Figure 5-8. Cross-sectional view of an LVDT

The primary coil needs to be excited, in order to induce a voltage in the secondary coils. The excitation needs to be an alternating voltage, in the 400 Hz to 20 KHz range usually. Square, trapezoid and other wave shapes can be used, but a sinusoidal shaped wave will yield the best results. The voltage that is applied to the primary coil produces a current whose magnitude depends on the impedance of the primary coil at the chosen frequency. This current induces currents in the secondary coils of the LVDT. The amount of current induced in each secondary coil depends on the mutual inductance between the primary coil and each secondary coil. This mutual inductance, in turn, depends on the position of the core, with relation to each secondary coil. The outputs of the LVDT are these two AC voltages, which can be added together to form one AC voltage. This voltage varies approximately linearly with the axial position of the core. A typical LVDT signal conditioning electronics will convert this AC voltage to DC voltage.

When the primary coil is energized by an external AC source, voltages are induced in the two secondary coils. These are connected in series and in opposing direction so the two voltages are of opposite polarity. Therefore, the net output of the

transducer is the difference between these voltages, which is zero when the core is at the centre or null position. When the core is moved from the null position, the induced voltage in the coil toward which the core is moved increases, while the induced voltage in the opposite coil decreases. This action produces a differential voltage output that varies linearly with changes in core position. The phase of this output voltage changes abruptly by 180° as the core is moved from one side of null to the other. Figure 5-9 shows the core displacement and the respective voltage changes that occur in the coil.

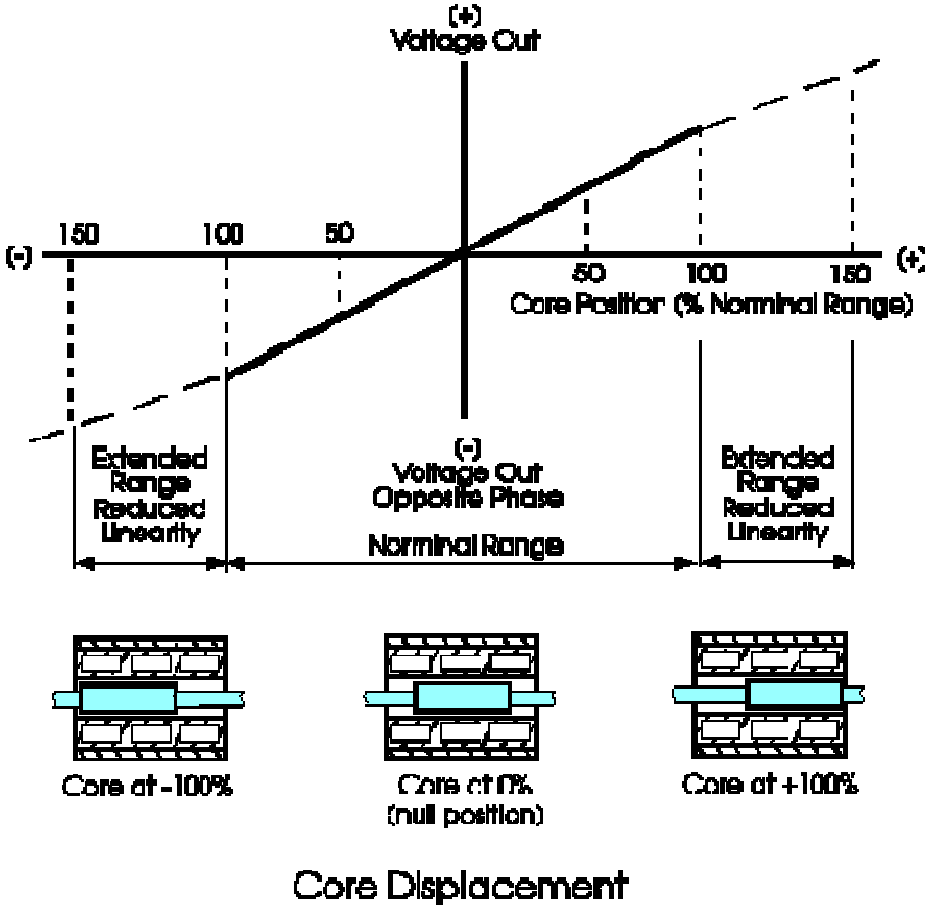

Figure 5-9. LVDT core displacement and the respective voltage change

The LVDT used was a CD375-025 by Macro Sensors and Figure 5-10 shows a close-up picture of the LVDT inside the LVDT holder. Figure 5-11 shows a close-up picture of the holder for the rod for the LVDT core.

E

Figure 5-10. LVDT holder and a portion of the rod that is connected to the other holder

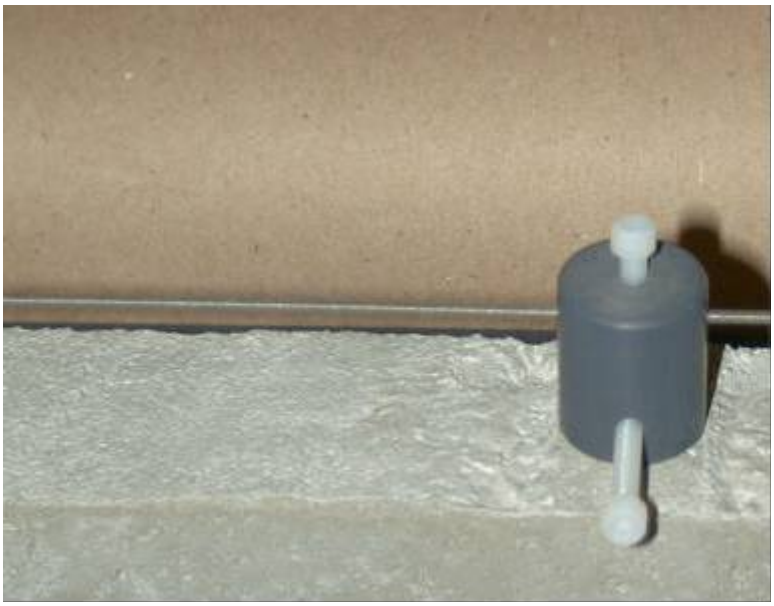

Figure 5-11. The holder for the rod that passes through the LVDT core

This LVDT has a stroke of ±0.025 in. (0.635 mm), a weight of 0.1 oz (2.8 grams) and gives an output of 10 mV per 0.001 in. (0.0254 mm) of deformation under the normal operating condition. An AC voltage source is used to supply an excitation voltage of 3.0 RMS V at 2.5 kHz. The displacement (in inches) between the two gage points is computed from the RMS voltage output as:

$$\text{(Displacement in 0.001 in.)} = \text{(RMS voltage in mV)} \times 0.1$$

The strain is then computed from the displacement as:

$$\text{Strain} = \text{Displacement} / \text{(Gage Length)} = \text{Displacement} / \text{(10 in. or 254 mm)}$$

5.3.3 Load Cell for Measurement of Stress

A load cell was used to measure the force experienced by the concrete specimen during a test. The load cell used was a LCCB-1K by Omega. It is a tension and compression "S" type load with a maximum capacity of 1000 lb (4450 N). The rated output is 3mV/V for the full load of 1000 lb (4450 N). A DC voltage source is used to supply an excitation voltage of 10 V. With the 10 V excitation input, the load cell gives an output of 30 mV/1000 lb, or 0.03 mV/lb. The axial force in the concrete sample is computed from the DC output voltage from the load cell as:

$$\text{(force in lb.)} = \text{(dc voltage in mV)} \times 33.33$$

The stress in the concrete sample is then calculated from the force as:

$$\text{Stress} = \text{Force} / \text{(Cross-sectional area of concrete)}$$

$$= \text{Force} / (2.25 \text{ in}^2 \text{ or } 1451.6 \text{ mm}^2)$$

The load cell attached to the frame of the specimen is shown in Figure 5-12.

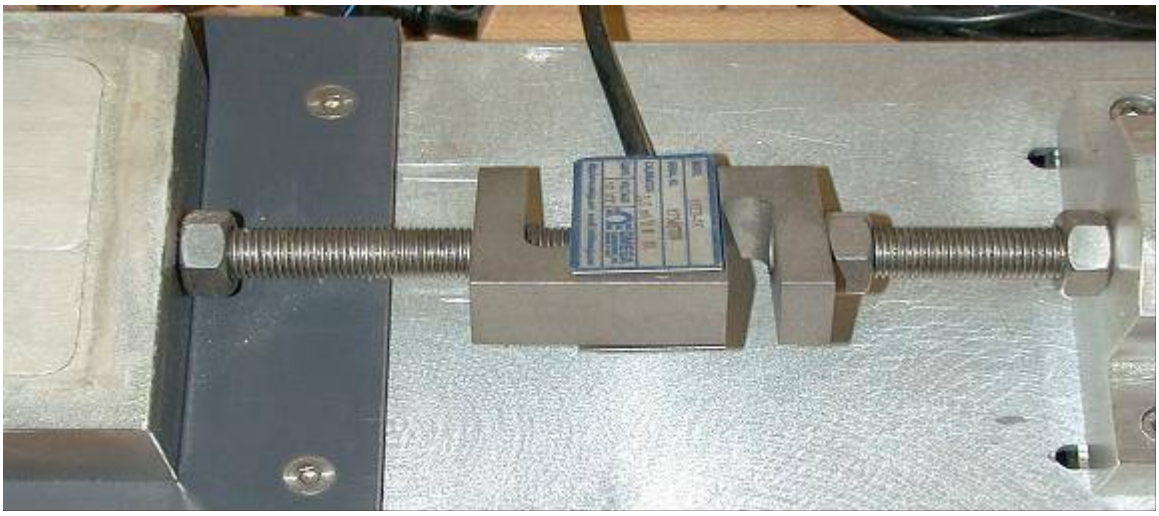

Figure 5-12. The load cell attached to the frame of the concrete specimen

5.3.4 Data Acquisition System

The output ends from the LVDT and the load cell were connected to an automatic data acquisition system, an Agilent 34970A unit (by Agilent Technologies) with a HP 34901A (20-channel armature multiplexer) plug-in module. The Data Acquisition System unit is shown in Figure 5-13. The DAS unit can be set up to take readings at

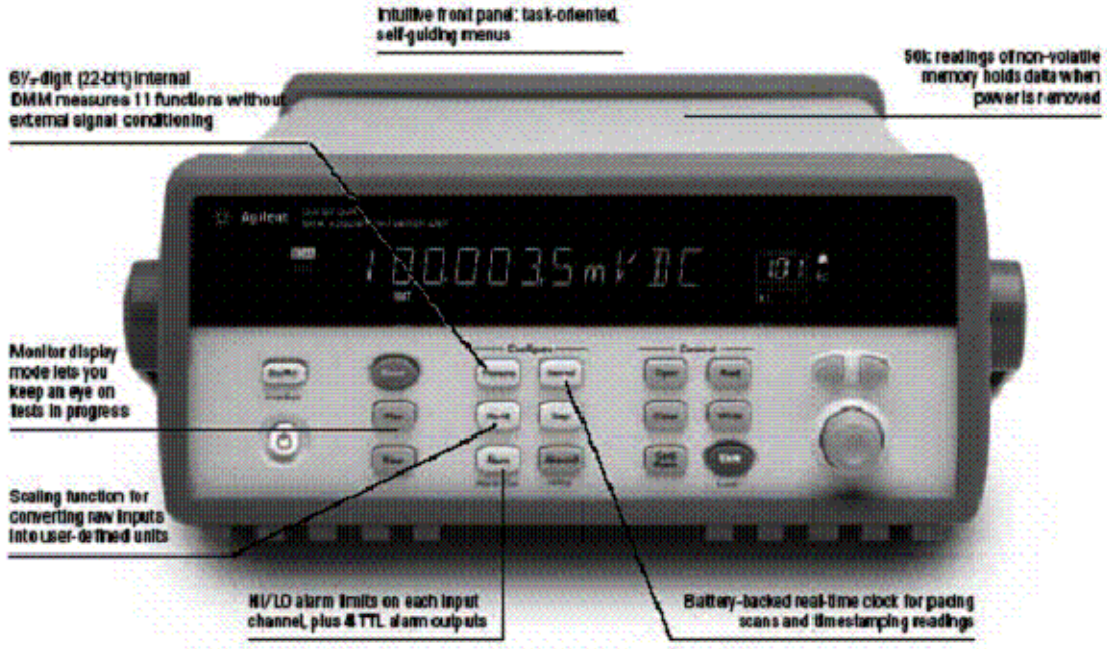

Figure 5-13. Agilent 34970A data acquisition system unit

specified time intervals and for a specified length of time. The HP 34901A multiplexer module can read up to 20 channels of AC or DC voltages with a maximum capacity of 300 V. It has a switching speed of up to 60 channels per second. It also has a built-in thermocouple reference junction for use in temperature measurement by means of thermocouples.

The Agilent 34970A unit can take up to three plug-in modules. The stored data can be downloaded to a personal computer via a RS232 cable connection. The data files are in CSV format and can be read readily by spreadsheet software such as Excel.

After satisfactory performance was observed from a prototype of the developed constrained long specimen apparatus equipped with a LVDT, a load cell and a data acquisition system, ten of such apparatuses were constructed. Five of the ten apparatuses were equipped each with both a LVDT and a load cell, and were to be used to perform the constrained shrinkage test. The other five apparatuses were equipped each with only a LVDT, and were to be used to perform the free shrinkage test. All the apparatuses were constructed to be identical to one another so that they could perform equally in measuring shrinkage. A load cell could be added easily to the apparatus if there was no load cell attached, prior to running the constraint shrinkage test. Similarly, the load cell could be taken off easily from the apparatus to run the free shrinkage test. The schematics of the set-up for the constrained shrinkage test using a LVDT and a load cell is shown in Figure 5-14.

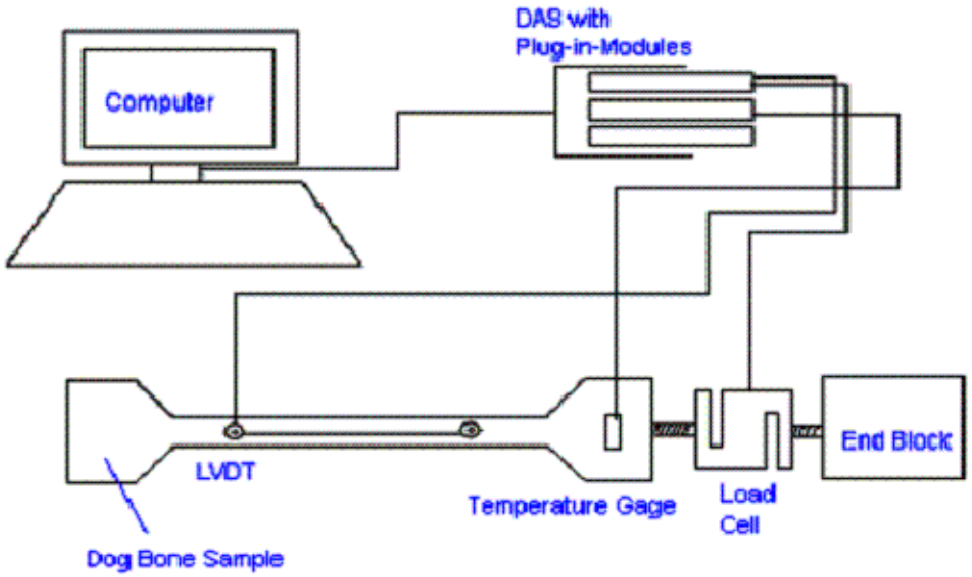

Figure 5-14. Setup for the constrained long specimen test with a LVDT and a load cell

5.3.5 Modified Instrumentation for the LVDTs

One major instrumentation problem was encountered when these ten apparatuses were evaluated. The problem was caused by the fact that only one AC Voltage Function Generator was used to power all of the AC LVDTs. The AC LVDT requires an excitation voltage of 3 RMS V at a frequency 2.5 kHz. However, when one voltage function generator was used to power several LVDTs at the same time, the function generator was not able to deliver the required voltage. In addition, interferences between the outputs from the different LVDTs were noted. The instrumentation for the LVDTs was subsequently modified to take care of this problem.

Eleven LVDT signal conditioners (Model LPC-2100 by Micro Sensors) were acquired. Each of these LVDT signal conditioners was connected to each of the AC LVDTs (CD375-025 by Macro Sensors) to provide the needed excitation voltage of 3.0 RMS V at 2.4 kHz, to demodulate the AC output signal from the LVDT into a DC signal, and to amplify the DC signal before outputting it to the data acquisition system.

According to the specification sheet, the LVDT signal conditioner had been calibrated such that a full stroke of the LVDT (±0.025 inch) would produce an output of ±10.0 DC V from the signal conditioner. A LVDT signal conditioner is shown in Figure 5-15. According to this assumed calibration, the displacement between the two gage points could be computed from the voltage output as follows:

$$\text{(Displacement in 0.001 inch)} = \text{(voltage in V)} \times 2.5$$

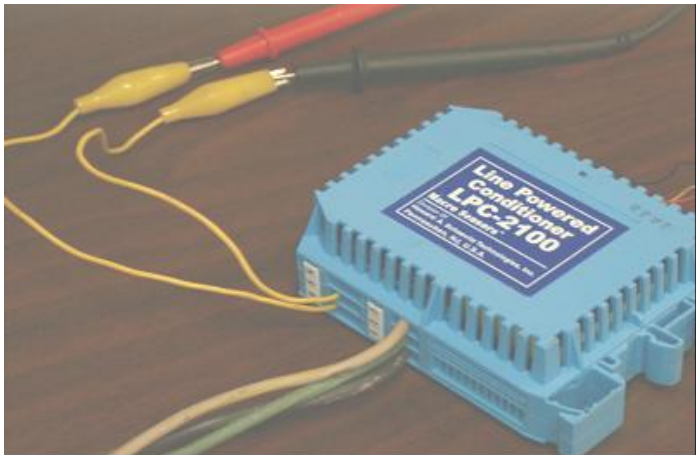

Figure 5-15. A LVDT line powered LPC-2100 signal conditioner

Figure 5-16 shows the schematics of an individual constrained long specimen connected to the LVDT and other instrumentations.

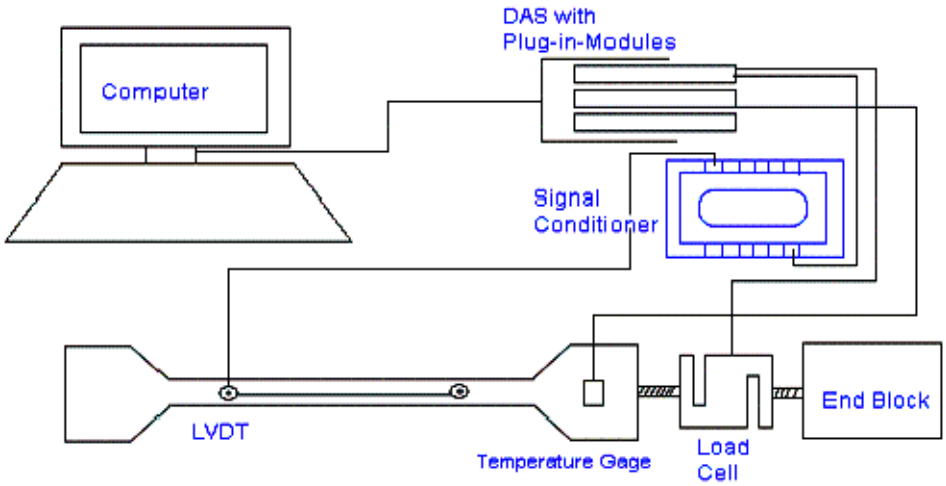

Figure 5-16. Individual constrained long concrete specimen connected to an LVDT, LVDT signal conditioner, DAS and the computer

5.3.6 Calibration of the LVDT/Signal Conditioner System

When the assumed calibration of the LVDT/signal conditioner system was used, the measured shrinkage from the long specimen apparatus appeared to be too low and erroneous. Thus, a special calibration setup using a micrometer was built to calibrate the LVDT/signal conditioner system. It consisted mainly of a holder for the micrometer, a holder for the LVDT and a spring attachment for the extension rod for the core of the LVDT. This setup enabled a spring-loaded rod, which is connected to the core of the LVDT, to be aligned with the micrometer. The micrometer used had a range of 0.5 in. (12.7 mm) and a precision of 0.001 in. (0.0254 mm). The calibration was set up so that the core was positioned near the center of the LVDT. The core was then moved through the LVDT with the displacement read by the micrometer. The corresponding voltage output from the LVDT/conditioner was read by a digital voltmeter. A plot of the LVDT/conditioner output versus displacement is shown in Figure 5-17. A picture of the calibration setup is shown in Figure 5-18.

Results of the calibration indicated that the previously assumed calibration of the LVDT/signal conditioner system was in error. The previously assumed calibration was that 1 V of output from the LVDT/signal conditioner translated into 0.0025 in. (0.0635 mm) of displacement. However, the results of the actual calibration indicated that 1 V of output from the LVDT/conditioner system should translate into 0.013 in. (0.3302 mm) of displacement (as shown from the plot in Figure 5-17).

Equation for computation of displacement becomes:

$$\text{Displacement (in inches)} = \text{Output (in volts)} \times 0.013 \qquad \text{(Eq. 5.7)}$$

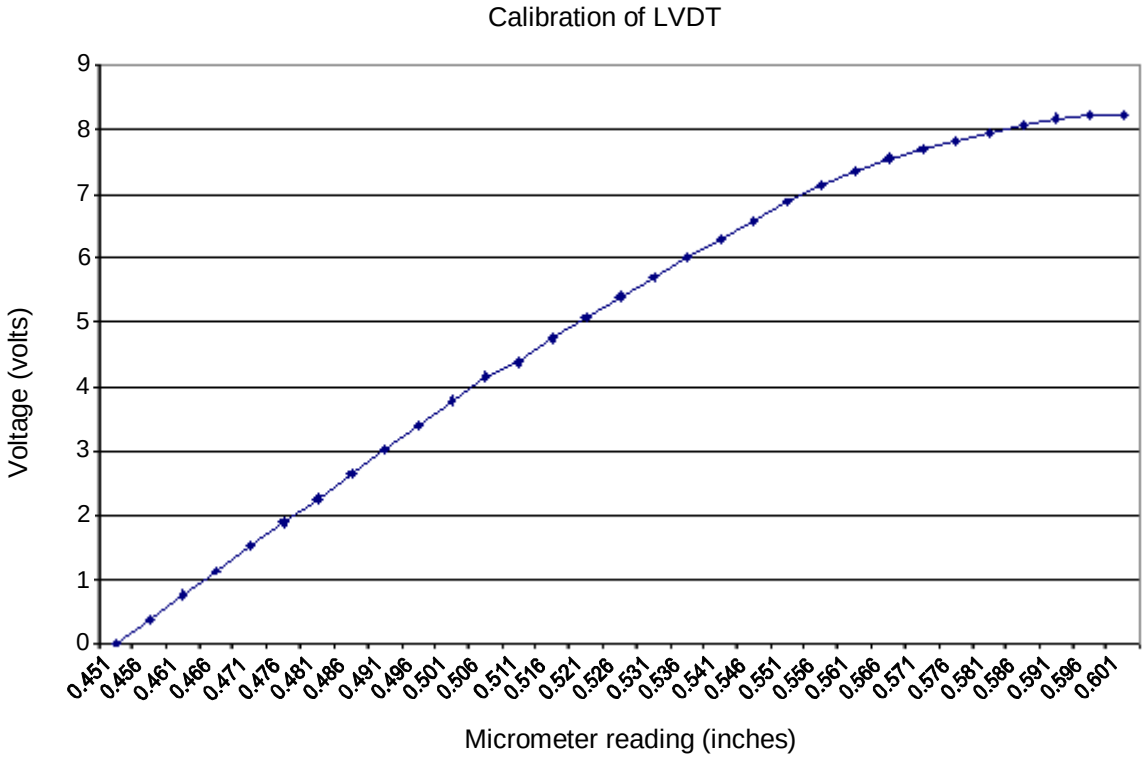

Figure 5-17. A plot of LVDT/conditioner output versus displacement (micrometer reading)

Equation for computation of strain becomes:

$$\text{Strain} = \text{Displacement} / (\text{Gage Length}) = \text{Displacement} / (10 \text{ in. or } 254 \text{ mm})$$

$$= \text{Output (in volts)} \times 0.0013 \qquad \text{(Eq. 5.8)}$$

5.4 Second Refinement of Apparatus – Use of Lubricated Base Plate

Another observed problem with the constrained long specimen apparatus was that the long concrete specimen appeared to be sticking to the steel plate below it.

A wax paper was placed over the steel base plate in an effort to reduce the friction between the concrete specimen and the base plate, as shown in Figure 5-19. However, the wax paper got soaked by the wet concrete and it worsened the problem further. This idea was thus abandoned.

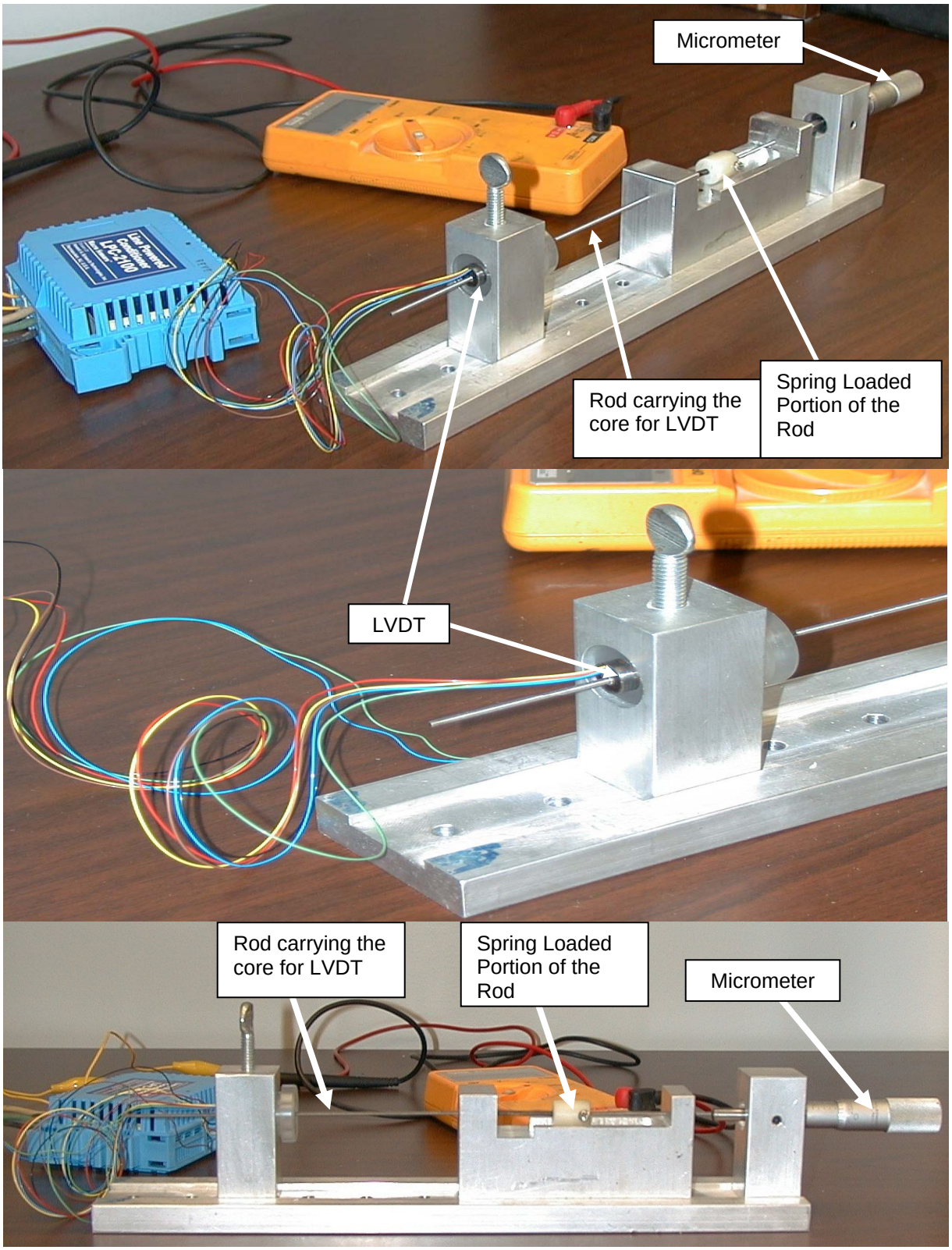

Figure 5-18. Set-up for calibration of LVDTs used in the long specimens

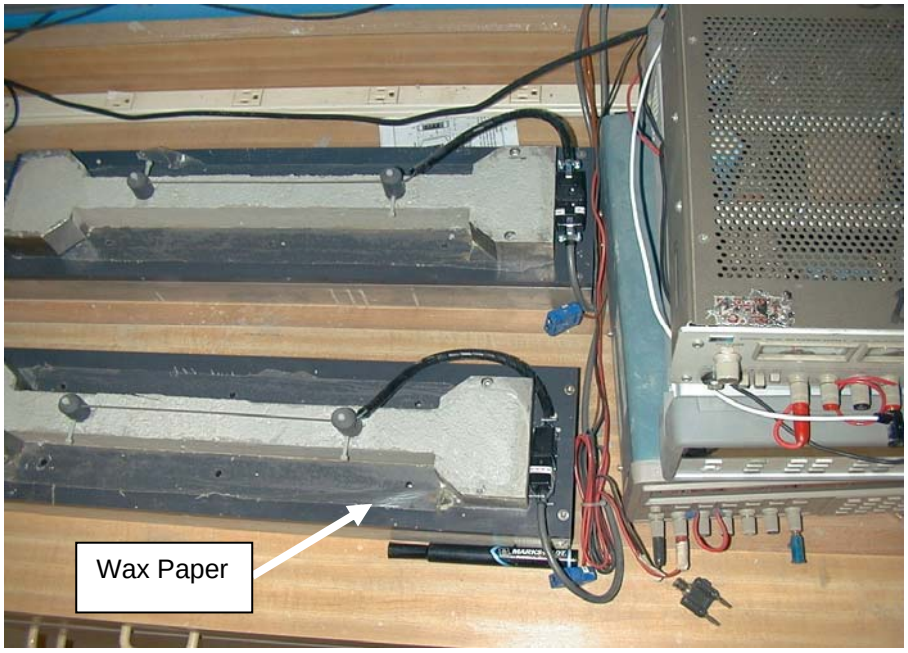

Figure 5-19. Use of wax paper to reduce friction between concrete and base plate

Finally, a water-resistant and low-friction Teflon sheet was used as the base plate of the long constrained specimen apparatus to minimize the friction between the concrete specimen and its supporting base. Figure 5-20 shows a picture of the modified apparatus with the Teflon base plate. The use of Teflon sheets as base plates appears to give good results, and was adopted in this study.

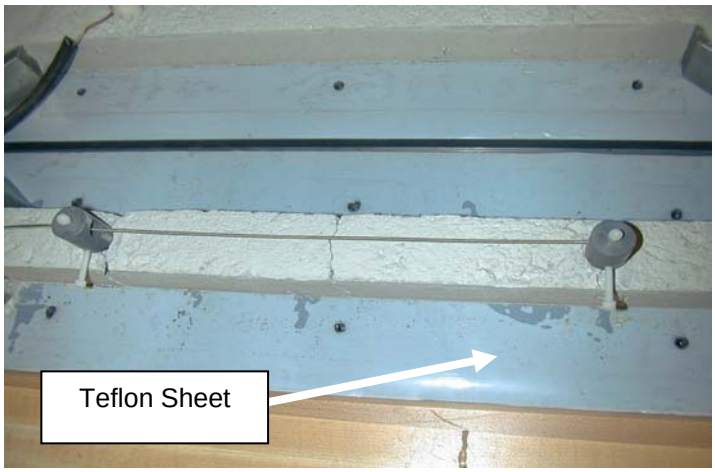

Figure 5-20. Constrained long specimen apparatus with a Teflon base plate

5.5 Third Refinement of Apparatus – Use of Embedment Strain Gages

5.5.1 Embedment Strain Gage

The constrained long specimen apparatus using LVDT for strain measurement had one drawback in that the LVDT could be placed on the specimen only after the concrete has attained sufficient strength. Thus, the shrinkage of the concrete in the very early age could not be measured. In order to monitor the shrinkage of concrete at its very early age after placement, embedment strain gages were used for strain measurement. The embedment gage selected for this purpose was a 4.68-in. (120-mm) long embedment gage for concrete and mortar (KM-120-120-H2-11 made by Soltec-Kyowa Inc). This strain gage has a resistance of 120 Ohms and a gage factor of 2.0. Figure 5-21 shows a picture of two long specimen molds with the embedment strain gages in them.

Figure 5-21. Embedment strain gages inside the long specimen molds

5.5.2 Strain Gage Signal Conditioner

An OMEGA OM2-163 Backplane 8-channel signal conditioner was used to connect the embedment strain gages in a quarter bridge circuit and to amplify the output signals from the bridge circuits. OMEGA OM2-163 is a complete signal conditioning system designed for single half, or full bridge transducers. Figure 5-22 shows the schematics of the setup of the constrained long specimen apparatus using an embedment strain gage for strain measurement. Figure 5-23 shows a picture of the OMEGA OM2-163 Backplane 8-channel signal conditioner used.

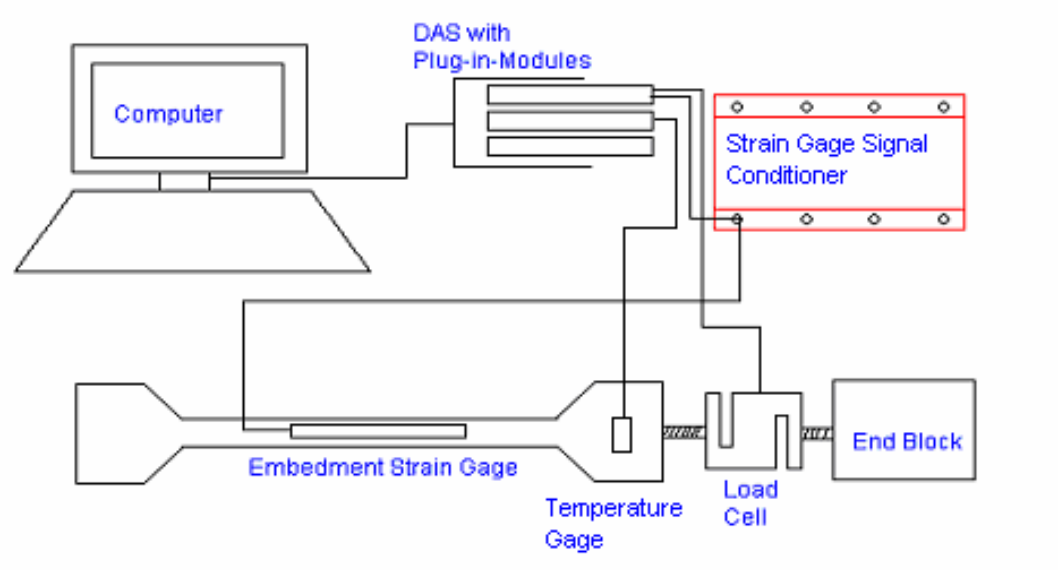

Figure 5-22. Schematics of the constrained long specimen apparatus using an embedment strain gage for strain measurement

Each embedment strain gage was connected to a channel of the signal conditioner in a quarter bridge configuration. An excitation voltage of 4 V and a gain of 333.33 for the output signal were used. The outputs from the signal condition were connected to the data acquisition system. The following equation relates the un-amplified voltage output to the measured strain:

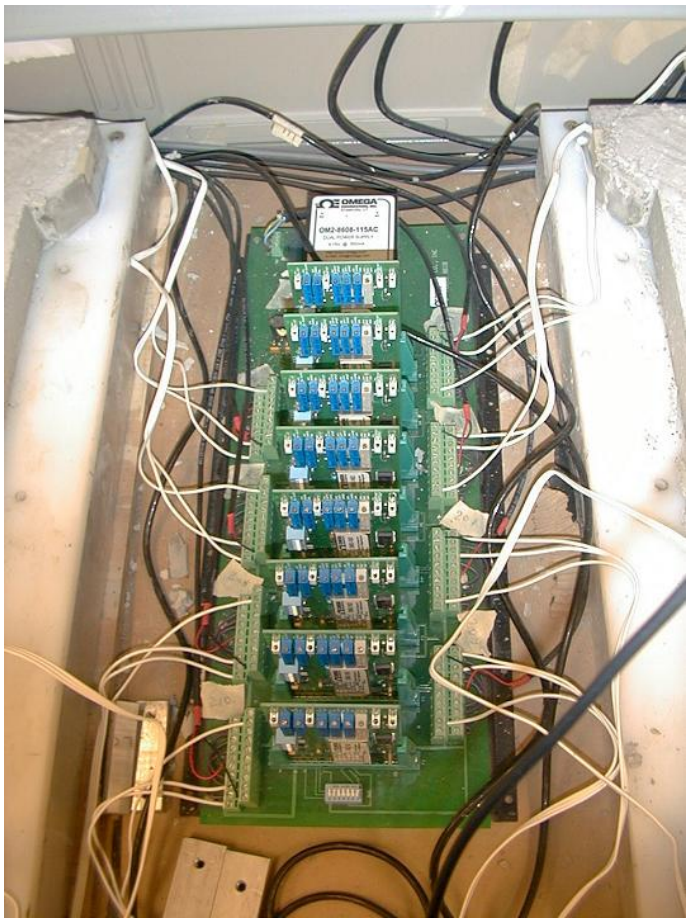

Figure 5-23. OMEGA OM2-163 Backplane 8-channel signal conditioner

$$\text{Strain} = 4\,(\text{Voltage output}) / (\text{Gage Factor})(\text{Excitation Voltage})$$

$$= 4\,(\text{Voltage output}) / 2.0\,(4\text{V})$$

$$= (\text{Voltage output in V}) / 2 \qquad \text{(Eq. 5.9)}$$

With a gain of 333.33 used, the measured strain is related to the amplified voltage output as follows:

$$\text{Strain} = (\text{Amplified voltage output in V}) / (2 \times 333.33)$$

$$= (\text{Amplified voltage output in V}) / (666.67) \qquad \text{(Eq. 5.10)}$$

The instrumentation for the embedment strain gages was set up and tested. The amplified voltage outputs from the strain gage connections were connected to the data acquisition system and tested to be working properly.

The test results appeared to be correct and this set-up was adopted for use to continue the testing of concrete for resistance to shrinkage cracking.

5.6 Fourth Refinement of Apparatus – Zeroing of Strain in the Constrained Specimen

From experimenting with testing of concrete in the constrained long specimen apparatus, it was found that the apparatus was not able to provide complete restraint to the concrete specimen to keep it from contracting during the constrained shrinkage test. Due to the contraction of the specimen during the test, a complete restrained condition was not achieved as intended.

It was decided to provide the correction to the specimen contraction by manually pulling the specimen during the test such that the strain in the specimen would be kept as close to zero as possible. The manual pulling of the test specimen was done by turning a nut on a threaded rod on the test apparatus, which would result in pulling of the test specimen. Figure 5-24 shows how this was done.

The strain reading from the strain gage was used as a guide on how much the specimen needed to be pulled. Every time the specimen was to be pulled for correction for contraction, the specimen would be pulled until the strain was as close to zero as possible. Ideally, this pulling of specimen to zero out the strains in the test specimen should be done as often as possible and as early as possible, so that the strains would remain close to zero throughout the test.

Figure 5-24. Manual pulling of a test specimen to correct for specimen contraction

This manual method of correcting the contraction strains in the constrained long specimen appeared to give acceptable results. Thus, this method was adopted for use in testing the concrete mixtures in the laboratory testing program of this study.

CHAPTER 6
RESULTS OF LABORATORY TESTING PROGRAM

6.1 Introduction

This chapter presents the results of the laboratory testing program which is described in Chapter 4. It includes: (1) the evaluation of the five different methods for measurement of free shrinkage of concrete; (2) the evaluation of the effects of a shrinkage-reducing admixture on the compressive strength, splitting tensile strength, elastic modulus, free shrinkage and resistance to shrinkage cracking of concrete; and (3) the comparison of the resistance to shrinkage cracking of concrete containing fly ash with that containing ground blast-furnace slag as mineral admixture.

6.2 Evaluation of Different Methods of Free Shrinkage Measurement

6.2.1 Methods Evaluated

Five different methods for measuring free shrinkage of concrete were evaluated. These five methods were:

1. Shrinkage measurement using a Whittemore gage in the long specimen apparatus (as described in Section 4.3.6).
2. Shrinkage measurement using a LVDT in the long specimen apparatus (as described in Section 5.3.2).
3. Shrinkage measurement using an embedment gage in the long specimen apparatus (as described in Section 4.3.5).
4. Shrinkage measurement using a Whittemore gage on a 6 in. × 12-in. (152.4 × 304.8-mm) cylindrical specimen (as described in Section 4.3.7).

5. Shrinkage measurement using a LVDT on a 3 in. × 3 in. × 11.25-in. (76 × 76 × 286-mm) square prism specimen according to ASTM C157 procedure (as described in Section 4.3.4).

6.2.2 Comparison of Test Results

Free shrinkage measurements using these five different methods were made on the 15 pairs of concrete mixtures (with and without the addition of a shrinkage-reducing admixture) used in this study. The mix designs for these concrete mixtures are described in Tables 3.1 through 3.15 in Chapter 3. Table 6-1 presents the results of these free shrinkage strain measurements in units of microstrain (10^{-6}) using these five different methods along with their means and variances.

From the comparison of the free shrinkage strain measurements using the different methods, it can be seen that strain measurements using the embedment gage in the long specimen apparatus showed the best repeatability with the lowest variance, with an overall average variance (s^2) of 263, or an overall average standard deviation (s) of 16.2 microstrains. This was followed by the ASTM C157 method using LVDT with an overall average s^2 of 662, or an overall average s of 25.7 microstrains. The strain measurements from the other three methods had much higher variances, with overall average s^2 of 2987, 4695 and 5511, or overall average s of 54.7, 68.5 and 74.2 microstrains.

The shrinkage strains as measured by the ASTM C157 method and the Whittemore gage on the cylindrical specimens were much lower than those from the other three methods using the long specimens. This can be explained by the relatively larger size of the cylindrical concrete specimens and the square prism specimens, which have lower surface area per unit mass, and thus lower drying rates. The long specimens

Table 6-1. Free Shrinkage Strains of the 15 Pairs of Concrete Mixtures as Measured by the Different Methods

Free Shrinkage Strains as Measured by Different Methods, in 10^{-6}																					
Time (Days)	Whittemore Gage on Long Specimen				LVDT on Long Specimen				Embedment Gage on Long Specimen				Whittemore Gage on Cylinder				LVDT on ASTM C157 Prism				
	1	2	μ	s^2	1	2	μ	s^2	1	2	μ	s^2	1	2	μ	s^2	1	2	3	μ	s^2
Mix 1 Standard																					
3	200	180	190	200	358	312	335	1066	155	141	148	96	42	68	55	356	53	84	67	68	240
7	330	305	318	313	377	354	366	247	317	283	300	563	43	93	68	1250	161	200	177	179	376
14	350	320	335	450	473	452	462	214	406	354	380	1340	123	135	129	68	242	298	264	268	788
Mix 1 SRA																					
3	90	40	65	1250	142	-	142	-	75	71	73	6	40	20	30	200	23	15	19	19	15
7	180	240	210	1800	238	-	238	-	183	182	183	0	52	130	91	3003	87	80	86	84	12
14	230	250	240	200	343	-	343	-	264	249	257	105	60	220	140	12800	158	145	153	152	39
Mix 2 Standard																					
3	220	300	260	3200	319	242	281	3005	196	182	189	104	25	53	39	378	67	83	124	91	847
7	370	500	435	8450	461	381	421	3199	323	316	320	25	67	133	100	2113	189	209	242	213	715
14	380	520	450	9800	478	469	474	43	404	390	397	103	32	113	72	3200	258	276	306	280	568
Mix 2 SRA																					
3	75	140	107	2113	80	110	95	464	88	97	92	42	48	58	53	50	22	22	21	22	0
7	140	125	132	112	138	171	154	529	174	160	167	93	57	78	68	200	119	71	103	98	590
14	195	205	200	50	176	192	184	135	241	233	237	25	38	35	36	3	159	108	136	134	651
Mix 3 Standard																					
3	180	10	95	14450	390	292	341	4810	178	149	163	409	43	38	40	13	30	77	-	53	1083
7	330	160	245	14450	523	473	498	1208	314	332	323	163	58	70	64	78	131	201	-	166	2425
14	380	160	270	24200	523	540	531	133	376	414	395	718	218	155	186	1953	221	309	-	265	3849
Mix 3 SRA																					
3	-	15	15	-	25	37	31	74	107	86	97	230	20	25	22	13	54	33	28	38	193
7	-	171	171	-	143	188	166	996	227	210	219	144	205	57	131	10878	78	79	57	71	149
14	-	380	380	-	218	247	233	402	307	299	303	32	220	348	284	8128	140	142	114	132	236

Table 6-1– continued

Free Shrinkage Strains as Measured by Different Methods, in 10^{-6}																				
Time (Days)	Whittemore Gage on Long Specimen				LVDT on Long Specimen				Embedment Gage on Long Specimen				Whittemore Gage on Cylinder				LVDT on ASTM C157 Prism				
	1	2	μ	s^2	1	2	μ	s^2	1	2	μ	s^2	1	2	μ	s^2	1	2	3	μ	s^2
Mix 4 Standard																					
3	8	50	29	903	164	233	198	2355	132	151	142	192	80	170	125	4050	42	68	37	49	282
7	260	129	194	8646	283	362	323	3141	238	262	250	289	140	183	161	903	130	162	126	139	393
14	535	308	421	25878	343	428	385	3620	302	331	317	407	233	330	281	4753	230	268	228	242	521
Mix 4 SRA																					
3	85	95	90	50	56	44	50	71	27	61	44	598	70	65	67	12	2	0	1	1	0
7	100	130	115	450	125	112	118	76	96	125	110	433	77	148	113	2450	44	41	43	43	1
14	240	225	232	113	166	199	183	561	165	197	181	505	110	153	131	903	101	101	103	102	1
Mix 5 Standard																					
3	100	125	113	312	182	116	149	2190	122	105	114	145	72	275	173	20672	37	69	34	47	370
7	185	250	218	2113	334	252	293	3363	278	230	254	1123	183	420	301	28203	110	151	109	123	572
14	290	250	270	800	352	301	327	1264	343	281	312	1942	338	518	428	16200	204	253	200	219	876
Mix 5 SRA																					
3	110	35	72	2813	18	33	25	111	41	48	44	26	93	10	51	3403	10	13	8	10	6
7	210	110	160	5000	113	65	89	1169	111	123	117	62	168	275	221	5778	41	44	43	43	2
14	340	225	282	6612	288	165	226	7536	181	187	184	21	265	340	303	2813	96	100	95	97	6
Mix 6 Standard																					
3	8	50	29	903	34	91	62	1675	47	43	45	10	150	173	161	253	55	52	54	54	3
7	260	129	194	8646	209	433	321	25099	248	231	240	147	305	203	254	5253	167	170	168	168	2
14	535	308	421	25878	274	580	427	47099	336	315	326	220	353	300	326	1378	258	271	261	263	47
Mix 6 SRA																					
3	60	110	85	1250	16	16	16	0	16	9	13	29	265	133	199	8778	7	50	11	23	563
7	135	215	175	3200	144	93	118	1302	141	140	141	1	283	345	314	1953	68	10	6	28	1206
14	165	290	228	7812	203	163	183	832	211	217	214	17	325	423	374	4753	130	71	7	70	3784

Table 6-1– continued

Free Shrinkage Strains as Measured by Different Methods, in 10^{-6}																				
Time (Days)	Whittemore Gage on Long Specimen				LVDT on Long Specimen				Embedment Gage on Long Specimen				Whittemore Gage on Cylinder				LVDT on ASTM C157 Prism				
	1	2	μ	s^2	1	2	μ	s^2	1	2	μ	s^2	1	2	μ	s^2	1	2	3	μ	s^2
Mix 7 Standard																					
3	200	180	190	200	125	92	108	565	105	107	106	2	42	68	55	356	42	54	37	44	77
7	330	305	318	313	264	193	228	2560	207	205	206	1	43	93	68	1250	110	128	103	113	163
Mix 7 SRA																					
3	-	-	-	-	10	29	19	178	24	26	25	2	40	20	30	200	5	9	8	7	4
7	-	-	-	-	70	109	89	752	86	85	85	0	52	130	91	3003	29	38	37	35	23
Mix 8 Standard																					
3	39	132	86	4356	113	70	91	949	105	100	103	9	30	50	40	200	96	89	80	88	63
7	174	152	163	247	222	132	177	4075	197	191	194	23	68	153	110	3612	167	162	149	159	88
Mix 8 SRA																					
3	75	140	107	2113	24	28	26	12	33	32	32	0	27	58	42	465	41	37	38	39	5
7	140	125	132	112	83	68	76	118	86	86	86	0	75	95	85	200	68	63	65	66	7
Mix 9 Standard																					
3	50	45	48	13	100	83	91	137	65	70	68	13	27	18	22	38	9	16	10	12	16
7	160	185	173	313	275	259	267	132	199	208	204	42	62	82	72	200	77	84	75	79	19
Mix 9 SRA																					
3	-	-	-	-	13	12	12	1	21	23	22	4	28	12	20	113	1	2	1	1	0
7	-	-	-	-	75	106	90	479	83	83	83	0	60	45	52	112	17	15	23	18	15
Mix 10 Standard																					
3	75	105	90	450	153	119	136	576	83	76	79	28	22	32	27	50	56	51	50	52	10
7	180	135	158	1013	246	199	223	1114	186	180	183	17	45	57	51	78	112	115	111	113	5
Mix 10 SRA																					
3	-	-	-	-	33	1	17	522	22	8	15	93	30	33	31	3	23	21	18	20	4
7	-	-	-	-	22	58	40	646	70	40	55	448	75	80	77	12	44	42	41	42	3

Table 6-1– continued

Free Shrinkage Strains as Measured by Different Methods, in 10^{-6}																				
Time (Days)	Whittemore Gage on Long Specimen				LVDT on Long Specimen				Embedment Gage on Long Specimen				Whittemore Gage on Cylinder				LVDT on ASTM C157 Prism				
	1	2	μ	s^2	1	2	μ	s^2	1	2	μ	s^2	1	2	μ	s^2	1	2	3	μ	s^2
Mix 11 Standard																					
3	70	15	43	1512	166	47	107	7162	96	109	102	84	15	27	21	78	46	149	55	83	3279
7	150	220	185	2450	342	61	202	39447	240	253	247	87	80	95	87	113	149	255	153	185	3589
Mix 11 SRA																					
3	-	-	-	-	43	14	29	438	35	42	38	28	35	15	25	200	25	31	25	27	15
7	-	-	-	-	167	124	145	947	118	128	123	58	55	45	50	50	64	69	66	66	5
Mix 12 Standard																					
3	75	190	132	6612	331	133	232	19525	210	173	191	666	135	115	125	200	52	108	60	73	906
7	690	350	520	57800	459	249	354	21985	336	290	313	1076	175	150	163	313	198	211	108	172	3163
Mix 12 SRA																					
3	-	-	-	-	37	76	56	766	90	77	83	85	80	80	80	0	34	60	52	49	173
7	-	-	-	-	133	165	149	525	168	159	164	37	110	110	110	0	116	95	95	102	154
Mix 13 Standard																					
3	90	180	135	4050	267	218	242	1208	198	226	212	392	45	92	69	1128	69	103	120	97	691
7	155	305	230	11250	430	366	398	2026	371	410	390	746	95	153	124	1653	241	241	249	244	25
Mix 13 SRA																					
3	-	-	-	-	121	96	108	304	93	79	86	102	55	35	45	200	26	17	52	32	321
7	-	-	-	-	234	214	224	217	190	176	183	106	110	92	101	168	103	52	103	86	888

Table 6-1– continued

Free Shrinkage Strains as Measured by Different Methods, in 10^{-6}																					
Time (Days)	Whittemore Gage on Long Specimen				LVDT on Long Specimen				Embedment Gage on Long Specimen				Whittemore Gage on Cylinder				LVDT on ASTM C157 Prism				
	1	2	μ	s^2	1	2	μ	s^2	1	2	μ	s^2	1	2	μ	s^2	1	2	3	μ	s^2
Mix 14 Standard																					
3	65	-	65	-	148	61	105	3844	98	90	94	28	27	5	16	253	26	26	34	29	25
7	130	-	130	-	194	91	142	5349	172	151	162	225	83	73	78	50	99	90	73	87	173
Mix 14 SRA																					
3	-	-	-	-	68	78	73	48	38	36	37	2	18	52	35	584	34	17	52	34	296
7	-	-	-	-	109	99	104	50	86	82	84	11	65	78	72	89	146	120	138	135	173
Mix 15 Standard																					
3	155	-	155	-	137	131	134	22	156	143	149	87	30	100	65	2450	52	60	69	60	74
7	185	-	185	-	156	138	147	163	238	217	228	222	65	128	96	1953	112	103	112	109	25
Mix 15 SRA																					
3	-	-	-	-	94	99	97	11	77	74	75	4	50	35	42	113	17	17	26	20	25
7	-	-	-	-	139	153	146	92	127	120	124	20	90	75	82	112	34	34	34	34	0
Overall Average																					
			147	5511		159	4695			137	263			96	2987					75	662

had a relatively lower thickness and higher surface area per unit mass, and thus a higher drying rate. Among the three methods of measuring free shrinkage of the long specimens, the embedment gage method gave lower strain measurements than those by the Whittemore gage or the LVDT methods. This can be explained by the fact that the Whittemore gage points and the LVDT were attached to the surface of the specimen, which dried out faster than the inner part of the specimen where the embedment gage was placed.

Figures 6-1 through 6-5 show plots of free shrinkage strains versus time as measured by the five different methods for the first six standard mixes (without SRA). It can be observed that the strains as measured by the embedment gage method (as shown in Figure 6-3) and the ASTM C157 method (as shown in Figure 6-5) show much more even changes with time. These observations indicate that the data from these two methods appear to be more reasonable.

6.2.3 Observations on the Different Methods of Shrinkage Measurement

Whittemore Gage on the Long Specimen

This method has the advantage that the Whittemore gage is a simple mechanical gage that does not require any electronic system for it to work. It can be calibrated reliably with an invar bar before each measurement is made.

The limitation of this method is that the Whittemore gage is a manual gage, and thus the strains cannot be monitored conveniently. Another limitation is that it requires sufficient curing time before the gage points can be held securely by the concrete before readings can be taken with the Whittemore gage. For the concrete mixes evaluated in this study, it required a minimum of 24 hours before readings could be started.

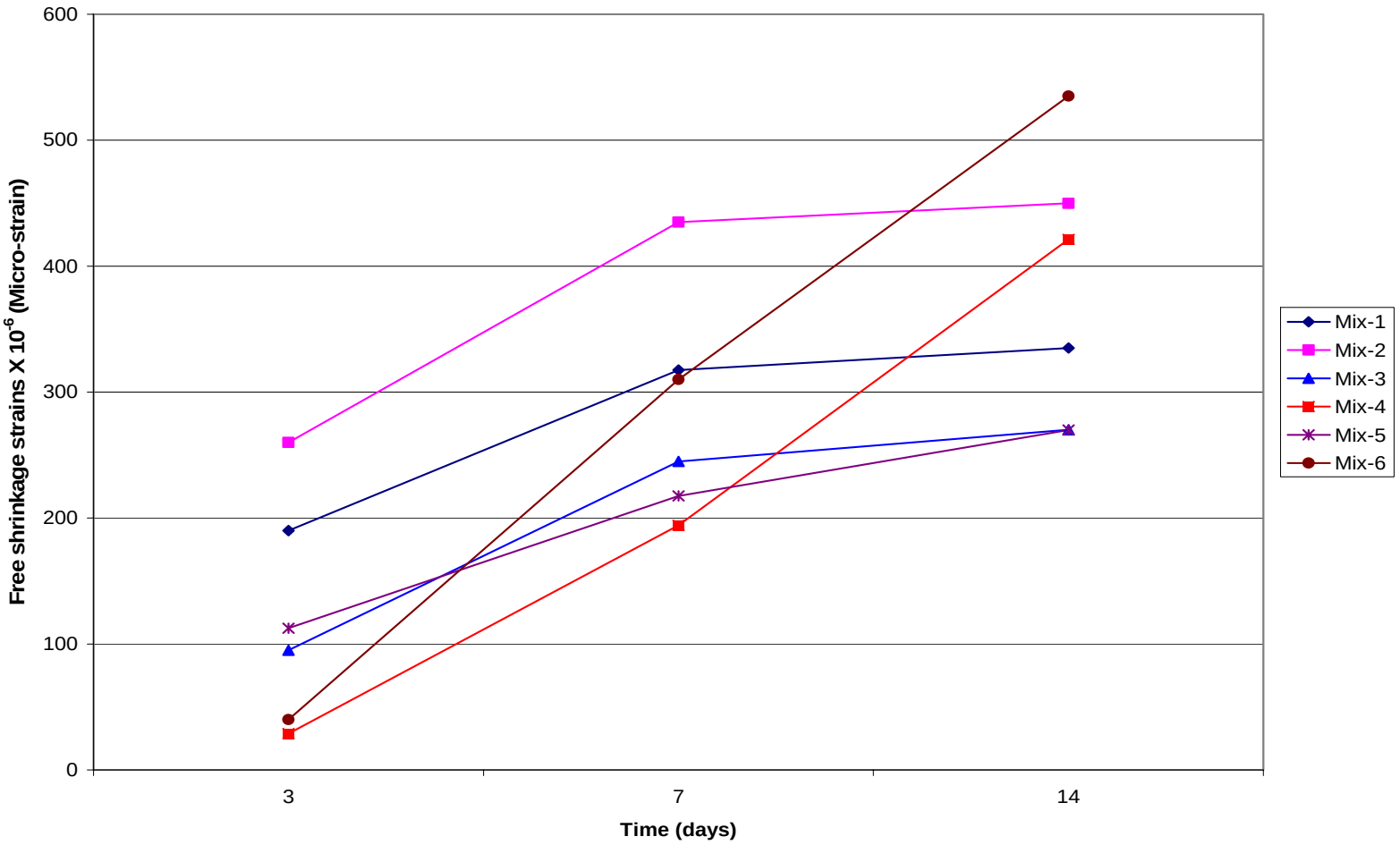

Figure 6-1. Free shrinkage strains as measured by Whittemore gage on the long specimens for six standard mixes

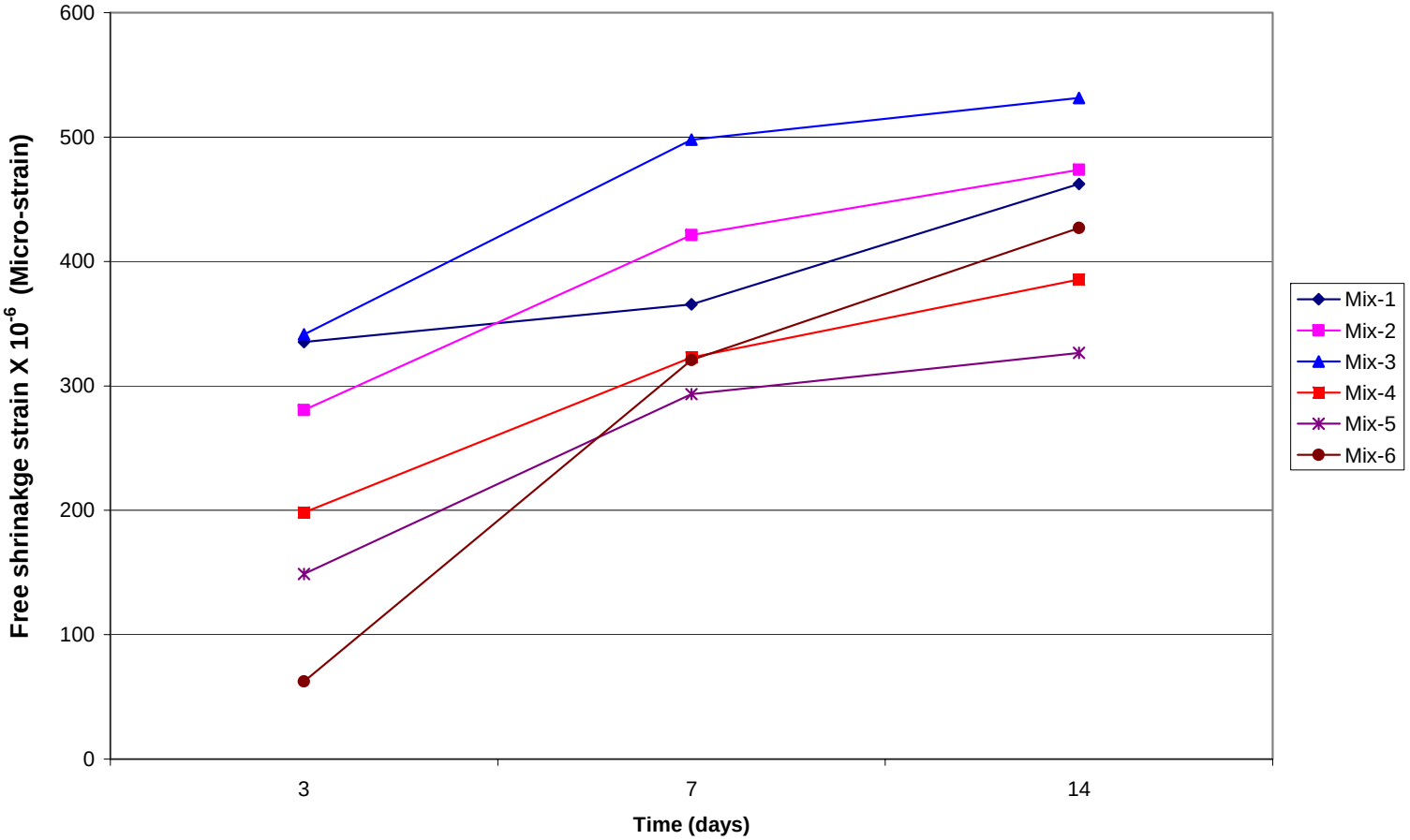

Figure 6-2. Free shrinkage strains as measured by LVDT on the long specimens for six standard mixes

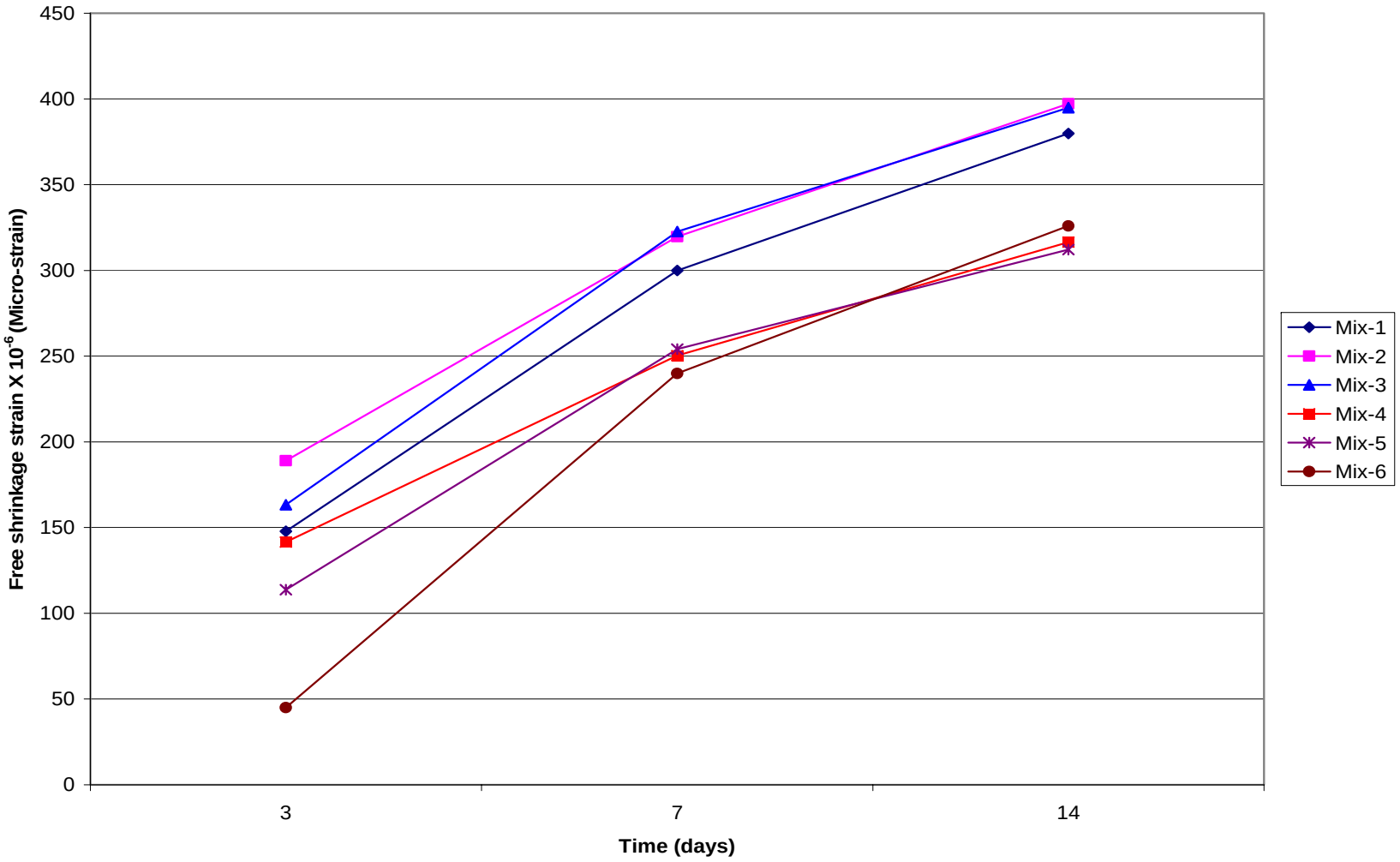

Figure 6-3. Free shrinkage strains as measured by embedment gages in the long specimens for six standard mixes

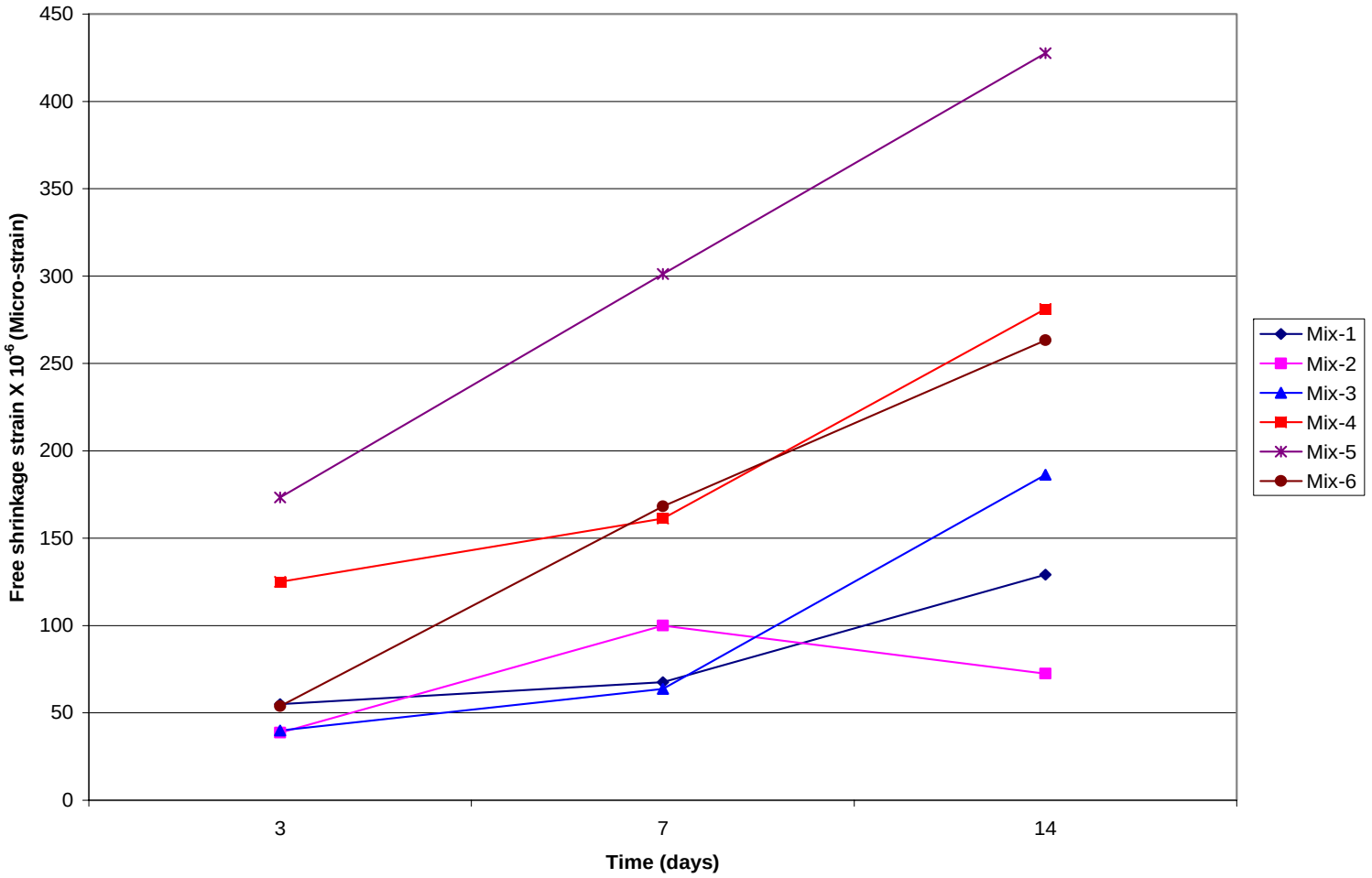

Figure 6-4. Free shrinkage strains as measured by Whittemore gage on the cylinders for six standard mixes

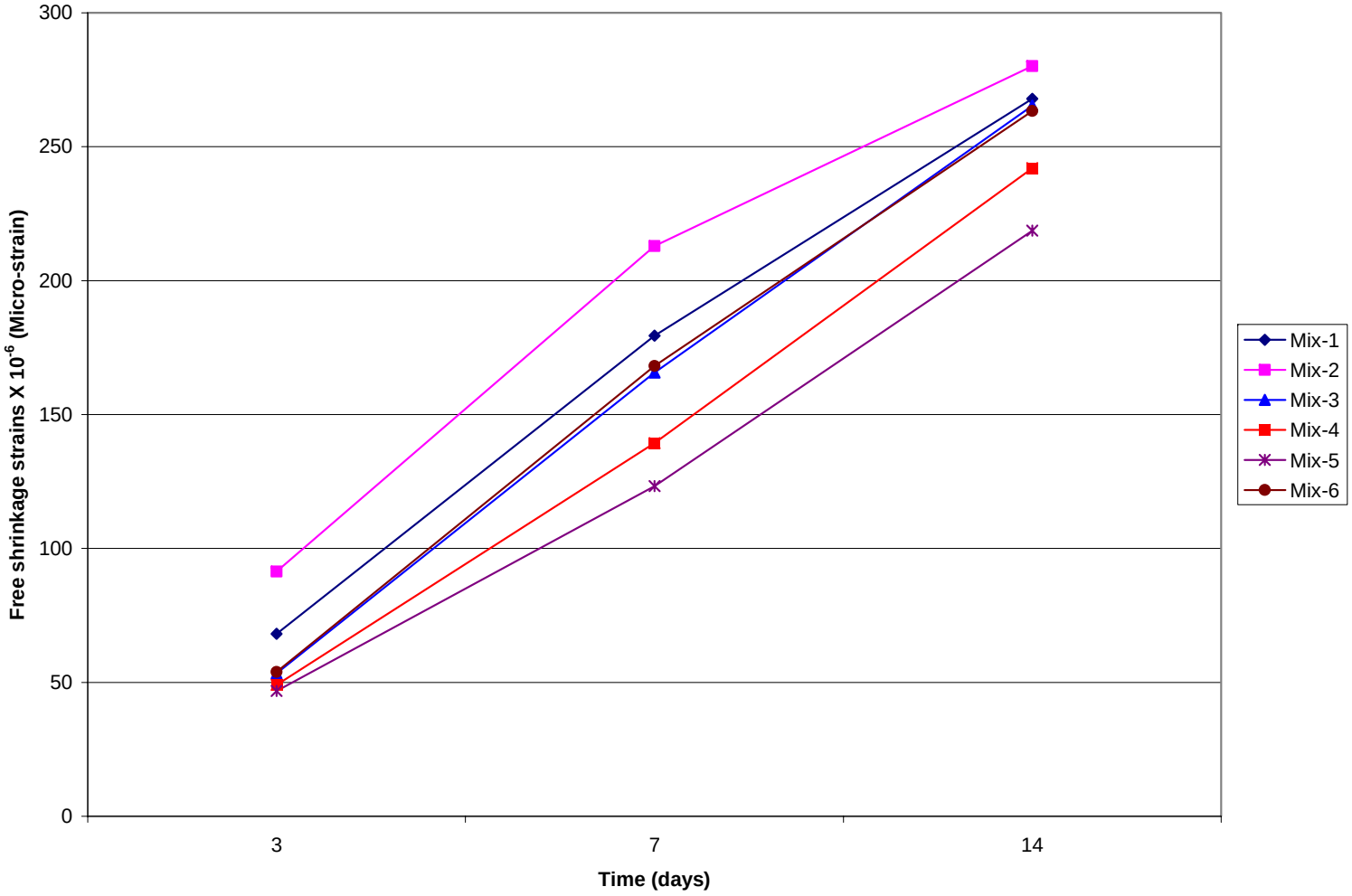

Figure 6-5. Free shrinkage strains as measured by ASTM C157 Method for six standard mixes

LVDT on the Long Specimen

This method has the advantage that strain readings can be taken automatically and continuously throughout the test.

The limitation of this method is that it requires sufficient curing time before the gage studs (that hold the LVDT and the core rod holder) can be held securely by the concrete before the LVDT and the core rod holder can be attached and readings can be taken with the LVDT. For the concrete mixes evaluated in this study, it required a minimum of 24 hours before readings could be started.

Embedment Gage in the Long Specimen

This method has the advantage that strain readings can be taken automatically and continuously throughout the test. Since embedment gage is embedded in the concrete from the very beginning, strain readings can be started at a very early age of the concrete.

The disadvantage of this method is the relatively higher cost of the test, as the embedment gage is not reusable after each test.

Whittemore Gage on a Cylindrical Specimen

This method has the advantage that the Whittemore gage is a simple mechanical gage that can be calibrated conveniently and reliably with an invar bar before each measurement is made.

The limitation of this method is that the Whittemore gage is a manual gage, and thus the strains cannot be monitored conveniently. Another limitation is that it requires sufficient curing time for the concrete to be able to hold the gage points securely before the molds can be removed and readings with the Whittemore gage can be started. For the

concrete mixes evaluated in this study, it required a minimum of 24 hours before readings could be started.

ASTM C157 Method using a LVDT

The advantage of this method is that it is already a fairly well developed procedure for measurement of shrinkage strains of concrete. With the use of a LVDT, the strains can be conveniently monitored throughout the test.

The limitation of this method is that sufficient curing time is needed before the specimens can be taken out from the mold and strain readings can be started. For concrete mixes evaluated in this study, it required a minimum of 24 hours before readings could be started. Another limitation of this method is that, since it uses a different specimen size from that for the constrained long specimen test, the free shrinkage measurements from this method cannot be applied directly to the constrained long specimen test without proper adjustments.

6.2.4 Recommended Method

In consideration of the good repeatability and reasonableness of the strain measurements, and that the strain measurements can be made from a very early age of the concrete, the embedment gage method was selected to be used for measurement of free shrinkage and for measurement of strain in the constrained long specimen test.

6.3 Evaluation of the Effects of a Shrinkage-Reducing Admixture

6.3.1 Effects on Free Shrinkage

Table 6-2 lists the average free shrinkage strains as measured by the embedment strain gages on the long specimens for the 15 pairs of concrete mixtures (with and without the addition of a shrinkage-reducing admixture), which were evaluated

Table 6-2. Percentage Reduction in Free Shrinkage Strains of the SRA Mixtures as Compared With the Standard Mixtures as Measured by the Embedment Strain Gages in the Long Specimens

% Reduction in Free shrinkage strains of SRA Mixtures over Standard							
Mix	Type	Curing time (days)					
		3		7		14	
		Average Strain, 10^{-6}	% Reduction	Average Strain, 10^{-6}	% Reduction	Average Strain, 10^{-6}	% Reduction
1	Standard	148	51	300	39	380	32
	SRA	73		183		257	
2	Standard	189	51	320	48	397	40
	SRA	92		167		237	
3	Standard	163	41	323	32	395	23
	SRA	97		219		303	
4	Standard	142	69	250	56	317	43
	SRA	44		110		181	
5	Standard	114	61	254	54	312	41
	SRA	44		117		184	
6	Standard	45	72	240	41	326	34
	SRA	13		141		214	
7	Standard	106	76	206	59	N/A	N/A
	SRA	25		85		N/A	N/A
8	Standard	103	68	194	56	N/A	N/A
	SRA	32		86		N/A	N/A
9	Standard	68	68	204	59	N/A	N/A
	SRA	22		83		N/A	N/A
10	Standard	79	81	183	70	N/A	N/A
	SRA	15		55		N/A	N/A
11	Standard	102	62	247	50	N/A	N/A
	SRA	38		123		N/A	N/A
12	Standard	191	57	313	48	N/A	N/A
	SRA	83		164		N/A	N/A
13	Standard	212	59	390	53	N/A	N/A
	SRA	86		183		N/A	N/A
14	Standard	94	61	162	48	N/A	N/A
	SRA	37		84		N/A	N/A
15	Standard	149	50	228	46	N/A	N/A
	SRA	75		124		N/A	N/A
μ			62		51		36

in this study. The percentage reduction in free shrinkage strains of the mixtures containing SRA as compared with the standard mixtures without SRA were computed and presented in this table. It can be seen that the addition of SRA reduced the free

shrinkage substantially for all mixes. The percentage reduction varies from 41 to 81% at 3 days, from 32 to 70% at 7 days, and from 23 to 43% at 14 days. The comparison of free shrinkage strains between the standard and the SRA mixtures are plotted in Figures 6-6 through 6.8 for 3, 7 and 14 days of curing, respectively.

6.3.2 Effects on Shrinkage-Induced Stress

The modified constrained long specimen test, as described in Section 5.3 and with the refinements as described in Sections 5.4, 5.5 and 5.6, was performed on the 15 pairs of concrete mixtures (with and without the addition of SRA). The analysis method as described in Section 5.2.3 was used to analyze the test results and to compute the induced shrinkage stresses under a fully constrained condition. Table 6-3 presents the test results and the computed shrinkage-induced stresses for all the mixtures evaluated along with the splitting tensile strength of the concrete at the corresponding curing times. When the computed shrinkage-induced stress exceeds the tensile strength of the concrete at the corresponding curing time, it means that the concrete would have cracked due to drying shrinkage under a fully constrained condition.

It can be seen from Table 6-3 that the SRA mixtures had substantially lower computed induced shrinkage stresses than their corresponding standard mixtures. The results predict that 6 of the 15 standard mixtures would have cracked within 3 days under a fully constrained condition, while none of the SRA mixtures would crack under a similar condition. The comparison of the shrinkage-induced stresses of the standard and SRA mixtures is shown in Figures 6-9 and 6-10 for the curing times of 3 and 7 days, respectively. Table 6-4 presents the percentage reduction of computed induced shrinkage stresses due to the addition of SRA. The percentage reduction ranges from 20 to 88%

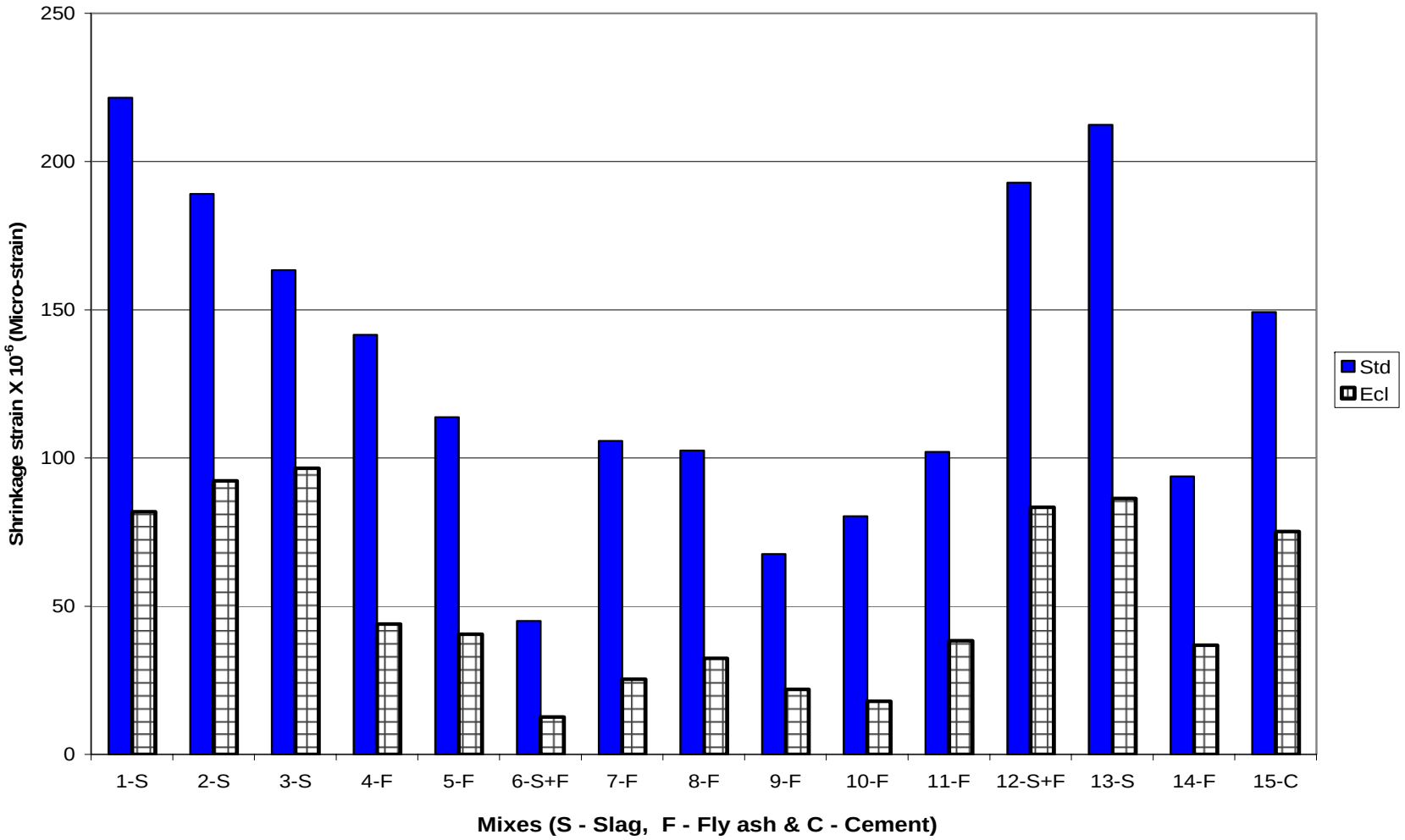

Figure 6-6. Comparison of free shrinkage strains of Standard and SRA mixtures at 3 days curing

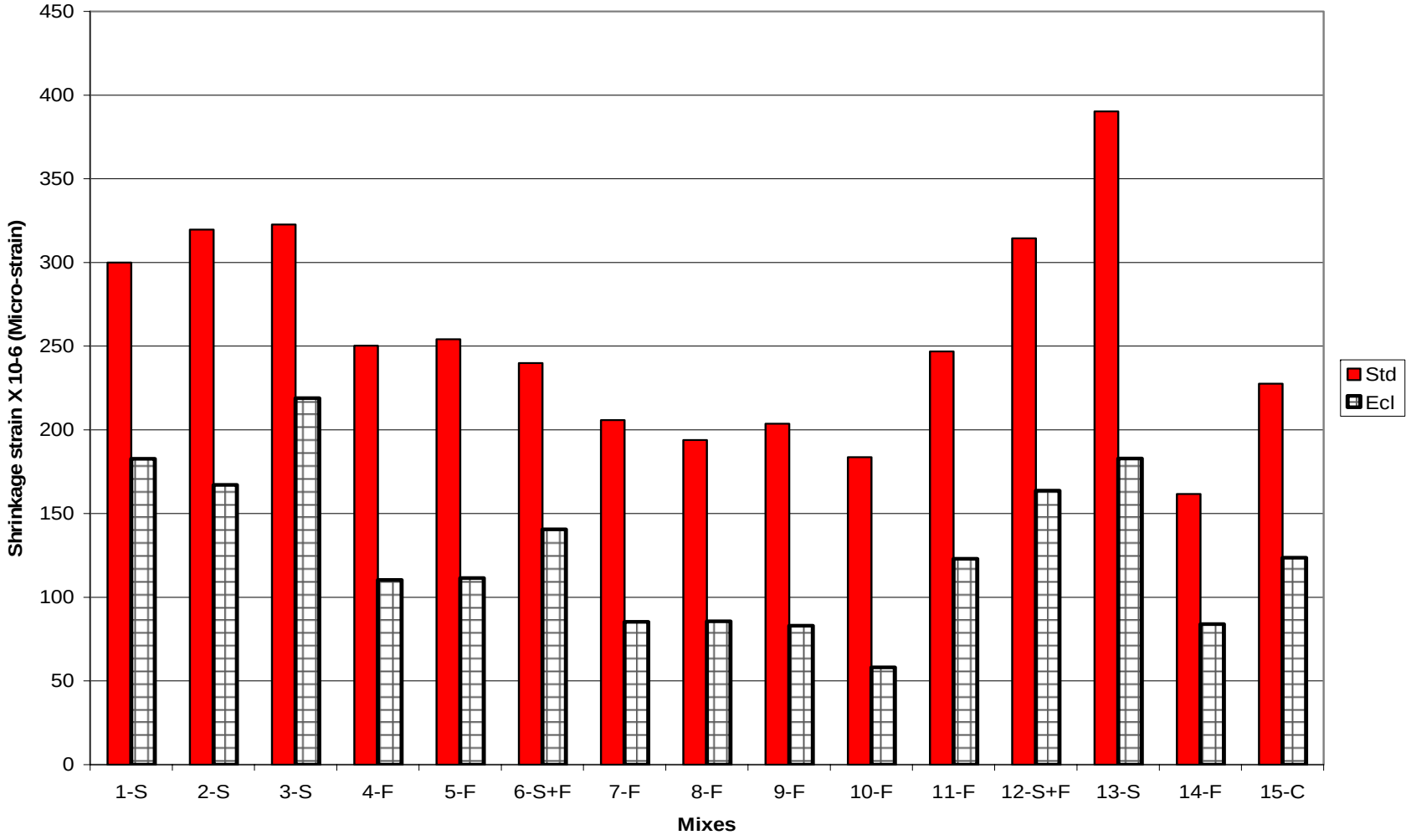

Figure 6-7. Comparison of free shrinkage strains of Standard and SRA mixtures at 7 days curing

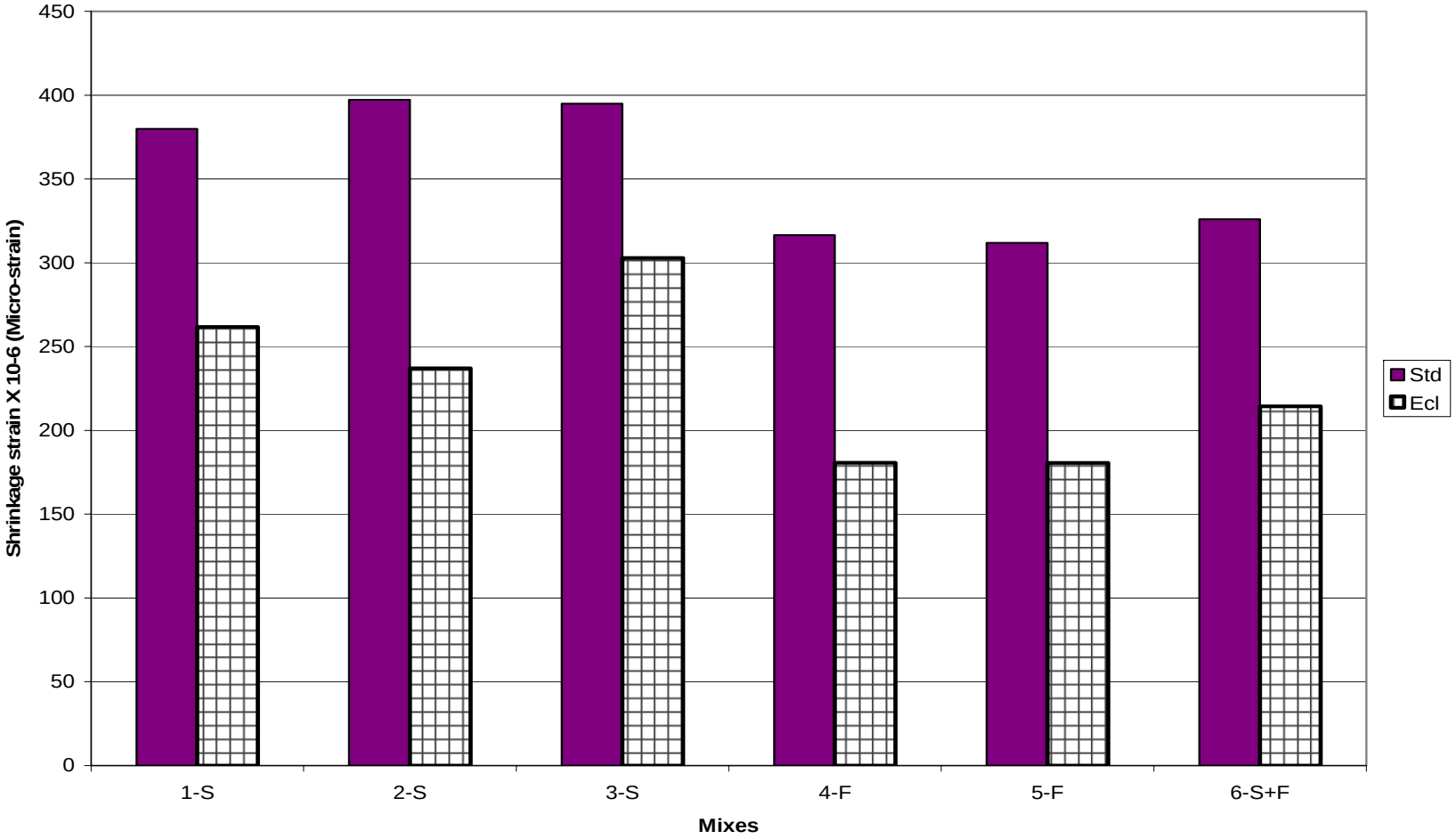

Figure 6-8. Comparison of free shrinkage strains of Standard and SRA mixtures at 14 days curing

Table 6-3. Results of Constrained Long Specimen Test on the 15 Pairs of Concrete Mixtures

Time (Days)	E (psi)	Specim. Stress, σ_E (psi)	Elastic Strain, ε_E	Free Shrinkage Strain, ε_{sh}	Total Specimen Strain, ε_{CL}	Creep Strain, ε_{CR}	Computed Shrinkage Stress, σ_{FC} (psi)	Splitting Tensile Strength (psi)
Mix - 1								
Standard								
3	4455155	103	0.000023	0.000222	0.000104	0.000094	569*	381
7	5150415	157	0.000030	0.000300	0.000194	0.000076	1151*	594
14	5535946	185	0.000033	0.000380	0.000204	0.000142	1314*	614
SRA								
3	4731254	106	0.000022	0.000082	0.000026	0.000033	234	397
7	5404991	164	0.000030	0.000183	0.000043	0.000110	394	603
14	5716239	175	0.000031	0.000262	0.000072	0.000159	588	718
Mix - 2								
Standard								
3	6427326	138	0.000022	0.000189	0.000084	0.000083	682*	376
7	7168223	194	0.000027	0.000320	0.000120	0.000172	1058*	617
14	7285077	192	0.000026	0.000397	0.000154	0.000217	1316*	695
SRA								
3	6538004	23	0.000003	0.000092	0.000012	0.000077	95	395
7	6981284	60	0.000009	0.000167	0.000112	0.000047	813*	607
14	7068646	88	0.000012	0.000237	0.000171	0.000054	1290*	644
Mix - 3								
Standard								
3	2905150	28	0.000010	0.000163	0.000115	0.000270	362	381
7	3427850	210	0.000061	0.000323	0.000204	0.000058	908*	594
14	4082624	236	0.000058	0.000395	0.000247	0.000090	1243*	614
SRA								
3	3650126	10	0.000003	0.000097	0.000076	0.000018	288	397
7	4185281	138	0.000033	0.000219	0.000153	0.000033	779*	603
14	4193226	168	0.000040	0.000303	0.000215	0.000048	1069*	718

Table 6-3 – continued

Time (days)	E (psi)	Specim. Stress, σ_E (psi)	Elastic Strain, ε_E	Free Shrinkage Strain, ε_{sh}	Total Specimen Strain, ε_{CL}	Creep Strain, ε_{CR}	Computed Shrinkage Stress, σ_{FC} (psi)	Splitting Tensile Strength (psi)
Mix - 4								
Standard								
3	3055865	51	0.000017	0.000142	0.000065	0.000060	249	376
7	3462333	108	0.000031	0.000250	0.000147	0.000072	618*	617
14	3901191	139	0.000036	0.000317	0.000195	0.000086	899*	695
SRA								
3	3008550	79	0.000026	0.000044	0.000004	0.000013	92	395
7	3343896	151	0.000045	0.000110	0.000034	0.000031	267	607
14	3856788	167	0.000043	0.000181	0.000090	0.000047	507	644
Mix - 5								
Standard								
3	2861518	59	0.000021	0.000114	0.000045	0.000048	187	381
7	3441955	154	0.000045	0.000254	0.000123	0.000087	575	594
14	3619022	180	0.000050	0.000312	0.000167	0.000095	783*	614
SRA								
3	2869918	47	0.000016	0.000041	0.000010	0.000014	76	397
7	3336697	102	0.000030	0.000111	0.000057	0.000024	293	603
14	3568982	120	0.000034	0.000181	0.000128	0.000019	576	718
Mix - 6								
Standard								
3	4455155	48	0.000011	0.000045	0.000003	0.000031	1314*	381
7	5150415	70	0.000014	0.000240	0.000132	0.000094	753*	594
14	5535946	76	0.000014	0.000326	0.000188	0.000124	1121*	614
SRA								
3	5404263	57	0.000011	0.000013	0.000013	-0.000011	127	397
7	6250985	71	0.000011	0.000141	0.000140	-0.000011	947*	603
14	6457045	76	0.000012	0.000214	0.000225	-0.000023	1530*	718

Table 6-3 – continued

Time (Days)	E (psi)	Specim. Stress, σ_E (psi)	Elastic Strain, ε_E	Free Shrinkage Strain, ε_{sh}	Total Specimen Strain, ε_{CL}	Creep Strain, ε_{CR}	Computed Shrinkage Stress, σ_{FC} (psi)	Splitting Tensile Strength (psi)
Mix - 7								
Standard								
3	3606318	51	0.000014	0.000106	0.000069	0.000023	300	381
7	3992038	130	0.000033	0.000206	0.000141	0.000032	696*	594
SRA								
3	3388225	35	0.000010	0.000025	0.000008	0.000007	64	397
7	3785151	110	0.000029	0.000085	0.000042	0.000014	269	603
Mix - 8								
Standard								
3	3684585	99	0.000027	0.000103	0.000067	0.000009	346	381
7	4046461	149	0.000037	0.000194	0.000128	0.000029	667*	594
SRA								
3	4161028	48	0.000012	0.000032	0.000018	0.000003	122	397
7	4293893	89	0.000021	0.000086	0.000057	0.000008	334	603
Mix - 9								
Standard								
3	2820558	51	0.000018	0.000068	0.000024	0.000026	118	381
7	3273363	130	0.000040	0.000204	0.000112	0.000052	497	594
SRA								
3	2963033	35	0.000012	0.000022	0.000006	0.000004	53	397
7	3300901	110	0.000033	0.000083	0.000029	0.000021	204	603

Table 6-3 – continued

Time (Days)	E (psi)	Specim. Stress, σ_E (psi)	Elastic Strain, ε_E	Free Shrinkage Strain, ε_{sh}	Total Specimen Strain, ε_{CL}	Creep Strain, ε_{CR}	Computed Shrinkage Stress, σ_{FC} (psi)	Splitting Tensile Strength (psi)
Mix - 10								
Standard								
3	3052549	89	0.000029	0.000080	0.000047	0.000004	233	381
7	3280739	154	0.000047	0.000184	0.000109	0.000028	512	594
SRA								
3	3114178	55	0.000018	0.000018	0.000005	-0.000005	71	397
7	3298157	101	0.000031	0.000058	0.000035	-0.000007	216	603
Mix - 11								
Standard								
3	3226966	149	0.000046	0.000102	0.000049	0.000007	306	381
7	3666718	158	0.000043	0.000247	0.000164	0.000040	758*	594
SRA								
3	3189941	125	0.000039	0.000038	0.000001	-0.000002	127	397
7	3507181	128	0.000037	0.000123	0.000082	0.000004	417	603
Mix - 12								
Standard								
3	3992077	134	0.000034	0.000193	0.000103	0.000055	549*	381
7	4239146	157	0.000037	0.000314	0.000199	0.000079	999*	594
SRA								
3	3880440	104	0.000027	0.000083	0.000037	0.000019	246	397
7	4417371	118	0.000027	0.000164	0.000102	0.000035	568	603

Table 6-3 – continued

Time (Days)	E (psi)	Specim. Stress, σ_E (psi)	Elastic Strain, ε_E	Free Shrinkage Strain, ε_{sh}	Total Specimen Strain, ε_{CL}	Creep Strain, ε_{CR}	Computed Shrinkage Stress, σ_{FC} (psi)	Splitting Tensile Strength (psi)
Mix - 13								
Standard								
3	3861868	119	0.000031	0.000212	0.000138	0.000043	654*	381
7	4539476	139	0.000031	0.000390	0.000281	0.000079	1413*	594
SRA								
3	4138054	107	0.000026	0.000086	0.000048	0.000013	304	397
7	4757098	132	0.000028	0.000183	0.000131	0.000025	754*	603
Mix - 14								
Standard								
3	3842707	100	0.000026	0.000094	0.000068	0.000000	361	381
7	3886822	134	0.000034	0.000162	0.000120	0.000008	599*	594
SRA								
3	3556466	93	0.000026	0.000037	0.000008	0.000002	122	397
7	4001058	119	0.000030	0.000084	0.000037	0.000017	269	603
Mix - 15								
Standard								
3	4167444	101	0.000024	0.000149	0.000108	0.000017	552*	381
7	4962452	144	0.000029	0.000228	0.000160	0.000039	936*	594
SRA								
3	4384647	111	0.000025	0.000075	0.000036	0.000014	266	397
7	4887643	155	0.000032	0.000124	0.000072	0.000020	508	603

Note: * Concrete would have cracked due to shrinkage under a fully constrained condition.

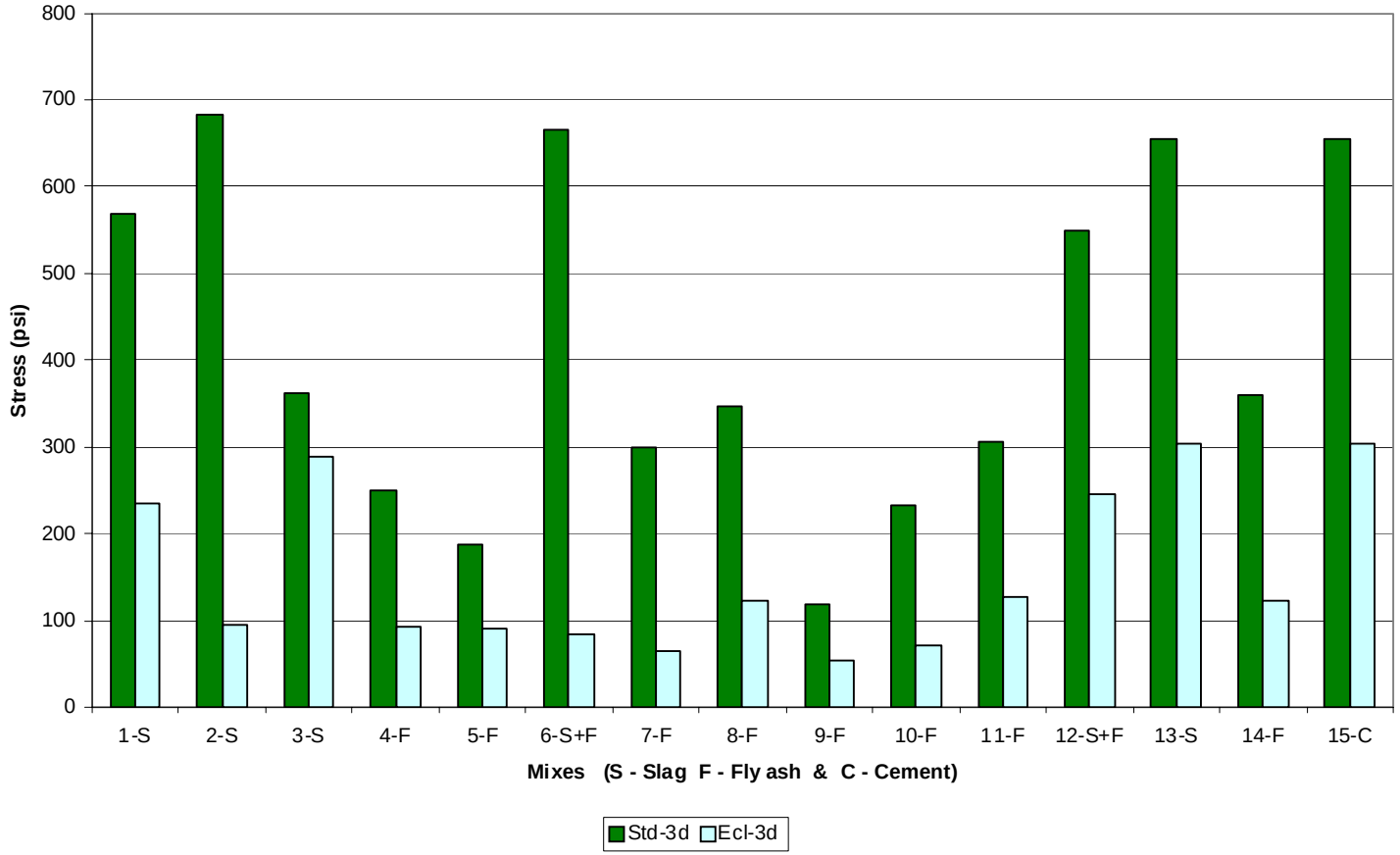

Figure 6-9. Comparison of computed shrinkage-induced stresses of Standard and SRA mixtures at 3 days curing

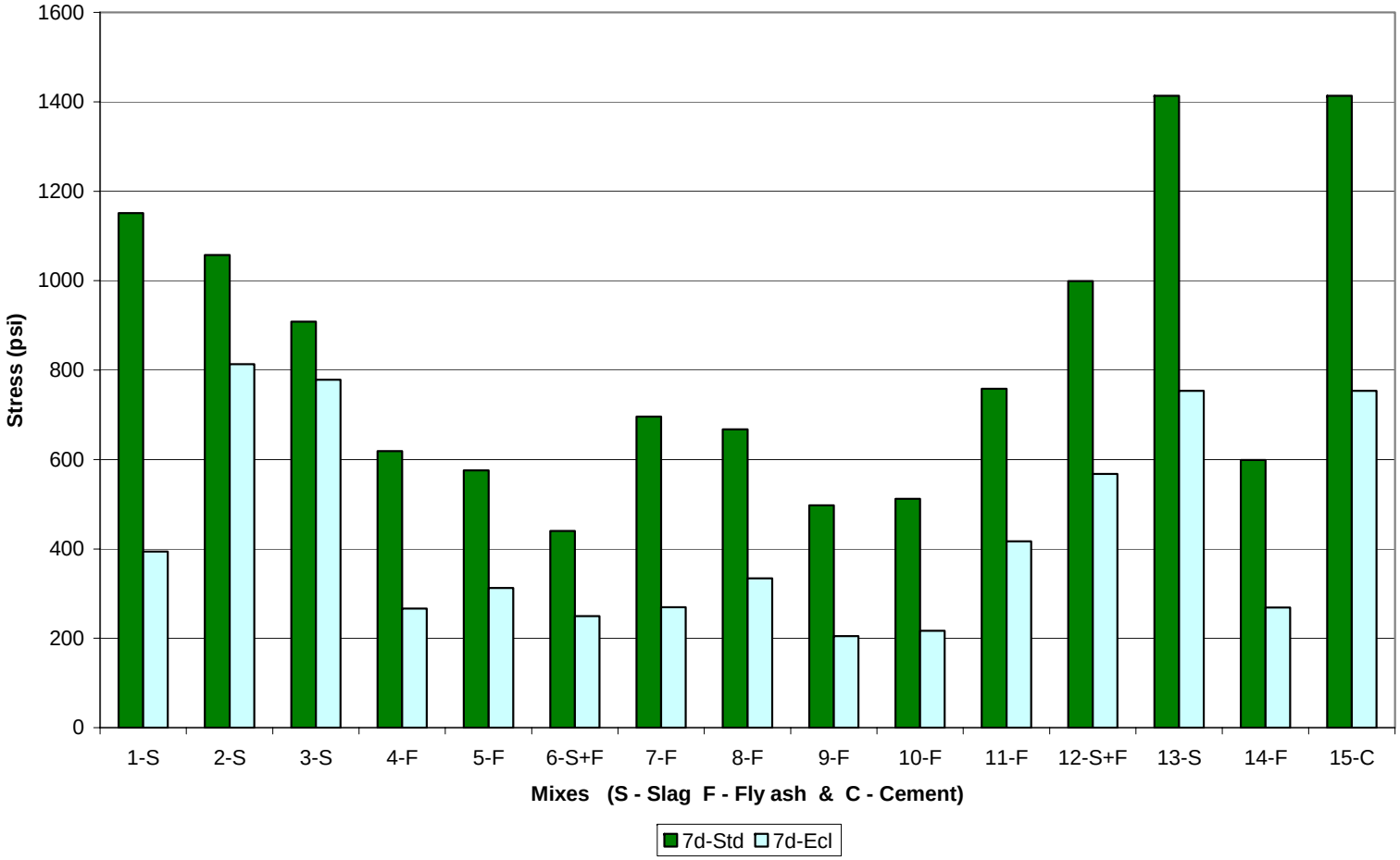

Figure 6-10. Comparison of computed shrinkage-induced stresses of Standard and SRA mixtures at 7 days curing

Table 6-4. Percentage Reduction of Computed Shrinkage-Induced Stresses of SRA Mixtures as Compared With the Standard Mixtures

% Reduction of Computed Induced Shrinkage Stress of SRA Mixes							
Mix	Type	Curing time (days)					
		3		7		14	
		Stress (psi)	% Reduction	Stress (psi)	% Reduction	Stress (psi)	% Reduction
1	Standard	569	59	1151	66	1314	55
	SRA	234		394		588	
2	Standard	682	86	1058	23	1316	2
	SRA	95		813		1290	
3	Standard	362	20	908	14	1243	14
	SRA	288		779		1069	
4	Standard	249	63	618	57	899	44
	SRA	92		267		507	
5	Standard	187	52	575	46	783	23
	SRA	90		312		600	
6	Standard	665	88	440	43	673	26
	SRA	83		250		497	
7	Standard	300	79	696	61	N/A	N/A
	SRA	64		269		N/A	N/A
8	Standard	346	65	667	50	N/A	N/A
	SRA	122		334		N/A	N/A
9	Standard	118	55	497	59	N/A	N/A
	SRA	53		204		N/A	N/A
10	Standard	233	70	512	58	N/A	N/A
	SRA	71		216		N/A	N/A
11	Standard	306	58	758	45	N/A	N/A
	SRA	127		417		N/A	N/A
12	Standard	549	55	999	43	N/A	N/A
	SRA	246		568		N/A	N/A
13	Standard	654	53	1413	47	N/A	N/A
	SRA	304		754		N/A	N/A
14	Standard	361	66	599	55	N/A	N/A
	SRA	122		269		N/A	N/A
15	Standard	654	53	1413	47	N/A	N/A
	SRA	304		754		N/A	N/A
Mean			62		48	N/A	27

with an average of 62% at 3 days curing. The percentage reduction ranges from 14 to 66% with an average of 48% at 7 days curing. The percentage reduction ranges from 2 to 55% with an average of 27% at 14 days curing.

6.3.3 Effects on Strengths and Elastic Modulus

The results of the compressive strength, splitting tensile strength and elastic modulus tests on the 15 pairs of concrete mixtures evaluated in this study are presented in Table 6-5. It can be seen from these data that, in some mixes, the SRA mixtures appeared to give slightly higher increase the strengths and elastic modulus, while for the other mixes, the SRA mixtures appeared to have slightly lower strengths and elastic modulus. Were these observed differences statistically significant, or were they due primarily to the variability of the test data? The Student's t-test was used to answer this question.

For each pair of concrete mixtures, the Student's t-test was performed to compare the means of each of these three mechanical properties from the SRA and the standard mixtures to determine if they were significantly different from one another with respect to each of these three mechanical properties.

For each t-test, the t statistic was calculated as follows:

$$t = \frac{X_1 - X_2}{s\left(\frac{1}{n_1} + \frac{1}{n_2}\right)^{0.5}} \qquad \text{(Eq. 6.1)}$$

where X_1 and X_2 are means of the samples from populations 1 and 2; n_1 and n_2 are sample sizes for the samples from populations 1 and 2; s is the square root of the pooled variance (s^2) given by:

$$s^2 = \frac{(n_1 - 1)(s_1)^2 + (n_2 - 1)(s_2)^2}{n_1 + n_2 - 2} \qquad \text{(Eq. 6.2)}$$

where $(s_1)^2$ and $(s_2)^2$ are variances of the samples from populations 1 and 2.

Table 6-5. Compressive Strength, Splitting Tensile Strength and Elastic Modulus of the 15 Pairs of Concrete Mixtures

Mixes	Time (days)	E (psi)			Compressive Strength (psi)				Splitting Tensile Strength (psi)			
		1	2	Average	1	2	3	Average	1	2	3	Average
Mix - 1 (C-50, S-50), Standard (w/c - 0.33)	3	4416855	4493455	4455155	4810	4470	5004	4761	461	396	428	429
	7	5308886	4991944	5150415	6950	7050	6790	6930	654	577	551	594
	14	5640288	5431603	5535946	7700	8160	7740	7867	614	551	676	614
Mix - 1 (C-50, S-50), SRA (w/c - 0.33)	3	4584048	4878461	4731254	5030	4830	5020	4960	441	423	504	456
	7	5438242	5371741	5404991	7090	7120	7400	7203	640	613	557	603
	14	5642459	5790019	5716239	8220	8150	8410	8260	788	696	670	718
Mix - 2 (C-30, S-70), Standard (w/c - 0.25)	3	6224478	6630175	6427326	6700	6440	6520	6553	493	486	495	492
	7	7063727	7272718	7168223	8710	8434	8430	8525	658	636	602	632
	14	7271631	7298524	7285077	9370	8760	8560	8897	694	726	680	700
Mix - 2 (C-30, S-70), SRA (w/c - 0.25)	3	6445834	6169017	6307425	4710	4810	4960	4827	383	366	403	384
	7	6689849	6790581	6740215	6550	6650	6830	6677	506	516	513	512
	14	6838769	7231382	7035076	7360	7270	7070	7233	607	599	595	600
Mix - 3 (C-30, S-70), Standard (w/c - 0.30)	3	2978144	2832156	2905150	4270	4310	4130	4237	314	384	365	354
	7	3386258	3469441	3427850	5695	5469	5442	5535	709	657	616	661
	14	4044965	4120283	4082624	7450	7570	7560	7527	773	656	667	699
Mix - 3 (C-30, S-70), SRA (w/c - 0.29)	3	3618629	3681622	3650126	3590	3530	3570	3563	322	360	304	329
	7	4208640	4161921	4185281	5399	5620	5570	5530	565	555	499	540
	14	4181911	4204542	4193226	7170	6870	6870	6970	610	651	660	640

Table 6-5 – continued

Mixes	Time (days)	E (Psi)			Compressive Strength				Splitting Tensile Strength (psi)			
		1	2	Average	1	2	3	Average	1	2	3	Average
Mix - 4 (C-80, F-20) Standard (w/c-0.35)	3	3138865	2972865	3055865	2910	2830	2970	2903	360	403	366	376
	7	3511892	3412774	3462333	6680	6750	6520	6650	604	660	587	617
	14	3881511	3920872	3901191	7870	7910	8100	7960	766	632	688	695
Mix - 4 (C-80, F-20) SRA (w/c-0.33)	3	3044235	2906975	2975605	2000	2040	2060	2033	391	400	395	395
	7	3275018	3464325	3369671	6400	6250	6370	6340	571	626	623	607
	14	3792704	3740321	3766512	7900	7940	7920	7920	646	656	630	644
Mix - 5 (C-65, F-35) Standard (w/c-0.33)	3	3000886	2722150	2861518	3440	3460	3430	3443	376	415	439	410
	7	3390959	3492951	3441955	4500	4560	4530	4530	533	590	519	547
	14	3661683	3576361	3619022	5580	5540	5640	5587	566	471	542	526
Mix - 5 (C-65, F-35) SRA (w/c-0.33)	3	2880273	2859563	2869918	3230	3300	3320	3283	406	436	331	391
	7	3382939	3290456	3336697	4710	4520	4510	4580	489	390	491	457
	14	3616783	3521181	3568982	5540	5540	5550	5543	529	487	464	494
Mix - 6 (C-30, S-50 & F-20), Standard (w/c-0.35)	3	2618982	2622861	2620921	2450	2410	2380	2413	381	345	372	366
	7	3120751	3162391	3141571	4690	4790	4620	4700	574	496	492	521
	14	3514496	3510558	3512527	6669	6465	6903	6679	669	726	664	686
Mix - 6 (C-30, S-50 & F-20), SRA (w/c-0.35)	3	2535208	2548807	2542007	2280	2210	2400	2297	376	303	284	321
	7	3349643	3362484	3356063	4720	4780	4690	4730	481	542	578	534
	14	3495439	3537646	3516542	6030	6450	6365	6282	649	588	607	615

Table 6-5 – continued

Mixes	Time (days)	E (Psi)			Compressive Strength				Splitting Tensile Strength (psi)			
		1	2	Average	1	2	3	Average	1	2	3	Average
Mix - 7 (C-80, F-20), Standard (w/c - 0.34)	3	3606318	3606318	3606318	4463	4439	4455	4452	465	467	467	467
	7	4076555	3900563	3988559	5855	6324	6006	6061	644	499	539	561
	14	4525851	4304663	4415257	7533	7509	7239	7427	581	478	606	555
	28	4537320	4525331	4531325	8002	8328	8265	8198	576	684	551	604
Mix - 7 (C-80, F-20), SRA (w/c - 0.34)	3	3388225	3388225	3388225	3516	3548	3572	3545	376	366	354	365
	7	3729430	3840872	3785151	5194	5417	5314	5308	493	447	557	499
	14	3983873	3991834	3987853	6356	6197	6339	6297	552	514	523	530
	28	4138115	4332631	4235373	7636	7422	7517	7525	616	598	676	630
Mix - 8 (C-80, F-20), Standard (w/c - 0.38)	3	3631600	3737570	3684585	4733	4781	4789	4767	483	512	516	504
	7	4056772	4036149	4046461	6539	6491	6658	6563	611	634	611	618
	14	4314802	4203692	4259247	7453	7557	7350	7453	718	718	704	713
	28	4497366	4609553	4553460	8178	8399	8341	8306	1970	2057	2100	2043
Mix - 8 (C-80, F-20), SRA (w/c - 0.38)	3	4019694	4260053	4139874	4964	4805	4932	4900	413	520	463	465
	7	4281844	4305943	4293893	6722	6499	6451	6557	616	611	561	596
	14	4728351	4441247	4584799	7525	7636	7366	7509	628	734	595	652
	28	4724886	4831122	4778004	7881	8227	8402	8170	693	745	610	683
Mix - 9 (C-65, F-35), Standard (w/c - 0.46)	3	2847699	2793418	2820558	2426	2490	2498	2471	326	290	326	314
	7	3230478	3316248	3273363	3651	3611	3611	3625	457	446	334	412
	14	3446445	3625646	3536046	4789	4653	4797	4746	479	557	563	533
	28	3599945	3822791	3711368	5878	5688	5823	5796	636	636	545	606
Mix - 9 (C-65, F-35), SRA (w/c – 0.46)	3	2997575	2928491	2963033	2538	2649	2561	2583	358	318	332	336
	7	3223592	3378211	3300901	3802	3938	3985	3908	369	377	368	371
	14	3607691	3715169	3661430	4828	4868	4852	4850	561	519	416	498
	28	3864973	3711668	3788320	5727	5759	5664	5717	531	614	601	582

Table 6-5 – continued

Mixes	Time (days)	E (psi)			Compressive Strength (psi)				Splitting Tensile Strength (psi)			
		1	2	Average	1	2	3	Average	1	2	3	Average
Mix - 10 (C-65, F-35), Standard (w/c - 0.41)	3	2936739	3168360	3052549	2657	2792	2919	2789	360	364	328	351
	7	3295355	3266124	3280739	3651	3699	3906	3752	457	461	485	468
	14	3466569	3496266	3481417	4598	4765	4741	4701	523	523	463	503
	28	3702587	3719864	3711225	5759	5775	5743	5759	573	602	507	561
Mix - 10 (C-65, F-35), SRA (w/c - 0.41)	3	3161160	3067196	3114178	2681	2705	2832	2739	360	382	378	373
	7	3240103	3356210	3298157	3866	3874	3930	3890	469	497	380	449
	14	3601638	3626390	3614014	5003	4860	4988	4950	507	459	581	516
	28	3712301	3959791	3836046	5839	5950	6157	5982	403	541	499	481
Mix - 11 (C-80, F-20), Standard (w/c - 0.46)	3	3258290	3195641	3226966	3691	3683	3747	3707	322	326	344	330
	7	3720572	3612864	3666718	5520	5409	5345	5425	464	612	447	508
	14	3862169	3827133	3844651	6064	6006	5979	6016	490	555	477	507
	28	4145363	4255670	4200516	7151	7199	7247	7199	542	441	537	506
Mix - 11 (C-80, F-20), SRA (w/c - 0.46)	3	3143982	3235900	3189941	3524	3516	3675	3572	346	439	320	368
	7	3498332	3516031	3507181	4956	5051	4972	4993	490	470	562	507
	14	3610294	3660458	3635376	5688	5823	5611	5707	549	542	604	565
	28	3834219	3949312	3891766	7151	7366	6889	7135	667	687	688	681
Mix - 12 (C-30, S-50 & F-20), Standard (w/c - 0.28)	3	3550043	4434111	3992077	4844	4645	5019	4836	414	414	527	451
	7	4203387	4274906	4239146	6618	6411	6634	6555	577	501	560	546
	14	4369976	4487084	4428530	7485	7533	7453	7491	594	543	652	596
	28	4591187	4564588	4577888	7803	8130	8225					
Mix - 12 (C-30, S-50 & F-20), SRA (w/c - 0.28)	3	4100167	3660713	3880440	3810	3922	3961	3898	362	430	360	384
	7	4442825	4391918	4417371	5727	5791	5759	5759	505	505	506	506
	14	4542769	4575835	4559302	6364	7016	6698	6692	593	577	614	595
	28	4794909	4926751	4860830	7247	7207	7151	7202	524	579	553	552

Table 6-5 – continued

Mixes	Time (days)	E (Psi)			Compressive Strength				Splitting Tensile Strength			
		1	2	Average	1	2	3	Average	1	2	3	Average
Mix - 13 (C-50, S-50), Standard (w/c - 0.41)	3	3735773	3987963	3861868	6189	6491	6523	6401	414	507	412	444
	7	4570450	4508502	4539476	8114	8193	8201	8169	556	498	659	571
	14	4747266	5123076	4935171	9259	9378	9514	9384	755	671	729	718
	28	4781950	5146989	4964470	9657	9736	9553	9649	911	656	867	811
Mix - 13 (C-50, S-50), SRA (w/c - 0.41)	3	4111928	4164180	4138054	5497	5314	5417	5409	406	410	396	404
	7	4658387	4855809	4757098	7398	7278	7613	7430	483	515	576	525
	14	5001046	5001046	5001046	8543	8519	8710	8591	509	562	646	572
	28	5177606	5134069	5155838	9044	9148	9108	9100	789	599	629	672
Mix - 14 (C-65, F-35), Standard (w/c - 0.30)	3	3858952	3826463	3842707	3475	3523	3378	3459	287	383	367	346
	7	3886822	2911755	3886822	4542	4470	4311	4441	467	436	453	452
	14	4423983	4366718	4395351	5505	5377	5170	5351	515	533	545	531
	28	5580151	4812471	5196311	7239	7382	6928	7183	611	509	723	615
Mix - 14 (C-65, F-35), SRA (w/c - 0.30)	3	3556466	3341947	3449206	3043	2954	2980	2993	313	327	331	324
	7	3965263	4036854	4001058	4176	4073	4120	4123	475	416	396	429
	14	4441069	4218399	4329734	5003	5338	4828	5056	481	515	561	519
	28	4592010	4711529	4651769	6618	6570	6284	6491	526	508	507	514
Mix - 15 (C-100), Standard (w/c - 0.29)	3	3803863	4510687	4157275	7764	8082	7835	7894	618	622	702	647
	7	5039900	5039900	5039900	10047	9561	9713	9773	651	722	722	698
	14	5315464	5123516	5219490	11192	10595	10206	10664	769	768	611	716
	28	5322837	5471778	5397307	11089	11526	11574	11396	597	692	716	668
Mix - 15 (C-100), SRA (w/c - 0.29)	3	4408573	4323830	4366202	6109	6173	6109	6130	528	472	585	528
	7	3366304	4917633	4917633	7692	7589	7772	7684	696	679	745	707
	14	5035781	5669101	5352441	9052	8480	8480	8670	627	504	532	554
	28	5234741	5439419	5337080	9076	9386	9593	9352	730	678	571	660

The null hypothesis that the two means were equal to one another was tested at an α level of 5%. The t value for $(n_1 + n_2 - 2)$ degrees of freedom and α level of 5% for a two-tail distribution was determined from the Student's t distribution table and was denoted as $t_{Critical}$. If the computed t value was smaller than $t_{Critical}$, the null hypothesis could not be rejected, and the two means were considered to be statistically not different from one another.

Tables 6-6, 6-7 and 6-8 present the results of the Student's t-test on the compressive strengths, splitting tensile strength and elastic modulus of elasticity, respectively, of the SRA mixtures versus the standard mixtures. It can be seen that for all the 15 pairs of mixtures evaluated, the compressive strength, splitting tensile strength and modulus of elasticity of the SRA mixtures were not significantly different from those of the standard mixtures.

6.4 Evaluation of the Effects of Fly Ash and Ground Blast Furnace Slag

The mix designs of all the 15 pairs of concrete mixtures evaluated in the laboratory testing program are presented in Section 3.2. All the concrete mixtures had a fixed cementitious materials content of 700 lb/yd^3 (415.7 kg/m^3) of concrete. The composition of the mixtures varied mainly by the type and amount of mineral admixtures. The mixtures can be divided into four categories. The first category includes eight mixtures containing fly ash as a mineral admixture. Of these eight fly ash mixtures, four (Mixes 4, 7, 8 and 11) contained 20% fly ash, and four (Mixes 5, 9, 10 and 14) contained 35% fly ash. The second category includes the four mixtures containing ground blast furnace slag as a mineral admixture. Of these four slag mixtures, two (Mixes 1 & 13)

Table 6-6. Results of t-Tests on the Compressive Strength of the SRA Mixtures Versus the Standard Mixtures

Mix	Admixture & w/c	Type	Sample size	Mean	$t_{Calculated}$	$t_{Critical}$ for 95% Confidence	Significantly Different?
1	S-50 & 0.33	Standard	3	6519	0.215	2.776	No
		SRA	3	6808			
2	S-70 & 0.25	Standard	3	7992	1.697	2.776	No
		SRA	3	6246			
3	S-70 & 0.30	Standard	3	5766	0.299	2.776	No
		SRA	3	5354			
4	F-20 & 0.33	Standard	3	5838	0.175	2.776	No
		SRA	3	5431			
5	F-35 & 0.33	Standard	3	4520	0.057	2.776	No
		SRA	3	4469			
6	S-50 & F-20 & 0.35	Standard	3	4597	0.095	2.776	No
		SRA	3	4436			
7	F-20 & 0.34	Standard	4	6535	0.736	2.447	No
		SRA	4	5669			
8	F-20 & 0.38	Standard	4	6772	0.011	2.447	No
		SRA	4	6784			
9	F-35 & 0.46	Standard	4	4160	0.107	2.447	No
		SRA	4	4264			
10	F-35 & 0.41	Standard	4	4250	0.148	2.447	No
		SRA	4	4390			
11	F-20 & 0.46	Standard	4	5587	0.226	2.447	No
		SRA	4	5352			
12	S-50 & F-20 & 0.28	Standard	4	6734	0.836	2.447	No
		SRA	4	5888			
13	S-50 & 0.41	Standard	4	8401	0.696	2.447	No
		SRA	4	7632			
14	F-35 & 0.30	Standard	4	5108	0.408	2.447	No
		SRA	4	4666			
15	C-100 & 0.29	Standard	4	9932	1.916	2.447	No
		SRA	4	7959			

Table 6-7. Results of t-Tests on the Splitting Tensile Strength of the SRA Mixtures Versus the Standard Mixtures

Mix	Admixture & w/c	Type	Sample size	Mean	$t_{Calculated}$	$t_{Critical}$ for 95% Confidence	Significantly Different?
1	S-50 & 0.33	Standard	3	545	0.489	2.776	No
		SRA	3	592			
2	S-70 & 0.25	Standard	3	608	1.246	2.776	No
		SRA	3	499			
3	S-70 & 0.30	Standard	3	571	0.479	2.776	No
		SRA	3	503			
4	F-20 & 0.33	Standard	3	563	0.115	2.776	No
		SRA	3	549			
5	F-35 & 0.33	Standard	3	494	0.904	2.776	No
		SRA	3	447			
6	S-50 & F-20 & 0.35	Standard	3	524	0.27	2.776	No
		SRA	3	490			
7	F-20 & 0.34	Standard	4	547	0.657	2.447	No
		SRA	4	506			
8	F-20 & 0.38	Standard	4	640	0.579	2.447	No
		SRA	4	600			
9	F-35 & 0.46	Standard	4	466	0.225	2.447	No
		SRA	4	447			
10	F-35 & 0.41	Standard	4	471	0.298	2.447	No
		SRA	4	455			
11	F-20 & 0.46	Standard	4	441	1.183	2.447	No
		SRA	4	530			
12	S-50 & F-20 & 0.28	Standard	4	576	0.951	2.447	No
		SRA	4	509			
13	S-50 & 0.41	Standard	4	636	0.946	2.447	No
		SRA	4	543			
14	F-35 & 0.30	Standard	4	486	0.622	2.447	No
		SRA	4	441			
15	C-100 & 0.29	Standard	4	678	1.398	2.447	No
		SRA	4	612			

Table 6-8. Results of t-Test on the Modulus of Elasticity of the SRA Mixtures Versus the Standard Mixtures

Mix	Admixture & w/c	Type	Sample size	Mean	$t_{Calculated}$	$t_{Critical}$ for 95% Confidence	Significantly Different
1	S-50 & 0.33	Standard	3	5047172	0.552	2.776	No
		SRA	3	5284162			
2	S-70 & 0.25	Standard	3	6960209	0.778	2.776	No
		SRA	3	6694239			
3	S-70 & 0.30	Standard	3	3471875	1.396	2.776	No
		SRA	3	4009544			
4	F-20 & 0.33	Standard	3	3473130	0.307	2.776	No
		SRA	3	3370596			
5	F-35 & 0.33	Standard	3	3307498	0.159	2.776	No
		SRA	3	3258533			
6	S-50 & F-20 & 0.35	Standard	3	3091673	0.117	2.776	No
		SRA	3	3138204			
7	F-20 & 0.34	Standard	4	4135365	1.033	2.447	No
		SRA	4	3849150			
8	F-20 & 0.38	Standard	4	4135938	1.348	2.447	No
		SRA	4	4449142			
9	F-35 & 0.46	Standard	4	3335334	0.107	2.447	No
		SRA	4	3428421			
10	F-35 & 0.41	Standard	4	3381483	0.148	2.447	No
		SRA	4	3465599			
11	F-20 & 0.46	Standard	4	3734713	0.226	2.447	No
		SRA	4	3556066			
12	S-50 & F-20 & 0.28	Standard	4	4309410	0.836	2.447	No
		SRA	4	4429486			
13	S-50 & 0.41	Standard	4	4575246	0.696	2.447	No
		SRA	4	4763009			
14	F-35 & 0.30	Standard	4	4330298	0.408	2.447	No
		SRA	4	4107942			
15	C-100 & 0.29	Standard	4	4953493	1.916	2.447	No
		SRA	4	4107942			

contained 50% slag, and two (Mixes 2 &3) contained 70% slag. The third category includes two mixtures (Mixes 6 & 12) containing both fly ash (20%) and slag (50%) as mineral admixtures. The fourth category is the reference mixture (Mix 15) containing no mineral admixture.

The effects of the mineral admixtures on free shrinkage of concrete were evaluated by comparing the free shrinkage strains of these four categories of concrete. Table 6-9 shows the comparison of the means and the ranges of the free shrinkage strains among the concrete in these four categories. It can be seen that the concrete mixtures containing fly ash had the lowest free shrinkage strains at both 3 days and 7 days curing, for both the standard mixes and the SRA mixes. The concrete mixtures containing slag generally had the highest free shrinkage strains among the four categories of concrete evaluated. The concrete mixtures containing both slag and fly ash generally had about the same free shrinkage strains as those of the concrete containing no mineral admixture. These two categories of mixes had relatively lower free shrinkage strains as compared with the concrete containing slag, and relatively higher free shrinkage strains as compared with the concrete containing fly ash.

Table 6-9. The Statistical Ranges of Free Shrinkage Strains of the Concrete Mixtures With Different Mineral Admixtures

Ranges of Free Shrinkage Strains in Microstrains								
Admixtures	**3 days**				**7 days**			
	Highest	**Lowest**	**Mean**	**Range**	**Highest**	**Lowest**	**Mean**	**Range**
	Standard							
Fly ash	142	68	101	74	254	162	213	92
Slag	222	163	197	58	390	300	333	90
Fly ash + Slag	193	45	119	148	314	240	277	75
None	N/A	N/A	149	N/A	N/A	N/A	228	N/A
	SRA							
Fly ash	44	18	32	26	123	58	93	65
Slag	97	82	89	15	219	167	188	52
Fly ash + Slag	83	13	48	71	164	141	152	23
None	N/A	N/A	75	N/A	N/A	N/A	124	N/A

Table 6-10 shows the comparison of the means and the ranges of the computed shrinkage-induced stresses among the four categories of concrete. It can be seen that the

concrete mixtures containing fly ash had the lowest shrinkage-induced stresses at both 3 days and 7 days curing, for both the standard mixes and the SRA mixes. The concrete mixtures in the other three categories did not show any clear rankings among themselves with regards to the shrinkage-induced stresses.

Table 6-10. The Statistical Ranges of Computed Shrinkage-Induced Stresses of the Concrete Mixtures with Different Mineral Admixtures

Ranges of computed shrinkage-induced stress in psi								
Admixtures	**3 days**				**7 days**			
	Highest	**Lowest**	**Mean**	**Range**	**Highest**	**Lowest**	**Mean**	**Range**
	Standard							
Fly ash	361	118	262	243	758	497	615	261
Slag	682	362	567	320	1413	908	1133	505
Fly ash + Slag	1314	549	932	766	999	753	876	247
None	N/A	N/A	552	N/A	N/A	N/A	936	N/A
	SRA							
Fly ash	127	53	91	74	417	204	284	212
Slag	304	95	230	209	813	394	685	419
Fly ash + Slag	246	127	187	118	947	568	757	380
None	N/A	N/A	266	N/A	N/A	N/A	508	N/A

From Table 6-3, which presents the computed shrinkage-induced stresses along with the splitting tensile strength of the concrete at the corresponding curing times, it can be seen that six of the standard mixtures would have cracked at 3 days curing due to shrinkage under a fully constrained condition. Of these six mixtures, three (Mixes 1, 2 and 13) contained slag, two (Mixes 6 and 12) contained fly ash and slag, and one (Mix 15) contained no mineral admixture. The only other concrete mix containing slag (Mix 3) had a computed shrinkage stress (362 psi) very close to the splitting tensile strength at 3 days (381 psi). All these results indicate that the addition of slag as a mineral admixture did not help to improve the resistance to shrinkage cracking of the concrete.

From Table 6-3, it can be seen that the three standard mixes that had the lowest shrinkage-induced stresses at 3 days curing are Mixes 5, 9 and 10. These three mixes all contained 35% fly ash. It can also be seen that the three SRA mixes that had the lowest shrinkage-induced stresses at 3 days curing are Mixes 7, 9 and 10. Mix 7 contained 20% fly ash, while Mixes 9 and 10 contained 35% fly ash. All these observations point to the effectiveness of fly ash in improving the resistance to shrinkage cracking of concrete.

CHAPTER 7
SUMMARY AND RECOMMENDATIONS

7.1 Development and Evaluation of the Modified Constrained Long Specimen Apparatus

The constrained long specimen apparatus, which was previously developed for the FDOT by the University of Florida for evaluation of resistance to shrinkage cracking of concrete, was further refined and evaluated in this study. Four main refinements were made to the test apparatus and procedure.

First, the long constrained specimen apparatus was refined by, (1) replacing the Whittemore gage, which was used to measure the deformation of the specimen, by a high-sensitivity Linear Variable Differential Transformer (LVDT); and (2) replacing the proving ring, which was used to measure the induced force in the constrained long specimen, by a load cell. The outputs from the LVDT and the load cell were connected to an automatic data acquisition system, which can be set up to take readings at specified time intervals and for a specified length of time.

One observed problem with the constrained long specimen apparatus was that the long concrete specimen appeared to be sticking to the steel plate below it. The second refinement to the apparatus was made to address this problem. A water-resistant and low-friction Teflon sheet was used as the base plate of the long constrained specimen apparatus to minimize the friction between the concrete specimen and its supporting base. The use of Teflon sheets as base plates appeared to give good results, and was adopted.

The constrained long specimen apparatus using LVDT for strain measurement had one drawback in that the LVDT could not be placed on the specimen until after the concrete has attained sufficient strength. Thus, the shrinkage of the concrete in the very

early age could not be measured. The third refinement was made to address this issue. In order to monitor the shrinkage of concrete at its very early age after placement, an embedment strain gage was used in place of the LVDT for strain measurement in the long specimen apparatus. The use of the embedment strain gages for strain measurement gave satisfactory performance, and thus was adopted.

Another observed problem was that the long specimen apparatus was not able to provide complete restraint to the concrete specimen to keep it from contracting during the constrained shrinkage test. Due to the contraction of the specimen during the test, a complete restrained condition was not achieved as intended. A modification to the test procedure was made to provide the correction to the specimen contraction by manually pulling the specimen (by turning a nut on a threaded rod on the test apparatus) during the test such that the strain in the specimen would be kept as close to zero as possible. The strain reading from the strain gage was used as a guide on how much the specimen needed to be pulled. This manual method of correcting the contraction strains in the constrained long specimen appeared to give acceptable results. Thus, this method was adopted for use in the laboratory testing program of this study.

7.2 Evaluation of Different Methods of Free Shrinkage Measurement

Five different methods for measuring free shrinkage of concrete were evaluated. These five methods were: (1) Whittemore gage in the long specimen apparatus; (2) LVDT in the long specimen apparatus; (3) embedment strain gage in the long specimen apparatus; (4) Whittemore gage on a 6 × 12-in. (152.4 × 304.8-mm) cylindrical

specimen; and (5) LVDT on a 3 × 3 × 11.25-in. (76 × 76 × 286-mm) square prism specimen according to ASTM C157 procedure.

Free shrinkage measurements using these five different methods were made on the 15 pairs of concrete mixtures (with and without the addition of a shrinkage-reducing admixture) used in this study. From the comparison of the free shrinkage strain measurements using the different methods, the strain measurements using the embedment strain gage in the long specimen apparatus showed the best repeatability with the lowest variance. The embedment strain gage method also has the advantage that the strain measurements can be made from a very early age of the concrete. Thus, the embedment gage method was used for measurement of free shrinkage and for measurement of strain in the constrained long specimen test in this study.

7.3 Evaluation of the Effects of a Shrinkage-Reducing Admixture

Fifteen pairs of concrete mixtures (with and without the addition of a shrinkage-reducing admixture, SRA) were evaluated for their free shrinkage, resistance to shrinkage cracking, compressive strength, splitting tensile strength and modulus of elasticity. The results from the free shrinkage test indicate that the addition of SRA reduced the free shrinkage substantially for all mixes. The percentage reduction varies from 41 to 81% at 3 days, from 32 to 70% at 7 days, and from 23 to 43% at 14 days.

The results from the constrained long specimen test indicate that the SRA mixtures had substantially lower computed induced shrinkage stresses than their corresponding standard mixtures. The results predict that 6 of the 15 standard mixtures would have cracked within 3 days under a fully constrained condition, while none of the

SRA mixtures would crack under a similar condition. The percentage reduction of computed induced shrinkage stresses due to the addition of SRA ranges from 20 to 88% with an average of 62% at 3 days curing. The percentage reduction ranges from 14 to 66% with an average of 48% at 7 days curing. The percentage reduction ranges from 2 to 55% with an average of 27% at 14 days curing.

The results of Student's t-test indicate that for all the 15 pairs of mixtures evaluated, the compressive strength, splitting tensile strength and modulus of elasticity of the SRA mixtures were not significantly different from those of the standard mixtures.

7.4 Evaluation of the Effects of Fly Ash and Ground Blast Furnace Slag

The mixtures evaluated in this study can be divided into four categories. The first category includes eight mixtures containing 20 to 35% fly ash as a mineral admixture. The second category includes the four mixtures containing 50 to 70% ground blast furnace slag. The third category includes two mixtures containing both fly ash (20%) and slag (50%) as mineral admixtures. The fourth category is the reference mixture containing no mineral admixture.

Among the four categories of concrete evaluated, the concrete mixtures containing fly ash showed the lowest free shrinkage strains. The concrete mixtures containing slag generally had the highest free shrinkage strains. The concrete mixtures containing both slag and fly ash generally had about the same free shrinkage strains as those of the concrete containing no mineral admixture.

The concrete containing fly ash also showed the lowest shrinkage-induced stresses. The concrete mixtures in the other three categories did not show any clear

rankings among themselves with regards to the shrinkage-induced stresses. All these observations indicate that addition of fly ash appeared to improve the resistance to shrinkage cracking of concrete. The results also indicate that the addition of ground blast furnace slag did not appear to improve the resistance to shrinkage cracking of concrete.

7.5 Recommendations

The following recommendations are made based on the results of this study:

1. The addition of a shrinkage-reducing admixture should be considered in the design of a concrete mixture for increased resistance to shrinkage cracking.
2. The addition of fly ash as a mineral admixture should be considered in the design of a concrete mixture for increased resistance to shrinkage cracking.
3. While the developed modified constrained long specimen apparatus was shown to be effective in evaluating the free shrinkage and resistance to shrinkage cracking of concrete in this study, the test procedure was somewhat laborious and time consuming due to the need to manually correct for the contraction strains in the long specimen. It is recommended that the apparatus be further refined such that the correction for the contraction strains can be done automatically rather than manually. It is recommended that a computer controlled servo-hydraulic actuator be used to pull the long specimen to correct for the possible contraction strains automatically. The outputs from the embedment strain gage in the long specimen can be read into the computer, which in turn can use this information to control the movement of the actuator to correction for the contraction strains in the constrained long specimen.

REFERENCES

Aictin, P. C. 1998. *High Performance Concrete*. E & FN Spon, London.

Almudaiheem, J. A., and Hansen, W. 1987. Effect of specimen size and shape on drying shrinkage. *ACI Materials Journal*, Vol. 84, No. 2, pp. 130-135.

Alsayed, S. H. 1998. Influence of superplasticizer, plasticizer, and silica fume on the drying shrinkage of high strength concrete subjected to hot-dry field conditions. *Cement and Concrete Research*, Vol. 28, No. 10, pp. 1405-1415.

Balogh, A. 1996. New admixture combats concrete shrinkage. *Aberdeens Concrete Construction*, Vol. 41, No. 75, pp. 1051-5526.

Bazant, Z. P., ed. 1986. *Proceedings*. Fourth RILEM International Symposium on Creep and Shrinkage of Concrete: Mathematical Modeling, August 26-29, Northwestern University.

Bazant, Z. P., and Carol, I., eds. 1993. *Proceedings*. Fifth International RILEM Symposium on Creep and Shrinkage of Concrete, September 6-9, Barcelona Spain.

Bentz D. P., Geikerb, M. R., and Hansenb, K. K. 2001. Shrinkage-reducing admixtures and early-age desiccation in cement pastes and mortars. *Cement and Concrete Research*, Vol. 31, pp. 1075-1085.

Berke, N. S., Dallaire, M. C., Hicks, M. C., and Kerkar, A. 1997. New developments in shrinkage-reducing admixtures, superplasticizers and other chemical admixtures in concrete. *Proceedings*. Fifth CANMET/ACI International Conference, Rome, Italy.

Bernader, S., and Emborg, M. 1995. Risk of cracking in massive concrete structures, new developments and experiences. *Proceedings*. International Symposium Thermal Cracking in Concrete at Early Ages, Munich, Germany, edited by R. Springenschmidt.

Bloom, R., and Bentur, A. 1995. Free and restrained shrinkage for normal and high strength concretes. *ACI Materials Journal*, Vol. 92, No. 2, pp. 211-217.

Duran, A. C., Kilic, A., and Sevim, U. K. 2004. Strength and shrinkage properties of mortar containing a nonstandard high-calcium fly ash. *Cement and Concrete Research*, Vol. 34, pp. 99-102.

Emborg, M. 1989. Thermal stresses in concrete structures at early ages. Ph.D. Thesis. Lulea University, Sweden.

Folliard, K. J., and Berke, N. S. 1997. Properties of high-performance concrete containing shrinkage-reducing admixture. *Cement and Concrete Research*, Vol. 27, No. 9, pp. 1357-1364.

Han, N., and Walraven, J. C. 1996. Creep and shrinkage of high-strength concrete at early and normal ages. *Advances in Technology*, pp. 73-94.

Haque, M. N. 1996. Strength development and drying shrinkage of high strength concretes. *Cement and Concrete Composites*, Vol. 18, No. 5, pp. 333-342.

Kraai, P. P. 1985. Proposed test to determine the cracking potential due to drying shrinkage of concrete. *Concrete Construction*, Vol. 30, No. 9, pp. 775-778.

Lyman, G. C. 1934. *Growth and Movement in Portland Cement Concrete*. Oxford, University Press, London, U. K., pp. 1-139.

Malhotra V. M. 2004. Properties of the high-volume fly ash concrete, and its role in sustainability of cement and concrete. *Proceedings*. Recent Advances in Cementitious Materials sponsored by University of Wisconsin at Milwaukee Center for By-Products Utilization, March 19-20.

Mindess, S., and Young, J. F. 1981. *Concrete*. Prentice-Hall, Englewood Cliffs, N.J., 671 pp.

Mehta, P. K. 1986. *Concrete: Structures, Properties and Materials,1st Edition*. Prentice-Hall, Englewood Cliffs, N. J., Chapters 6 and 8.

Mehta, P. K., and Monteiro, P. J. 1993. *Concrete: Structures, Properties, and Materials, 2nd Edition*. Prentice-Hall, Englewood Cliffs, N.J.

Neville, A. M. 1996. *Properties of Concrete, 4th Edition*. Addison Wesley Longman, Essex, England.

Persson, B. 1998. Self-desiccation and its importance on concrete technology. *Nordic Concrete Research*, Vol. 21, pp. 120-129. http://lu-research.lub.lu.se/php/gateway.php?who=lr&method=getfile&file=archive/00014056/

Powers, T. C., and Brownyard T. L. 1948. Studies on the physical properties of hardened Portland cement paste. *PCA Bulletin 22*, Chicago, Illinois.

Saito, M., Kawamura, M., and Arakawa, S. 1991. Role of aggregate in the shrinkage of ordinary Portland and expansive cement concrete. *Cement and Concrete Composites*, Vol. 13, No. 2, pp. 115-121.

Schaels, C. A., and Hover, K. C. 1988. Influence of mix proportions and construction operations on plastic shrinkage cracking in thin slabs. *ACI Material Journal*, Vol. 85, Nov-Dec, pp. 495-504.

Shah, S. P., Karaguler, M. E., and Sarigaphuti, M. 1992. Effects of shrinkage reducing admixtures on restrained shrinkage cracking of concrete. *ACI Materials Journal*, Vol. 89, No. 3, pp. 291- 295.

Shilstone, Sr., J. M. 1990. Concrete mixture optimization. *Concrete International: Design and Construction*, Vol. 12, No. 6, June, pp. 33-39.

Shilstone, J. M. 1999. The aggregate: The most important value-adding component in concrete. *Proceedings*. Seventh Annual International Center for Aggregates Research Symposium, Austin, Texas.

Springenschmidt, R., Gierlinger, E., and Kernozycki, W. 1985. Thermal stress in mass concrete: A new testing method and the influence of different cements. *Proceedings*. The 15th International Congress for Large Dams, Lausanne, R4, pp. 57-72.

Swamy, R. N., and Stavardes, H. 1979. Influence of fiber reinforcement on restrained shrinkage cracking. *ACI Journal*, Vol. 76, No. 3, pp. 443-460.

Tangtermsirikul, S., Sudsangium, T., and Nimityongsakul, P. 1995. Class C fly ash as a shrinkage reducer for cement paste. *Proceedings*. Fifth CANMET/ACI International Conference on Fly Ash, Silica Fume, Slag and Natural Pozzolans in Concrete, June 4-9, Milwaukee, Wisconsin, Vol. 1, pp. 385-401.

Tazawa, E., ed. 1998. Autoshrink-98. *Proceedings*. International Workshop on Autogenous Shrinkage of Concrete, Japan Concrete Institute, Hiroshima, Japan June 13-14, 358 pp.

Tazawa, E., and Miyazawa, S. 1995. Influence of cement and admixture on autogenous shrinkage of cement paste. *Cement Concrete Research*, Vol. 25, No. 2, pp. 281-287.

Tazawa, E., and Miyazawa, S. 1997. Effect of self-desiccation on volume change and flexural strength of cement paste and mortar. *Proceedings*. International Research Seminar on Self-Desiccation and Its Importance on Concrete Technology, held in Lund, Sweden.

Tazawa, E., and Miyazawa, S. 1997. Influence of constituents and composition on autogenous shrinkage of cementitious materials. *Magazine of Concrete Research*, Vol. 49, No. 178, pp. 15-22.

Tazawa, E., and Yonekura, A. 1986. Drying shrinkage and creep of concrete with condensed silica fume. *Proceedings*. The 2nd International Conference on the Use of Fly Ash, Silica Fume, Slag and Natural Pozzolans in Concrete, Madrid, Vol. 2, pp. 903-921.

Troxell, G., Harmer, D., and Kelly, J. 1996. *Composition and Properties of Concrete, 2nd edition*. McGraw-Hill, New York, pp. 290-320.

van Breugel, K., and de Vries, J. 1998. Mixture optimization of low water/cement ratio high strength concretes in view of autogenous shrinkage. *Proceedings*. International Symposium on High Performance and Reactive Powder Concrete, Sherbrooke, Canada, pp. 365-382.

Yunsheng Xu, D.D.L. Chung. 2000. Reducing the drying shrinkage of cement paste by admixture surface treatments. *Cement and Concrete Research*, vol. 30, pp. 241-245.

Yunsheng Xu, D.D.L. Chung. 2001. Silane-treated carbon fiber for reinforcing cement. *Carbon*, Vol. 39, Nov., pp. 1995-2001.

Washa, G. W. 1998. *Volume Changes, Chapter 9, Concrete Construction Handbook,4th edition*. Dobrowolski, J., ed. McGraw-Hill, New York.

Weiss, W. J. 1999. Prediction of early-age shrinkage cracking in concrete elements. Ph.D. Thesis. Northwestern University, Evanston, IL.

Wiegrink, K., Marikunte, S., and Shah, S. P. 1996. Shrinkage cracking of high strength concrete. *ACI Materials Journal*, Vol. 93, No. 5, pp. 409-415.